DOCUMENTING AND EXPLAINING RECENT GLOBAL-MEAN TEMPERATURE CHANGES

Final Report to the Natural Environment Research Council

Contract No. GR3/6565

G. Farmer, T.M.L. Wigley, P.D. Jones

and

M. Salmon

Climatic Research Unit,
School of Environmental Sciences,
University of East Anglia,
Norwich NR4 7TJ, U.K.

June 1989

CONTENTS

		Page
	ACKNOWLEDGEMENTS	ii
1.	INTRODUCTION	1
	1.1 Background	1
	1.2 Homogeneity of the data sets	2
	1.3 Correcting the marine data	3
	1.3.1 '*A priori*' corrections	3
	1.3.2 '*A posteriori*' corrections	5
	1.4 Implications of the different corrections	8
2.	THE LAND-BASED DATA	13
	2.1 Spatial representativeness of the land data	13
	2.2 Temporal changes in the seasonal cycle amplitude	20
3.	DESCRIPTION OF THE MARINE DATA SETS	24
	3.1 Introduction	24
	3.2 Construction of the data sets	24
	3.3 Coverage	25
	3.4 Spatial representativeness of the COADS data	29
	3.5 Air temperature series: COADS/UKMO comparison	41
	3.5.1 Hemispheric means	41
	3.5.2 Zonal means	46
	3.5.3 Land-marine comparison	46
	3.6 Sea surface temperature data: COADS/UKMO comparison	53
	3.6.1 Hemispheric means	53
	3.6.2 Zonal means	53
	3.7 Air-sea temperature differences	65
4.	AN *A PRIORI* BUCKET MODEL APPROACH	68
	4.1 Introduction	68
	4.2 The bucket model	69
	4.2.1 Theory	69
	4.2.2 Sensitivity analysis	70
	4.2.3 Effect of bucket/intake mix and different bucket types	72
	4.2.4 The ship speed effect	73
	4.2.5 The effect of bucket size and shape	75
	4.2.6 A more correct bucket equation	75
	4.3 Application of the bucket model	77
	4.3.1 Model input data	77
	4.3.2 Seasonal cycles in the uncorrected data	78
	4.3.3 Minimizing the spurious cycle	81
5.	SPATIAL ASPECTS OF SST DATA AND CORRECTION FACTORS	109
	5.1 Introduction	109
	5.2 The seasonal cycle of SSTs	109
	5.3 Seasonal cycles in the correction factor	112
	5.4 Time dependence of the hemispheric-mean correction factors	112
	5.5 Zonal and seasonal variations in the correction factors	118
6.	CORRECTING SSTs USING THE *A PRIORI* APPROACH	119
	6.1 Optimum exposure time	119
	6.2 The final correction factors	121
	6.3 The corrected SST data set	121
7.	SUMMARY AND CONCLUSIONS	128
	REFERENCES	139

ACKNOWLEDGEMENTS

This project would not have been possible without the cooperation of the Meteorological Office in the United Kingdom. The project has led to a formal agreement concerning future research collaboration between the Meteorological Office and the Climatic Research Unit. The authors are particularly grateful to C.K. Folland and D.E. Parker of the Synoptic Climatology Branch (Met. O.13) for numerous discussions and for supplying various marine data sets.

The Comprehensive Ocean-Atmosphere Data Set (COADS) used in this project was made available by Scott Woodruff of the Environmental Research Laboratories of the U.S. National Oceanic and Atmospheric Administration.

The results presented in this report are the culmination of many person-years of effort, the greater part of which has been funded by the U.S. Department of Energy, Carbon Dioxide Research Division. Specific results presented here were funded approximately equally by the Department of Energy and by the U.K. Natural Environment Research Council.

1. *INTRODUCTION*

1.1 Background

The data sets used to derive estimates of global-mean temperature changes over the last century are widely used in climatology. They form the basis for studies of climatic change on a variety of spatial scales and are central to assessing the sensitivity of the climate system to external forcing. However, these data sets have many shortcomings. The land-based data sets (e.g. Jones et al., 1986a,b; Jones, 1988, Vinnikov et al., 1987; Hansen and Lebedeff, 1987) only represent, at best, 30% of the Earth's surface. Information from oceanic areas, which make up 70% of the global surface area, has only very recently been added to the land-based data (although ocean island and weather ship data have been used previously to supply information from marine regions). To obtain global coverage it is essential to combine land and marine data. On century and longer time scales, the mean temperature changes of the ocean and land surface fractions of the globe must be in accord (Wigley et al., 1985), so either may be used as a reasonable proxy for global changes. However, the strength of land/ocean links must diminish as the time scale decreases and it is important to assess this relationship on shorter time scales.

Recently, two global compilations of marine data have been assembled. These are the United Kingdom Meteorological Office (UKMO) compilation (Shearman, 1983; Folland et al., 1984; Bottomley et al., 1989) and the Comprehensive Ocean-Atmosphere Data Set (COADS) (Slutz et al., 1985; Woodruff, 1985; Woodruff et al., 1987). The UKMO data set contains sea surface temperature (SST) observations and marine air temperatures (MAT), whilst COADS contains the complete set of shipboard observations. Although there is considerable overlap between the two data sets, the COADS set contains roughly 40% more raw individual SST observations than UKMO, mainly due to differences after 1960 (compare Woodruff et al., 1987, with Bottomley et al., 1989).

Previous analyses of hemispheric averages of SST and MAT have been confined to individual data sets, e.g. Folland et al. (1984) for UKMO and Jones et al. (1986c) for COADS. This report presents the first comparison of the two data sets.

1.2 Homogeneity of the data sets

Both marine data sets (UKMO and COADS) are compilations of raw observations taken on board so-called 'ships of opportunity' from the 1850s onwards. Since that time, considerable changes have been made both to shipping (in particular, the change during the late nineteenth century from sail to steam power ships), to shipping routes, and to the instrumentation used to take the MAT and SST measurements. These changes have introduced numerous inhomogeneities into both MAT and SST time series during the last 130 years. Thus, hemispheric-mean temperature estimates from the raw MAT and SST data show many features not apparent in homogeneous climatological time series. These inhomogeneities have been described by Folland et al. (1984) and Jones et al. (1986c).

It is generally agreed that raw marine data cannot be used without some form of adjustment or correction. This has been known for some time (e.g. Saur, 1963; Tabata, 1978). Nevertheless, some authors have failed to realise the primary importance of the inhomogeneities (e.g. Paltridge and Woodruff, 1981; Oort et al., 1987). The best way to correct the raw data would be to reduce all the individual readings to a common standard. It is, however, rarely known how and with what instruments individual readings were made. Such information was either never recorded or has been lost. When attempts have been made to use only observations of one type (e.g. in the case of SST measurements, bucket or intake measurements), it has been shown that compilations thought to contain only a single data type lead to time series with similar inconsistencies to those based on 'mixed' compilations (Barnett, 1984).

1.3 Correcting the marine data

The major question at present is how the two data compilations should be corrected in order to remove the inhomogeneities. There are two approaches, which can be classified as a priori or a posteriori adjustments.

1.3.1 'A priori' corrections

In the a priori approach, first used by Folland et al. (1984) in correcting MAT data, the adjustments are made on theoretical grounds. Corrections can, in this approach, only be made for known and understood causes.

Folland et al. (1984) argue that the MAT data set is affected by the positioning of the screen used to house the thermometers. Consequently, because solar heating during the day potentially affects many day-time readings, they use night-time MAT data only (NMAT). Through time, the mean ship height above mean sea-level has increased as ships have increased in both size and tonnage. Earlier readings would therefore tend to be warmer, even in the absence of any real temperature change. Corrections are applied to the pre-1961 NMAT data to cool the values by 0.02°C to 0.15°C based on estimates of the lapse rate near the ocean surface. From 1970, ship heights have continued to increase and it has become necessary to increase post-1970 NMAT values by 0.01 to 0.02°C (Bottomley et al., 1989). (The correction factors given above differ from those originally given in Folland et al. (1984) as more data on ship heights has become available recently requiring minor adjustments to earlier corrections.)

Complex corrections must be applied to the NMAT series during the years 1941-45, undoubtedly due to the problems of taking measurements in war-time (Bottomley et al., 1989). Corrections applied in these years are speculative in nature because both the areas with measurements and the temporal density of measurements reduced dramatically in this period. This

is also the case for the period 1914-18.

If one assumes the adjusted NMAT data to be homogeneous, then SST data can be corrected by comparison. In their analysis of the UKMO data set, Folland et al. (1984) found a fairly consistent difference of about 0.3°C between hemispheric means of the SST data and the corrected NMAT data prior to 1942. They then corrected their SST data using this empirical result. The reason for the positive correction to SST data before 1942 is that a rapid change in instrumentation took place around this time from measurements using uninsulated 'canvas' buckets beforehand to engine intake readings afterwards. Some (insulated) bucket measurements have been made since 1942, but the majority of measurements have been made via engine intakes (Bottomley et al., 1989). Furthermore, it is generally believed that since (except perhaps in recent years) the mix of engine intake and bucket readings has remained constant (Barnett, 1984). Recently, there has been a trend back towards bucket measurements, although the bucket fraction is still thought to be small. A bucket/intake correction of order 0.3-0.7°C is generally accepted due to the evaporative cooling of uninsulated buckets (Saur, 1963; James and Fox, 1972; Tabata, 1978). This is consistent with the empirical result noted above.

Folland and Parker (1986, 1989a,b) have extended the a priori approach to SSTs using a model of an uninsulated bucket. The basic assumption here is that a correction is required solely because of the evaporative cooling of a canvas bucket between sampling and measurement. Because evaporative cooling depends on temperature, relative humidity, etc., which vary spatially and temporally, this allows one to calculate corrections which vary according to month and to the region of the ocean. When the theoretical bucket correction is averaged over the hemispheres, the correction comes to a figure which is similar to the earlier empirical estimate (Folland and Parker, 1986, 1989a,b). Further details of the bucket model are given in Section 4.

Hemispheric estimates of mean NMAT and SST made using the above a priori approaches have been compared with land-based data from coastal and/or island regions by Folland and Parker (1989a). There are discrepancies of around 0.2°C in the twentieth century (pre 1942) and 0.1°C in the nineteenth century. Comparisons made between land and COADS data by Jones et al. (1986c) give somewhat larger differences in the nineteenth century. These discrepancies suggest either that the land data are in error, or that the assumptions made in applying the bucket model are incorrect. In the UKMO work, it has been assumed that canvas buckets, or buckets with similar characteristics, were in use continually over the period 1854-1941. As will be demonstrated below, this is debatable, as wooden buckets (with lower evaporative cooling rates) were widely used until at least the 1880s.

1.3.2 'A posteriori' corrections

In the a posteriori approach, exemplified by Jones et al. (1986c), adjustments are made so that the hemispheric means of MAT and SST are in accord with the near-propinquitous land-based data on decadal and longer time scales. For this approach to be valid the land-based data must be homogeneous, so let us consider this first.

It is well known that, for the land station data set, many stations are affected by inhomogeneities resulting from site changes, changing observation times, urbanization, etc. (Bradley and Jones, 1985). Fortunately, for many stations the homogeneity can be tested by comparing the record with neighbouring sites (Jones et al., 1985; Karl and Williams, 1987). Erroneous records can be corrected or removed if they prove to be badly affected, as has been done in developing the Jones et al. (1986a,b) land-based data set. Such techniques can be applied to most of the world's land-based stations, thus ensuring homogeneous results. Only stations with no suitably close neighbours cannot be checked.

The most likely source of residual error is urban warming. This has been discussed by Wigley and Jones (1988), Jones et al. (1989) and Karl and Jones (1989). Comparisons with rigorously homogenized U.S. data show that the maximum possible bias in the Jones et al. land data is a spurious warming trend of 0.1°C during the twentieth century.

The station intercomparison approach may fail if there were a major change in instrumentation which occurred at a similar time throughout the world. Although there have been such changes, e.g. in screens, thermometers and observation times, different countries have introduced changes to these factors at different times.

In the a posteriori approach as applied to the COADS data by Jones et al. (1986c), the MAT series is first corrected to be in accord with land-based data. Having corrected the MAT data, the SST series is adjusted to ensure conformity with MAT. Fifteen different regions of the world were chosen where both MAT measurements and adjoining coastal and/or island data from the land-based data set exist. In addition to these 15 regional comparisons, the hemispheric-mean MAT series for the NH and SH were compared with the appropriate averages of the coastal and island data. The similarity of all 17 annual difference time series indicates that the MAT data are affected by spatially consistent inhomogeneities, which are the same in both hemispheres. The corrections required to adjust the MAT series are -0.40°C over 1854-73, -0.48°C over 1874-89 and +0.17°C over 1903-40, with no correction required over 1946 to the present. During 1941-45, the required adjustments are somewhat anomalous, and differ between the hemispheres. This is presumably due to war-time observation difficulties over the oceans. A gradual change between the two levels of correction took place between 1890 and 1902. The large correction (downwards) of the MAT series differs markedly from that assumed by Folland et al. (1984).

The implied SST corrections necessary to ensure compatibility with the

MAT series are: 1854-89, +0.08°C; 1903-41, +0.49°C. No correction is required after 1945, and 1941-45 corrections are quite complex (c.f. Folland et al., 1984). As with MAT, gradual changes take place between 1890 and 1902.

How might these inhomogeneities have arisen? Jones et al. (1986c) argue that their correction to MAT in the 19th century (-0.48°C) implies that screens were either poorly exposed so that solar heating raised temperatures or, particularly in earlier times, screens were not used at all. The SST correction of +0.49°C required for readings between 1903 and 1941 is consistent with the change from uninsulated bucket measurements to engine intake readings. The value lies squarely in the range 0.3-0.7°C estimated for such a correction independently by James and Fox (1972), Barnett (1984) and Ramage (1984).

The implied corrections to SST data before 1890 and the gradual transition in the correction factor over 1890-1902 could be a combination of two factors. The change from sail to steam, which occurred most rapidly between 1890 and 1900 (Kirkaldy, 1919), means that early twentieth century readings could be cooler than those earlier because of the action of the propeller and greater keel depth. This, of course, would only be the case if the mixed layer were not isothermal, but showed a significant cooling with depth.

A more important contributing factor lies in the type of bucket used. There is considerable uncertainty regarding the types of bucket used in the nineteenth century. We can be sure that wooden buckets were the norm for at least a few decades beyond 1853, since their use was recommended at the first international meeting on marine data collection held in Brussels in 1853 (Quetelet, 1853; see also Maury, 1855). The proposed instructions to accompany the recording log were to "Haul up the water in a clean wooden bucket, place it in the shade, and, after the thermometer has remained in the bucket for two or three minutes, the thermometer should be read, the

bulb remaining immersed until the observation is completed". It is interesting to note that while the discussants at the meeting were in agreement with the sentiments of the instruction, they were also concerned that ships of different nations should be allowed to choose their own methods. It is not surprising, therefore, that the available evidence suggests that different nations used different types of bucket. Because of Maury's influence, the U.S. probably retained the use of wooden buckets for most of the century. U.K. and French ships may have switched to canvas buckets as early as the 1870s, while German and Italian ships used wooden buckets until well into the twentieth century. Krummel (1907), writing from the German perspective, refers to canvas buckets as a recent innovation. Bucket type is important because wooden buckets are considerably better insulated than their canvas counterparts and would not be affected as much by evaporative cooling.

Because of the transition from wooden to canvas buckets, we would expect a change in the SST correction factor between approximately 1870 and 1900. Unfortunately, it is impossible to pin-point the time of the transition because no firm information is available on the changes in measurement practice which must have occurred. The available history is, nevertheless, broadly consistent with the empirical result of Jones et al. (1986c) which shows a change over the period 1890-1902.

1.4 Implications of the different corrections

The major difference between the *a priori* and *a posteriori* approaches as they have been applied to date, apart from their basic assumptions, is in the implied mean hemispheric temperature levels during the nineteenth century. In Figure 1.1 we illustrate this showing the differences between the hemispheric and global mean SST values of Folland et al. (1984) and Jones et al. (1986c). These differences have two causes, differences in the basic data sets (which will be discussed further in a later section)

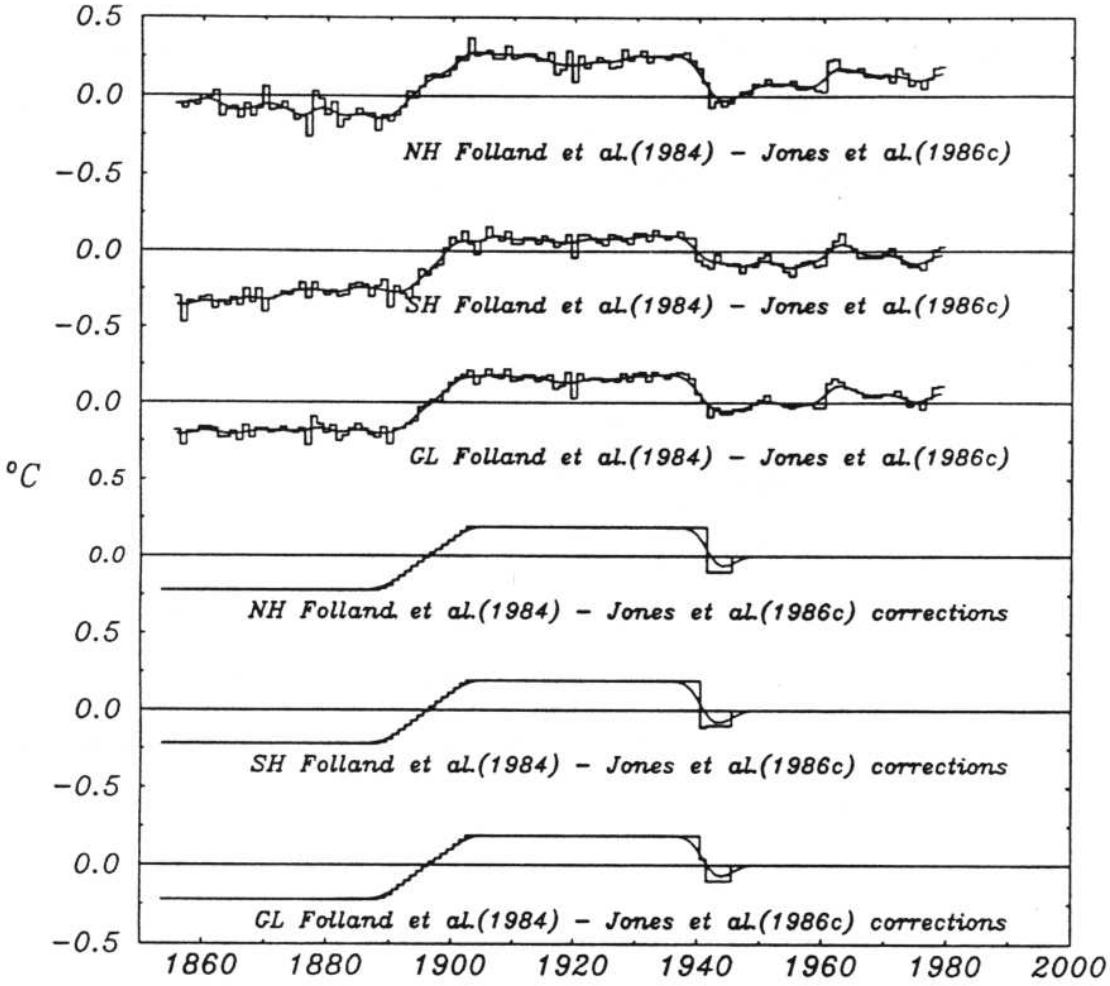

Fig. 1.1: Hemispheric and global SST UKMO-COADS using correction factors and (bottom) differences in correction factors.

and differences in the correction factors. The latter effect is shown separately in the bottom part of Figure 1.1. In Jones et al. (1986c), the nineteenth century temperature levels agree with the land-based data (this is ensured by the method), while in Folland et al. (1984) the marine temperatures are 0.2-0.3°C warmer than the land-based record. While such a difference may seem small, it represents one half of the long term warming of global-mean land-based temperatures that has occurred since 1900. Accurate knowledge of global-mean temperature changes during the middle to late nineteenth century is particularly important in estimating the natural, low frequency variability of the climate system. It is therefore important to determine which approach (if any) gives the better estimate of nineteenth century temperature fluctuations and levels.

In both their composite approach (Folland et al., 1984) and their a priori approach (Folland and Parker, 1986, 1989a,b; Bottomley et al., 1989) to the problem of correcting SST data, UKMO workers have assumed that the same measurement technique (mainly canvas buckets) was used over the whole period 1856-1941. We have suggested that this may be incorrect, largely because of the change from wooden to canvas buckets that probably occurred during the late nineteenth century. However, the information available on instrumentation is scanty, so the issue is still somewhat open. If the UKMO results are correct, then the land-based data must be incorrect in the nineteenth century. Let us consider this possibility in more detail.

Any changes in land-based temperature observation procedures in the nineteenth century would have been made at different times in different places. If these changes had affected land-based temperatures significantly, then one would expect this to show up as an inhomogeneity in the difference between the Northern and Southern Hemisphere land-based records over the last 130 years. No such difference is evident. Nevertheless, there are anomalous features in the land-based data that could point to an instrumentation problem; namely, a noticeable change in

the amplitude of the hemispheric-mean seasonal cycle for the Northern Hemisphere (but not in the Southern Hemisphere). There is, furthermore, an a priori reason to expect an inhomogeneity (of uncertain magnitude) in the land-based data, since, some time during the mid to late nineteenth century, there was a change from using Glaisher to using Stevenson Screens. Screen differences are likely to be seasonally specific. Apparent changes in the amplitude of the seasonal cycle are shown in Fig. 1.2. In the twentieth century, there are noticeable changes in the amplitude, manifest in the departures between the summer and winter curves. In the nineteenth century, these departures are greater. Is this a manifestation of natural variability in the seasonal cycle, or does it represent a basic data inhomogeneity (due, for example, to changing measurement techniques) or an inhomogeneity resulting, for example, from changes in coverage? We will address these questions in a later section.

There is one further possible explanation of the discrepancy between the marine data as corrected by UKMO workers and the Jones et al. land data, namely that both are correct and that the difference is a real change in the difference between land and marine temperature records which persisted for nearly 40 years from 1850-1890. This seems unlikely.

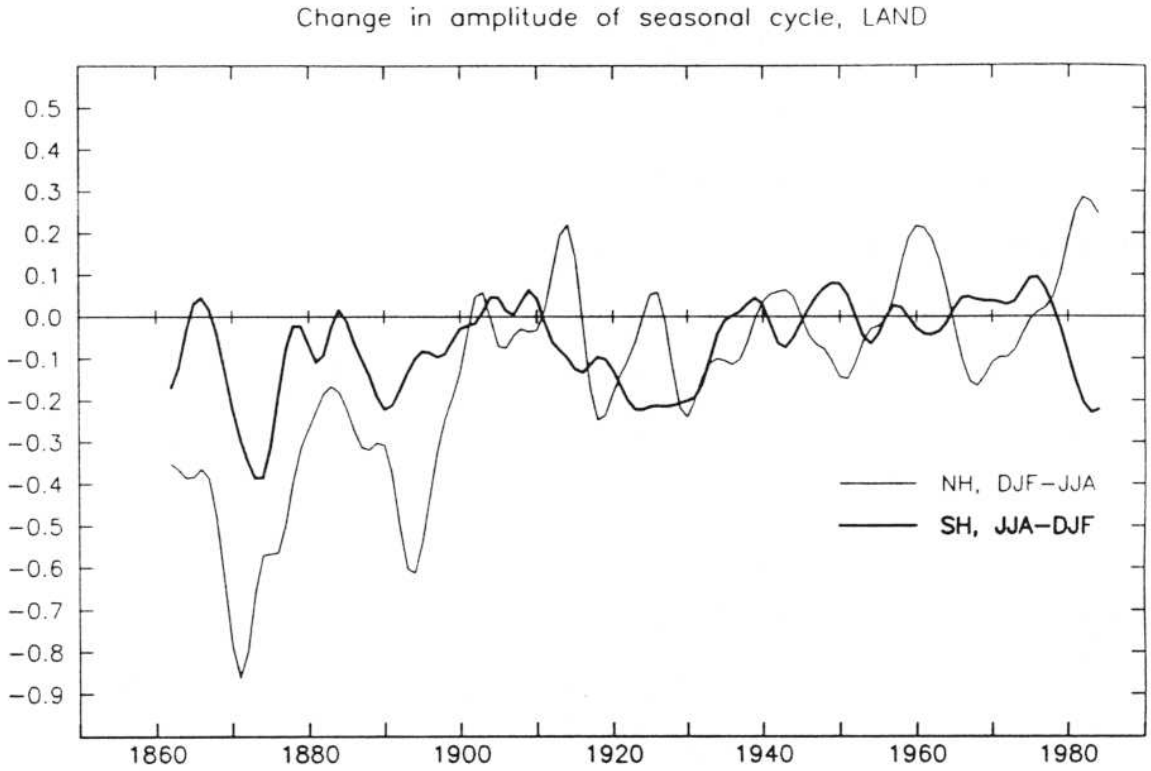

Fig. 1.2: Apparent changes in the amplitude of the seasonal cycle of land data.

2. *THE LAND-BASED DATA*

In the ensuing sections, land-based temperature series will be compared with marine data sets. We begin by discussing certain aspects of the land data set (Jones et al., 1986a,b; Jones, 1988).

2.1 Spatial representativeness of the land data

The land area represented by the two hemispheric temperature series has increased from the start of the record in the 1850s to the recent period. The percentage of the hemispheres covered can be seen in Figure 2.1. Equivalent figures for the marine data sets are given in Section 3 of this report. The change in coverage may give rise to concern as to the representativeness and homogeneity of the hemispheric averages. This issue has been investigated using a 'frozen grid' analysis (Jones et al., 1986a,b) where hemispheric-mean temperature estimates for the period 1941-80 are derived using only the grid points where data were present in the decade 1851-60, followed by identical procedures using the grids for 1861-70, 1871-80 and so on to 1931-40. We consider the Northern Hemisphere first.

Figure 2.2 shows the anomaly series (frozen grid minus full grid) for monthly-mean temperatures for grids available from decades 1851-60 to 1931-40. The greatest effects due to using an incomplete grid are for the period before 1881. This suggests that mean temperatures estimated before around 1875 are likely to incorporate twice the uncertainty of later estimates. The greatest differences occur in spring and autumn. As these differences are of opposite sign the effect of incomplete coverage on the annual mean is small. Over the whole period there is no systematic error in hemispheric-mean temperatures in any of the months April to September.

While biases in the area-averages due to coverage changes are most important, inter-annual variability values may also be biased. One would expect variability to decrease as coverage increased. Figure 2.3 gives the

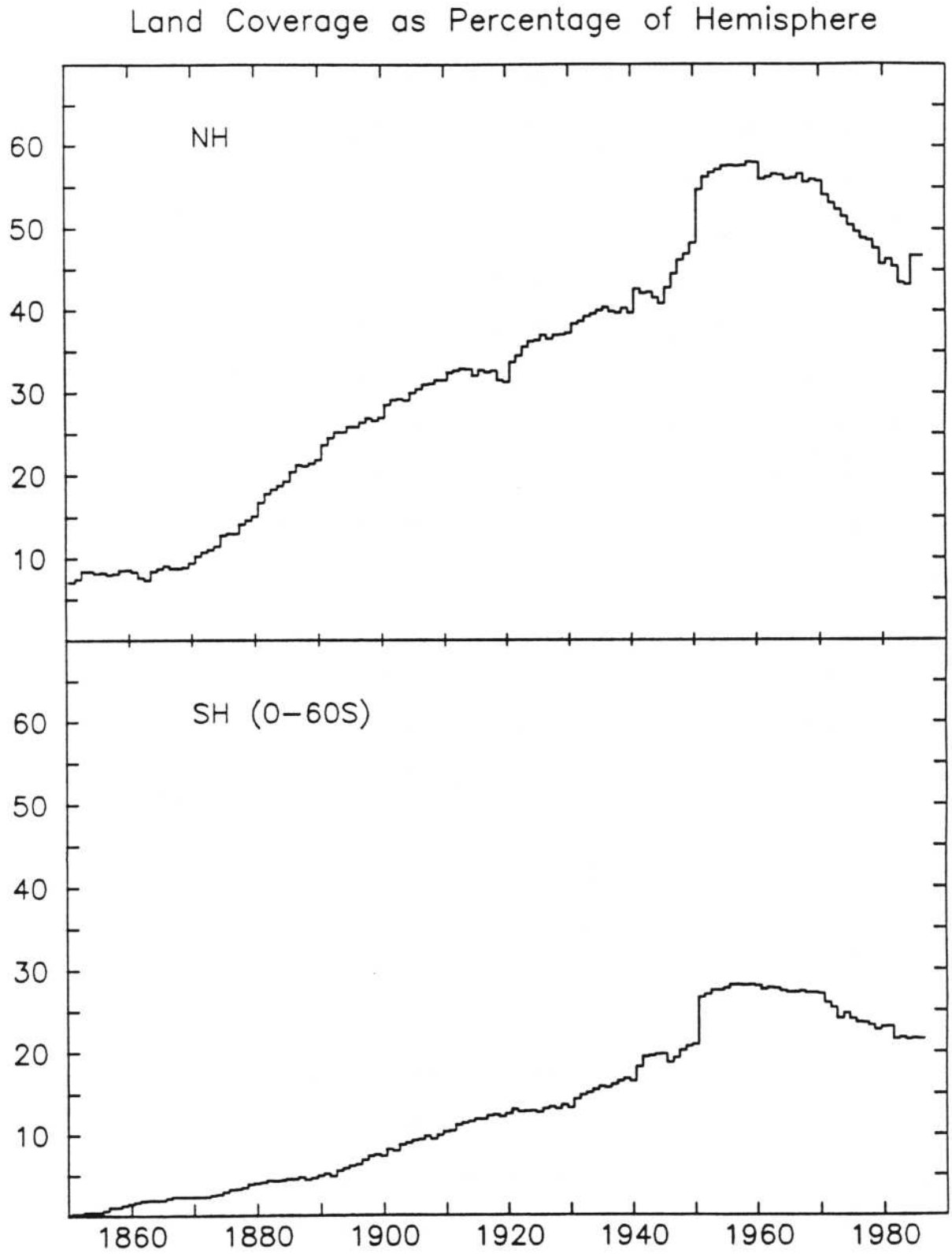

Fig. 2.1: Changes with time (1851 to 1986) in the spatial representatives, expressed as the percentage coverage for each hemisphere of the land temperature data set.

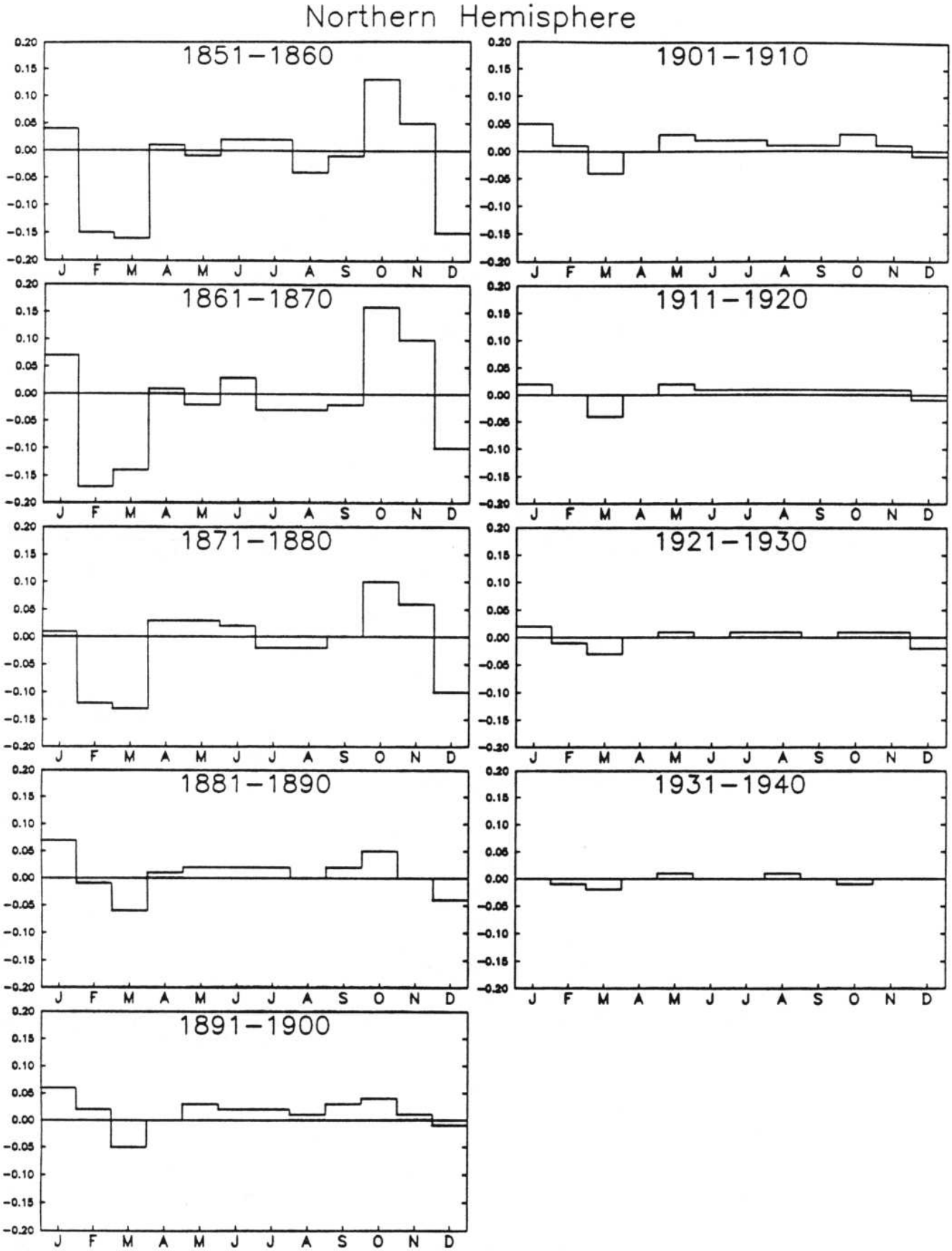

Fig. 2.2: Mean monthly anomalies (°C) for 1941-80 temperature estimates of the Northern Hemisphere using data grids present in 1851-60, 1861-70 and so on to 1931-40. Series for the decades to 1880 suggest higher uncertainty in spring and autumn in the mean estimated temperatures.

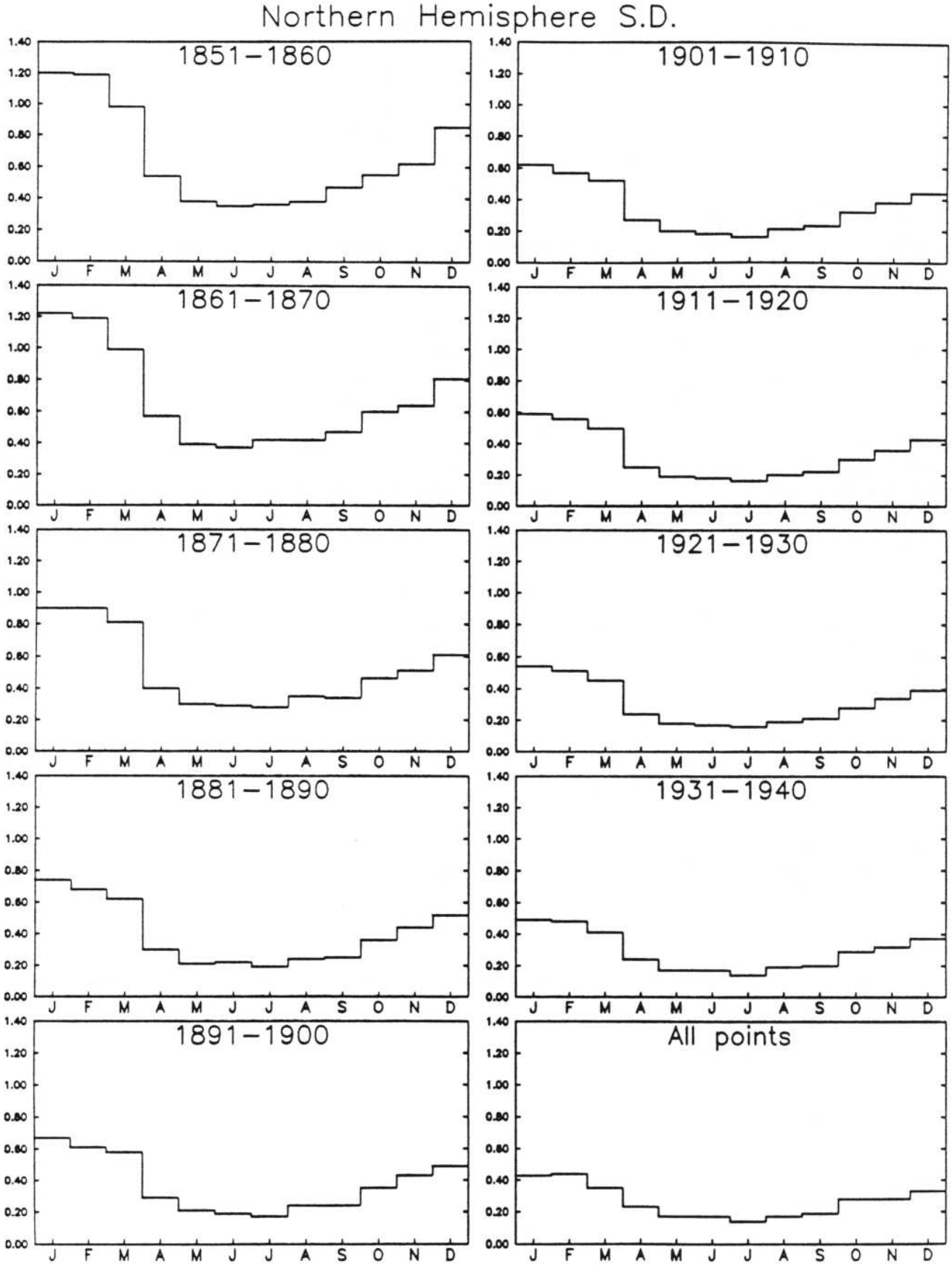

Fig. 2.3: Monthly standard deviation (°C) plots for the frozen grid analysis (Figure 2.2) where variability using the earlier grids can be compared to the full grid ('All points').

(Northern Hemisphere) standard deviations over 1941-80 for the 1851-60, 1861-70, etc., grids compared with those for the full grid (lower right corner). The summer months show the least increase (up to double for the 1851-60 grid) in variability when earlier, more sparse, grids are used. The greatest increases in variability (up to three times) come in the winter half-year. In the summer months, noticeable variability biases occur in all grids earlier than 1881, while in the winter months, the biases are clearly evident in all grids earlier than 1921.

A similar approach for the Southern Hemisphere shows smaller biases in the earlier estimates of means and standard deviations than in the Northern Hemisphere (Figures 2.4 and 2.5). For the means, there is a slight warming of hemispheric estimates when grids from the early twentieth century are used, but grids for the nineteenth century exhibit a more random spread of anomalies across the year. The standard deviations of temperatures based on earlier SH grids (Figure 2.5) show little change from using the present 'all points' grid back to about 1900. As with the Northern Hemisphere, the biggest variability biases occur in the winter months.

We can use these results to estimate the effect of coverage changes on the amplitude of the seasonal cycle. Prior to 1881, there is a Northern Hemisphere bias in winter relative to the summer of -0.07 to -0.09^{o}C, with winter temperatures relatively too cold. In the Southern Hemisphere the relative bias is negligible for 1861-70 and 1871-80, and slightly positive (i.e. winters relatively too warm) in 1881-90 and 1891-1900. The Northern Hemisphere result thus accounts for part of the winter-summer departure illustrated in Figure 1.2. Note, however, that this coverage effect does not noticeably influence annual mean temperatures; the required positive adjustment to winter temperatures prior to 1881 being largely offset by the need for a negative adjustment to autumn temperatures (see Figure 2.2).

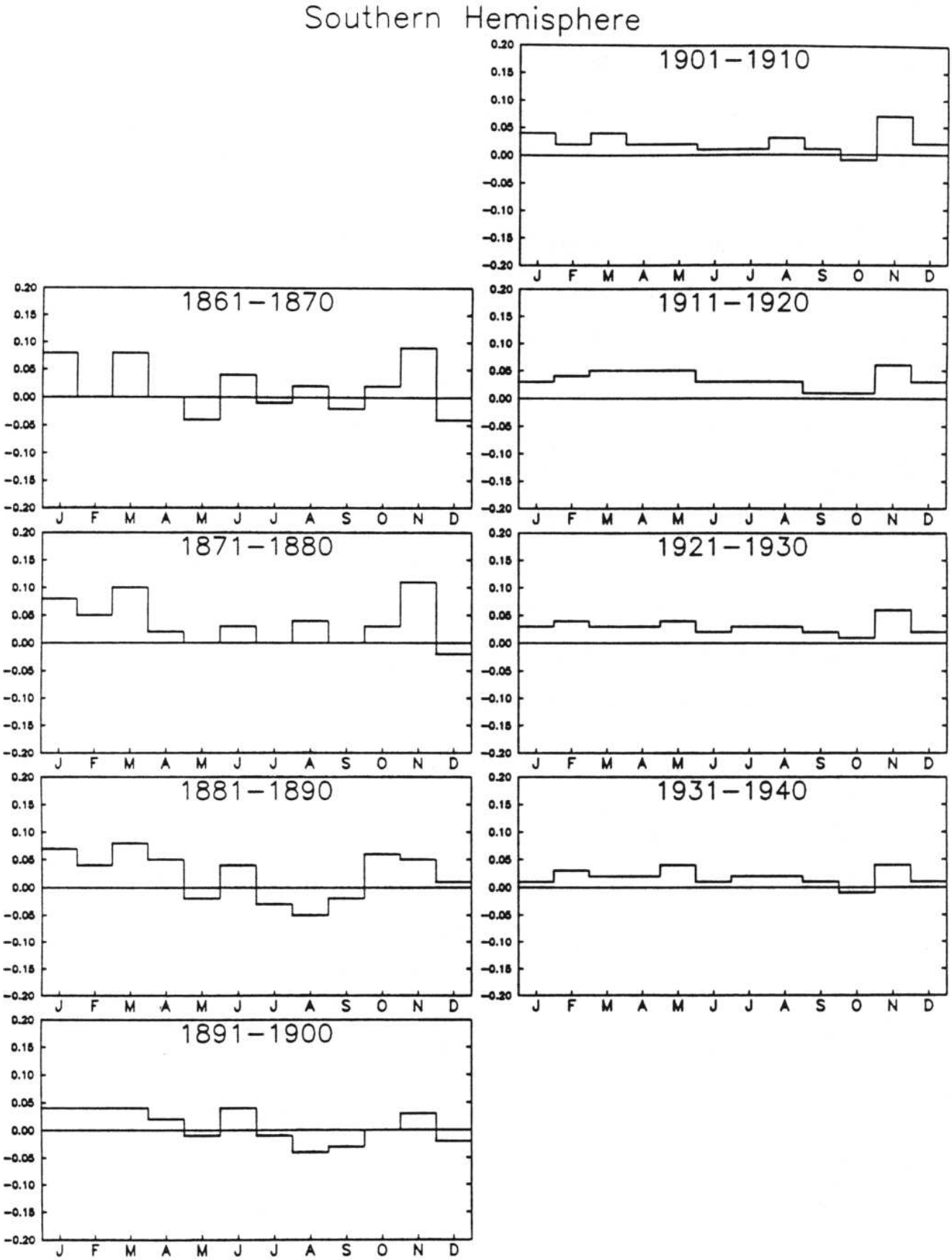

Fig. 2.4: Frozen grid analysis (°C) as in Figure 2.2 but for the Southern Hemisphere. Data are too sparse from 1851-60 to permit analysis.

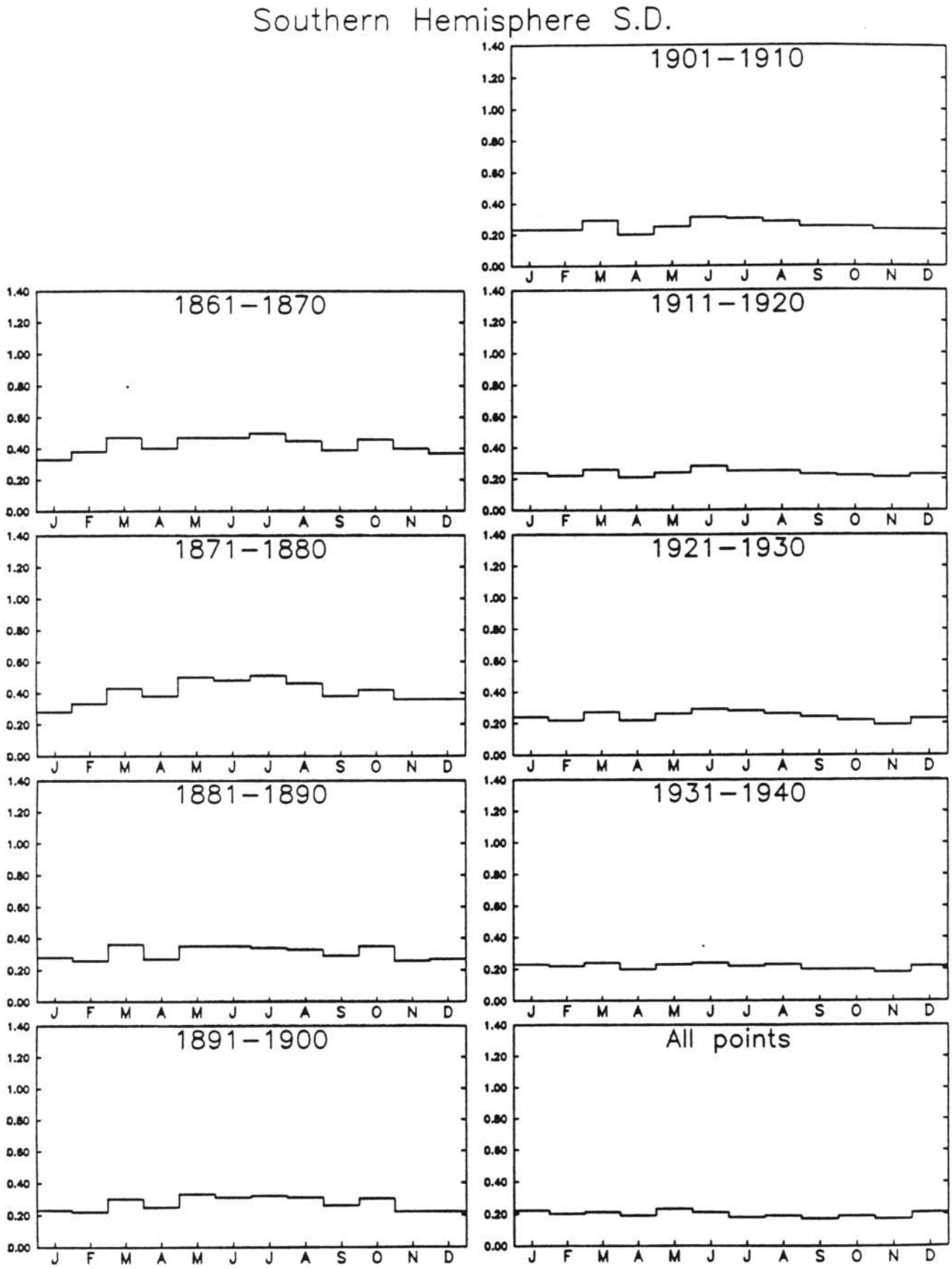

Fig. 2.5: Monthly standard deviations (°C) as in Figure 2.3 but for the Southern Hemisphere.

2.2 Temporal changes in the seasonal cycle amplitude

In the previous section we examined seasonal cycle changes in hemispheric-mean temperatures in an indirect way, and attributed some of these changes to coverage effects. Here we look at these changes directly and investigate the spatial patterns of change.

The basic data set uses 1951-70 as a reference period. Therefore, at each grid point, the mean anomaly over 1951-70 should be close to zero (identical if there are no missing data) and the mean seasonal-cycle amplitude over 1951-70 should also be close to zero. (This is indeed the case.) To study changes in the seasonal cycle amplitude, two periods were chosen, 1871-1900 and 1901-40. At each grid point where data were available, monthly means were derived for the study period being analysed. A sine curve with prescribed phase and amplitude was then fitted through the twelve monthly means, and the phase and amplitude progressively altered until a least-squares best fit was achieved. This was done for each grid point in turn. The resulting amplitudes, which represent deviations from the reference period, are plotted in Figure 2.6 for 1871-1900 and Figure 2.7 for 1901-40.

Since there is no evidence, neither from our knowledge of measurement procedures, nor empirically, to expect any noticeable inhomogeneities in the data back to 1901, the 1901-40 results should reflect the natural variability of the seasonal-cycle amplitude. These values are anomalies of 0.2-1.2^{o}C from a zero initial state (which corresponds to actual seasonal cycle amplitudes of a few to many tens of degrees Celsius). They represent, in general, quite small fractional changes. Do the results for 1871-1900 show changes which are incompatible with this natural variability? The evidence suggests not. Figure 2.8 shows the ratio, 1871-1900 amplitude divided by 1901-40 amplitude. Almost all values are in the range 1-2, with most close to unity. It is not possible to test the statistical significance of the ratios in Figure 2.8 rigorously, but values

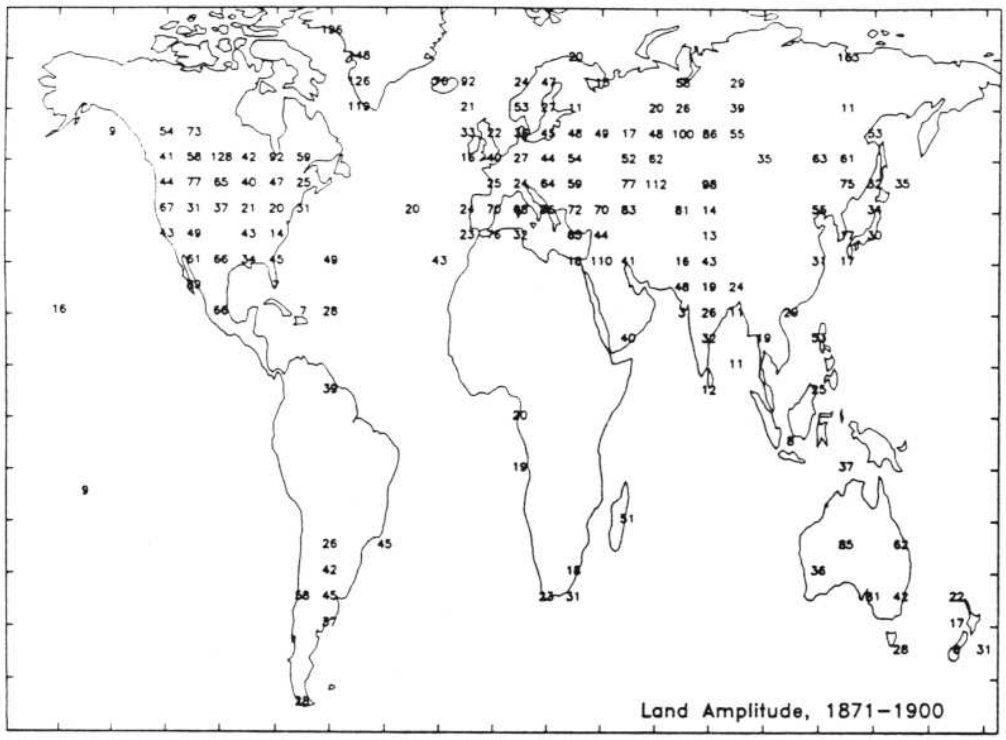

Fig. 2.6: Seasonal amplitude (°C x 0.01) in the 1871-1900 land temperature anomaly data. Anomalies are from the 1951-70 base period.

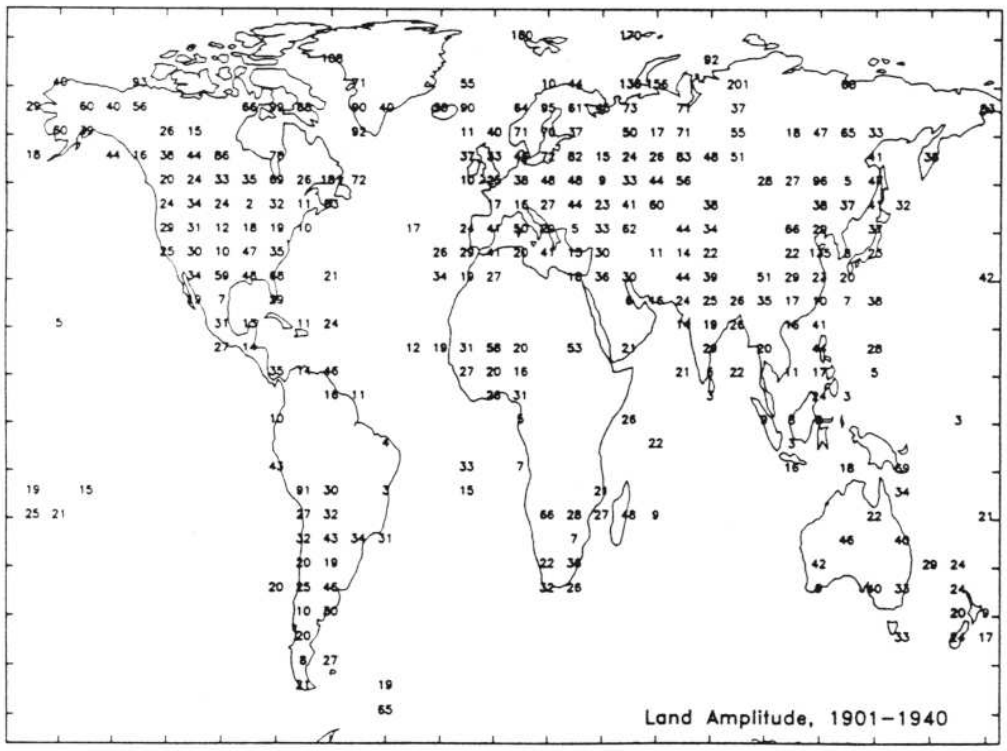

Fig. 2.7: Seasonal amplitude (°C x 0.01) in the 1901-40 land temperature anomaly data. Anomalies are from the 1951-70 base period.

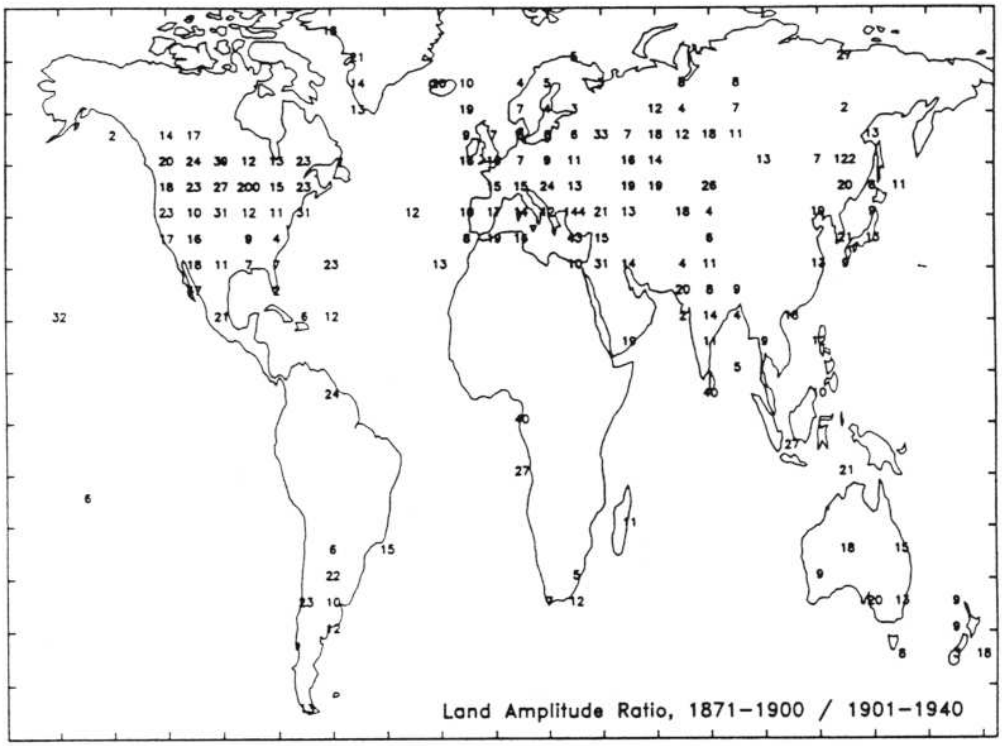

Fig. 2.8: The ratio of the two seasonal amplitudes (x10) from Figures 2.6 and 2.7, being the 1871-1900 amplitude divided by the 1901-40 amplitude.

below 2 cannot be judged unusual a priori. There is no evidence, therefore, of any significant, seasonally-specific bias in the nineteenth century land data.

3. *DESCRIPTION OF THE MARINE DATA SETS*

3.1 Introduction

In this section, we compare the UKMO and COADS marine data sets in terms of coverage and using hemispheric- and zonal-mean temperature series. These two data sets are often assumed to be essentially the same in character, but, as implied by Figure 1.1, there are some marked and important differences which will be discussed below. The discussion will focus on the UKMO Night-time Marine Air Temperature data (NMAT), the COADS marine air temperature data (MAT) and sea surface temperature data (SST) from both data sets.

3.2 Construction of the data sets

The basic raw UKMO and COADS data sets are made up of the mean SST or MAT value for each available 'square' of the ocean for each month since the beginning of recording during the 1850s. The only difference between the two data sets at this stage, apart from the greater number of raw SST observations in COADS and the rejection of day time MAT observations in UKMO, is that the box size for UKMO is 1° by 1°, while for COADS it is 2° by 2°. Because the grid box sizes are small, the coverage is 'spotty' in some regions and the number of boxes is unnecessarily large for studies of large-scale temperature fluctuations. The basic data have therefore been averaged to form monthly means and then combined to form larger boxes, $5^{o}x5^{o}$ for UKMO (Bottomley et al., 1989) and $4^{o}x10^{o}$ (SST) and $5^{o}x5^{o}$ (MAT) for COADS (Wright and Jones, 1986). (For the COADS data, the MAT observations have been gridded, as in Jones et al. (1986a,b) rather than simply averaged into boxes.)

Both data sets use very similar techniques to compress the data onto a more manageable grid. First, all small box values are reduced to anomalies from a common reference period (1951-80 for UKMO; 1950-79 for COADS). Small boxes with too few observations to form a reference-period mean or

individual monthly anomaly values are ignored. For COADS, at least nine years were required to form a reference period mean. In order to obtain a monthly-mean, only a small number of observations are required because of the high temporal autocorrelation between successive observations (Parker, 1984). Generally, only three measurements were considered sufficient for COADS (Wright and Jones, 1986) or three 5-day means for UKMO (Bottomley et al., 1989). With the COADS data, some effort was made to ensure that, if the number of observations was small, they were reasonably well distributed through the month - based on the mean day of the month for observations (see Wright and Jones, 1986). For the UKMO data, the use of at least three 5-day means largely achieves the same end. The small box values are then averaged to the larger units, with distance weighting in the COADS MAT case (cf. Jones et al., 1986a,b).

In data-sparse regions, only one small square was considered sufficient to produce a large box value. This assumption is <u>only</u> valid if anomaly values are used. Anomaly values for a $2^{o} \times 2^{o}$ (or $1^{o} \times 1^{o}$ for UKMO) square will be more representative of a larger square than the raw observations since most of the spatial variability in the latter is captured in the mean values. This technique not only optimizes coverage, but it also minimizes problems which might arise if the majority of readings came from one part of a large square, a problem which would be most acute in data-sparse regions or in regions of high temperature gradient across a $5^{o} \times 5^{o}$ or larger square (e.g. near the Gulf Stream).

3.3 Coverage

Since the 1850s, both the number of reporting ships and the areas of the oceans from which they report has altered. Changes from year to year in the number of observations and area covered, expressed as a percentage of the total hemisphere, are shown in Figures 3.1 and 3.2. Examples of the spatial variations in coverage can be seen for the UKMO SST dataset in

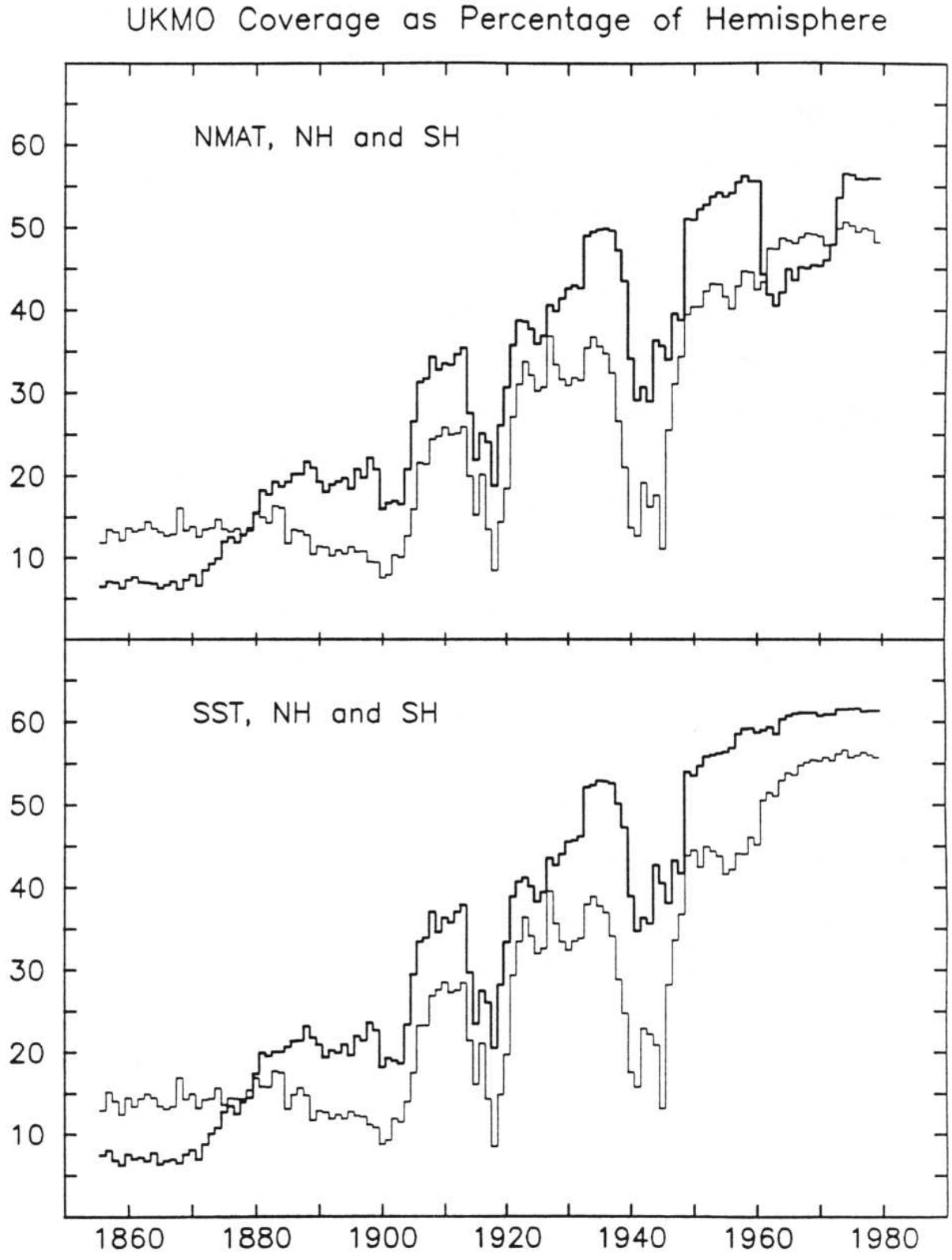

Fig. 3.1: Changes in the percentage of the hemisphere covered by UKMO NMAT (upper box) and SST (lower box) data, 1856 to 1979. Bold lines indicate Northern Hemisphere. Medium line shows Southern Hemisphere. The disparity between NMAT and SST in the 1960s is because extra SST data from another source have been included (see text for details).

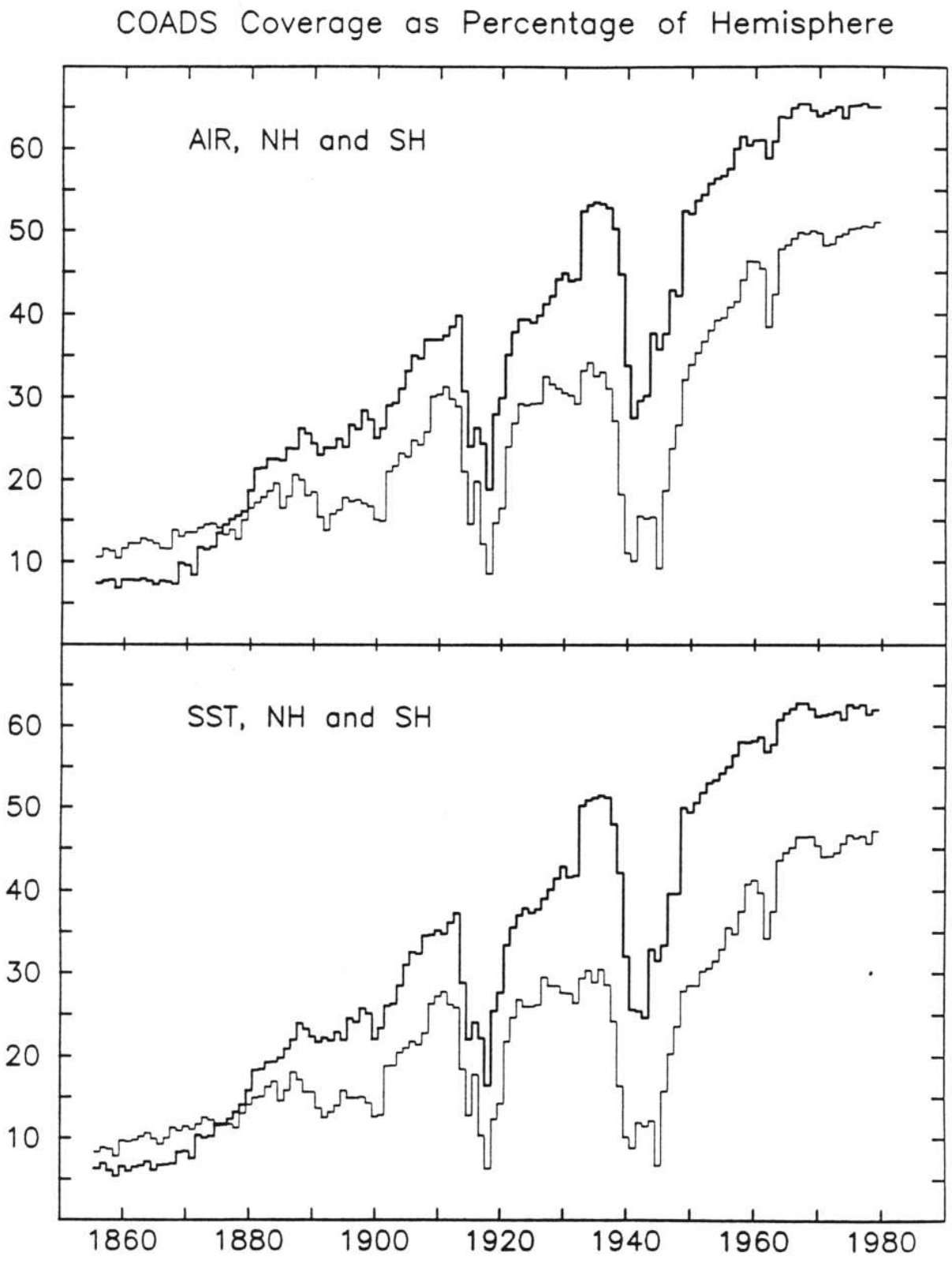

Fig. 3.2: Changes in the percentage of the hemisphere covered by COADS MAT (upper box) and SST (lower box) data. Heavy lines show Northern Hemisphere. Lighter lines show Southern Hemisphere.

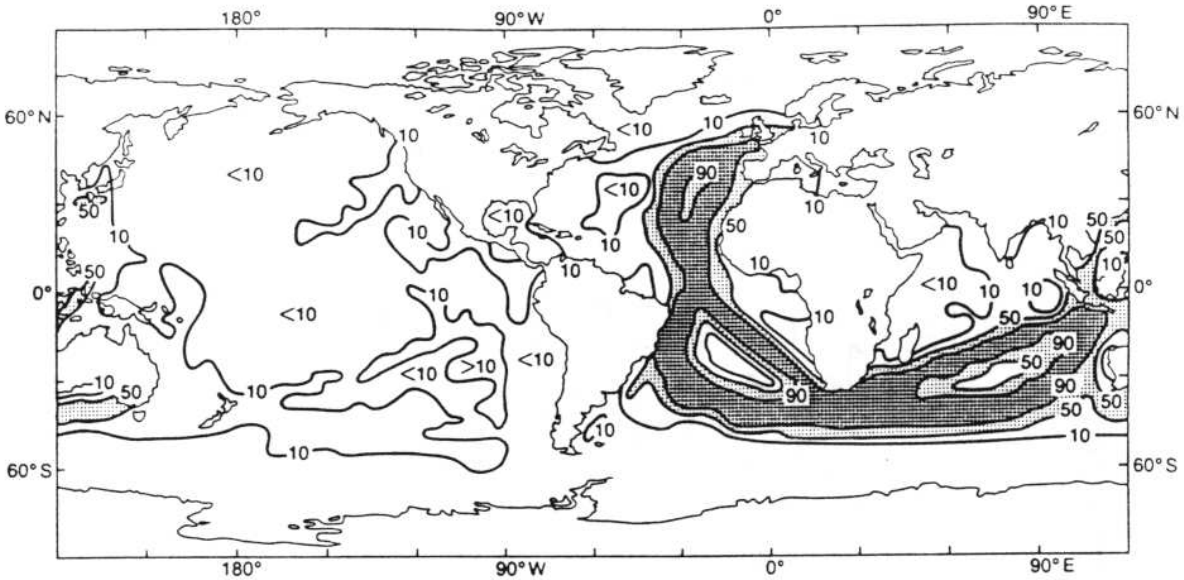

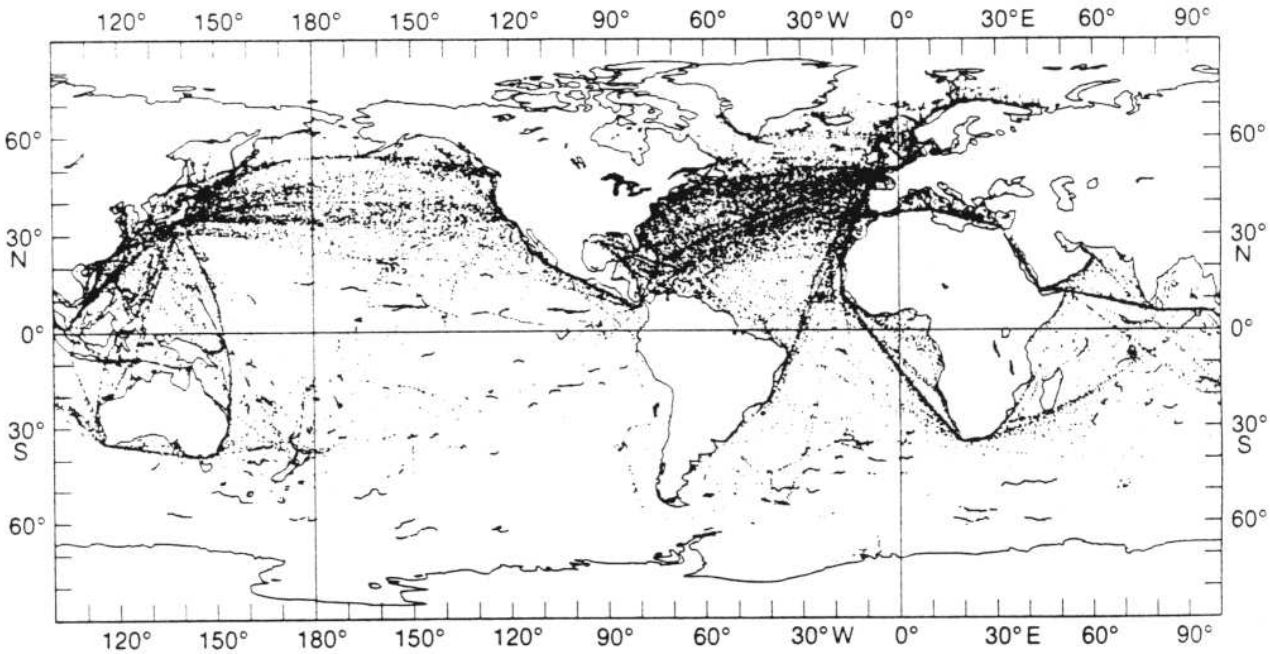

Fig. 3.3: a) Percentage of seasons with data (on a 5°x5° lat-long scale) in the UKMO SST data base for a sample decade of 1861-70. (from Bottomley et al., 1989)

b) Distribution of surface marine in situ (ship and buoy) observations received over the GTS for October 1986. Drifting buoys can be distinguished as nearly continuous wiggly lines. (From Reynolds, 1988)

Figure 3.3a (Bottomley et al., 1989), while an example of coverage for a recent month (October, 1986) is given in Figure 3.3b (Reynolds, 1988).

The main features in Figure 3.1 and 3.2 are as follows. First, after about 1880, the fractional coverage in the Northern Hemisphere always exceeds that for the Southern Hemisphere. Second, a decline in coverage in each of the two world wars can be seen in all eight time series. There is an additional drop in the NH UKMO NMAT series during the 1960s (Figure 3.1, top). This is primarily due to a lack of data for the North Pacific region. The marked difference in coverage between UKMO NMAT and UKMO SST during the 1960s is because additional SST data have been added from the Consolidated Data Set of the US Fleet Numerical Oceanography Centre (supplied by the Massachusetts Institute of Technology; Bottomley et al., 1989). Other than these periods of reduced coverage, the general picture for coverage of the NH is one of steady increase since the 1850s. In the SH, the steady increase did not start until around 1900.

3.4 Spatial representativeness of the COADS data

The effect of changes in coverage can be assessed using the frozen grid approach employed by Jones et al. (1986a,b) with the land data. But first we describe the spatial variations in coverage in more detail.

For each grid point in both COADS data sets, the first decade during which it had at least 40% of the monthly values was identified. These first decades for MAT are shown in Figure 3.4. The first decades for SST (Figure 3.5) differ little from those for MAT. There is one major area, the high southern latitudes, where there are never enough data to meet the 40% criterion. Smaller data-sparse areas also occur in the tropics. Shea (1986) shows similar data-poor regions in the tropics and high-latitude regions, but overall coverage shown by Shea is less because he considered raw rather than anomaly data (see above). Coverage changes are not always in a positive direction. For example, coverage is reduced almost

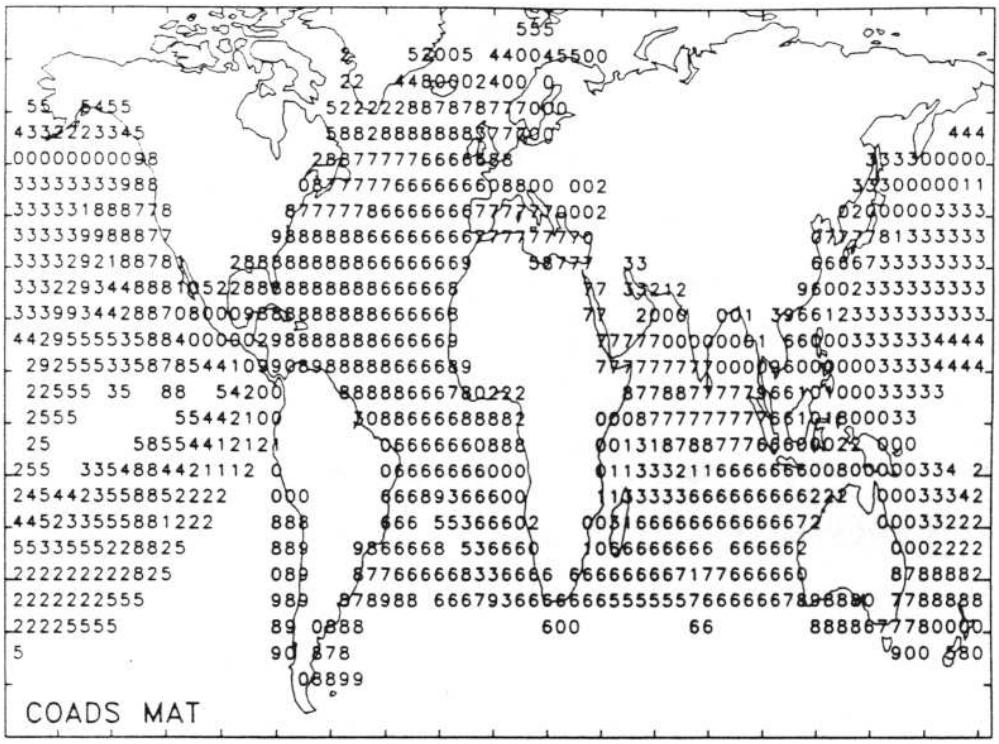

Fig. 3.4: First decade when at least 40% of the monthly values in the COADS MAT data base are present. A '6' indicates 1860s, '7' for 1870s and so on through to '5' for 1950s.

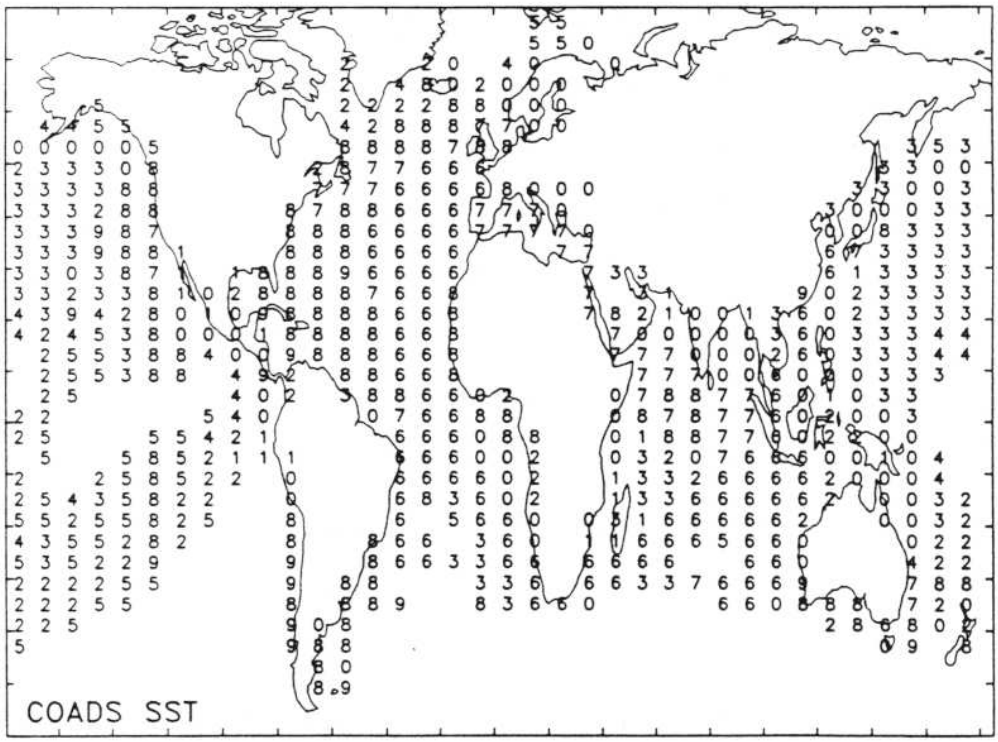

Fig. 3.5: First decade when at least 40% of the monthly values in the COADS SST data base are present. Numbers as for Figure 3.4.

everywhere during the years 1917-18 and 1942-45. The effects of the opening and closing of shipping routes can be seen in Figures 3.4 and 3.5, especially the routes from Europe to the Far East and Australia. The opening of the Suez Canal can be pin-pointed from coverage changes to around 1870 (it opened in 1869).

On a priori grounds, one might expect that a relatively small number of regularly spaced data points could give reliable estimates of hemispheric mean MAT and SST, because of the long spatial correlation decay length over oceanic areas. (The temporal analogue of this has already been exploited in obtaining the gridded data.) Spatial correlation would be a more useful property if the data-poor regions were small and numerous, but it can be seen from Figures 3.4 and 3.5 that the spatial gaps are simply too large to be filled in by extrapolation. Consequently, in many of the early years the hemispheric means in the Southern Hemisphere are based primarily on Atlantic data. Even today, there are large gaps in the Southern Hemisphere where no ocean information is available.

In order to assess the representativeness of the coverage available during the early decades relative to the best coverage, area average estimates for the years 1946-79 were made using the grids available for decades 1861-70, 1871-80, etc., up to 1941-50. The period 1946-79 has been chosen because it has near-optimum coverage and because no corrections are necessary to homogenize the COADS data. The results of this frozen grid analysis for annual data are given in Table 3.1. In both hemispheres and for both marine variables, the effect of coverage changes on the decadal-mean, area-average temperatures is small, with "errors" always 0.02°C or less.

It is, however, possible that these small annual differences obscure more marked month-to-month variations, as for the land data in the early decades of the record. Figures 3.6 to 3.13 show that this is not the case. These figures for MAT (Figures 3.6 to 3.9) and SST (Figures 3.10 to 3.13)

Table 3.1: Comparison of the difference between the decadally-reduced and full grids and the standard deviation of all grids: Annual data, 1946-79.

	NHMAT		NHSST		SHMAT		SHSST	
	Mean	SD	Mean	SD	Mean	SD	Mean	SD
1861-70	-0.01	0.16	0.01	0.16	0.01	0.16	0.02	0.17
1871-80	-0.01	0.13	0.00	0.14	0.00	0.16	0.02	0.17
1881-90	-0.01	0.13	0.00	0.14	0.00	0.16	0.00	0.16
1891-1900	-0.01	0.12	-0.01	0.13	-0.01	0.16	0.00	0.17
1901-10	-0.01	0.11	0.00	0.13	0.00	0.14	0.00	0.16
1911-20	-0.01	0.12	0.00	0.13	0.00	0.16	-0.01	0.17
1921-30	-0.01	0.11	-0.01	0.13	0.00	0.14	0.00	0.14
1931-40	0.00	0.11	0.00	0.12	0.00	0.14	0.00	0.16
1941-50	0.00	0.11	0.00	0.12	0.00	0.14	0.01	0.15
Time varying		0.11		0.12		0.15		0.15

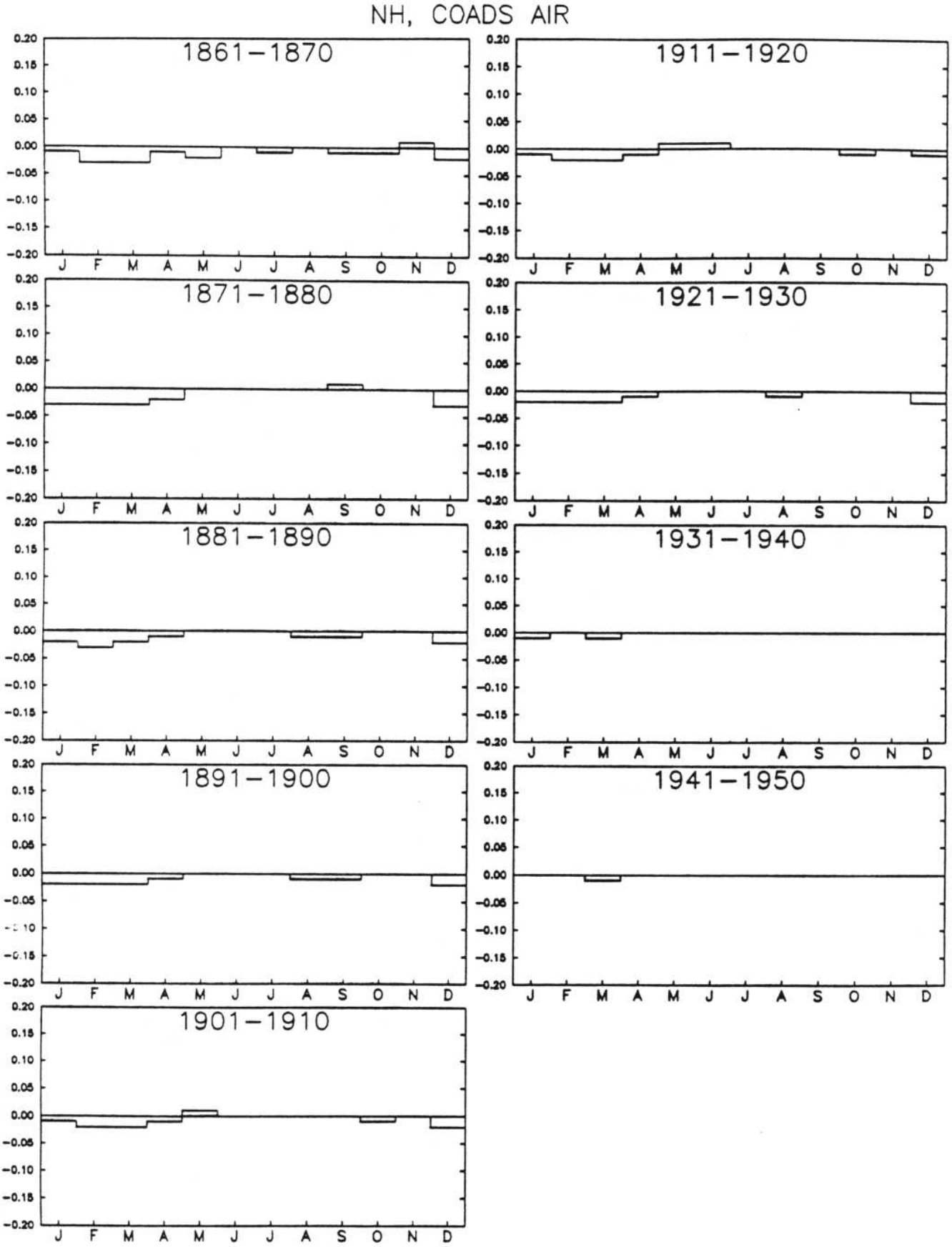

Fig. 3.6: Frozen grid analysis for NH COADS MAT. Values are mean monthly anomalies for 1946-79 based on grids available in 1861-70, 1871-80 and so on.

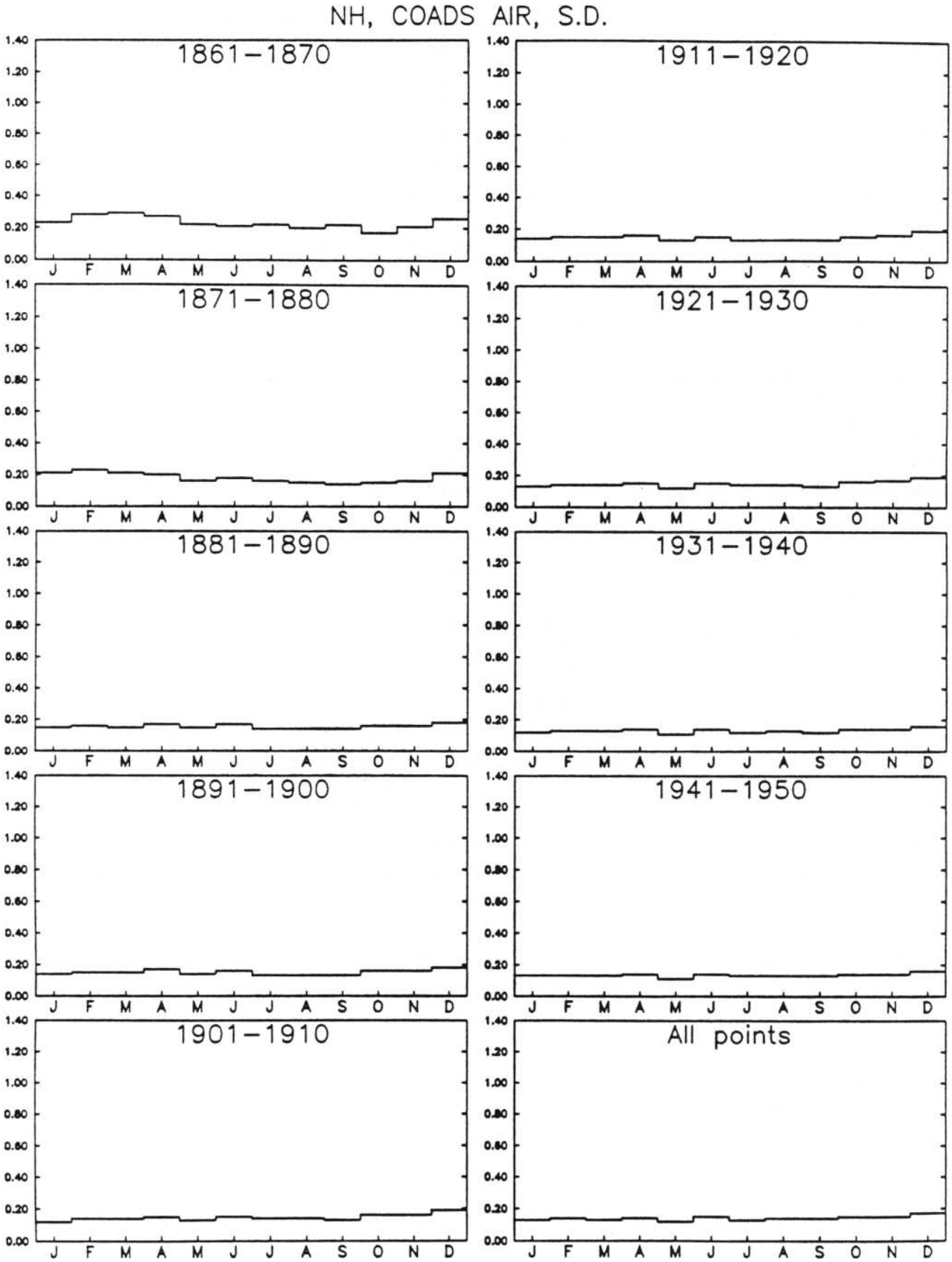

Fig. 3.7: Standard deviations of NH COADS MAT decadal frozen grids with comparison to that calculated over the full period of 1946-79 ('All points').

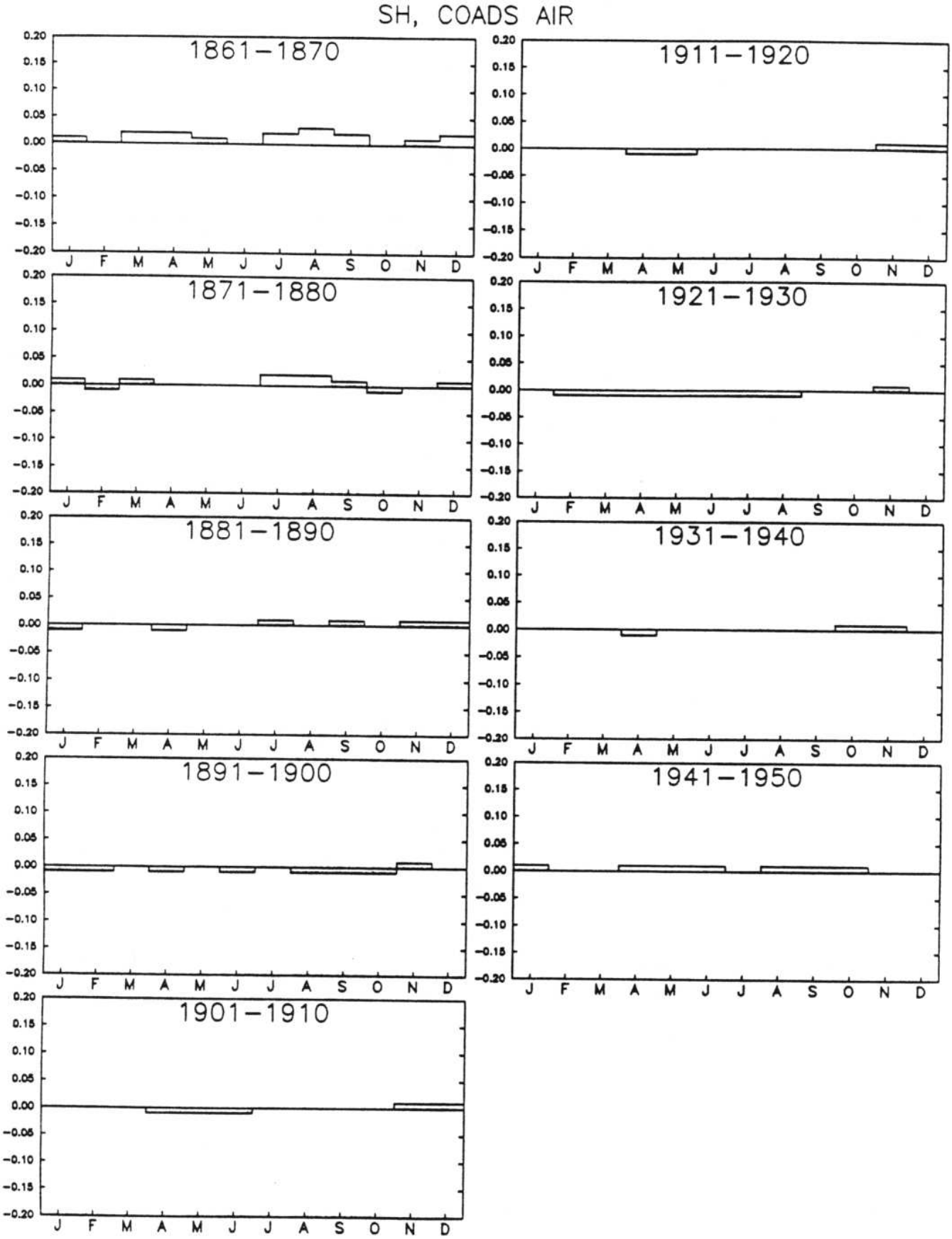

Fig. 3.8: Frozen grid analysis for SH COADS MAT. Values are mean monthly anomalies for 1946-79 based on grids available in 1861-70, 1871-80 and so on.

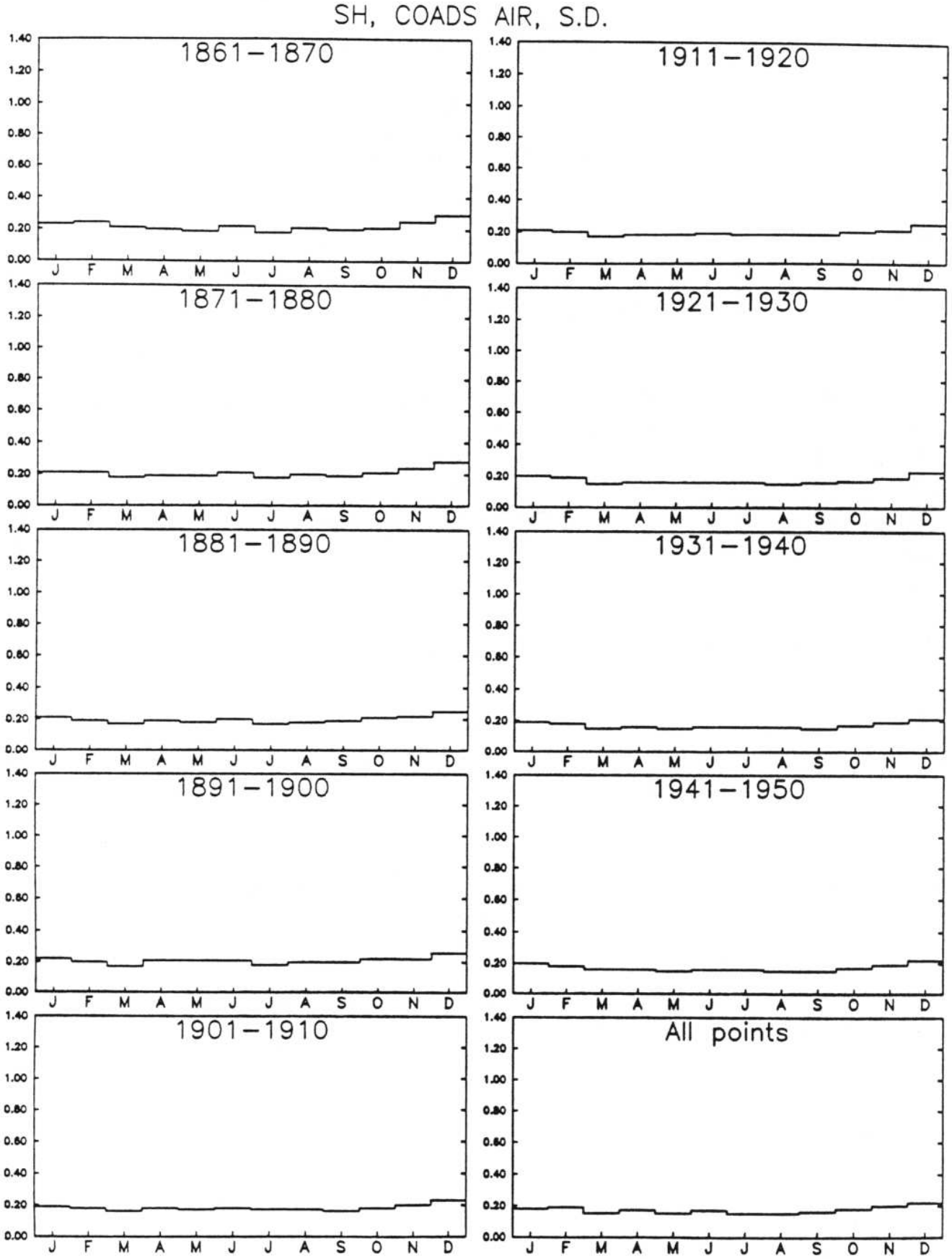

Fig. 3.9: Standard deviations of SH COADS MAT decadal frozen grids.

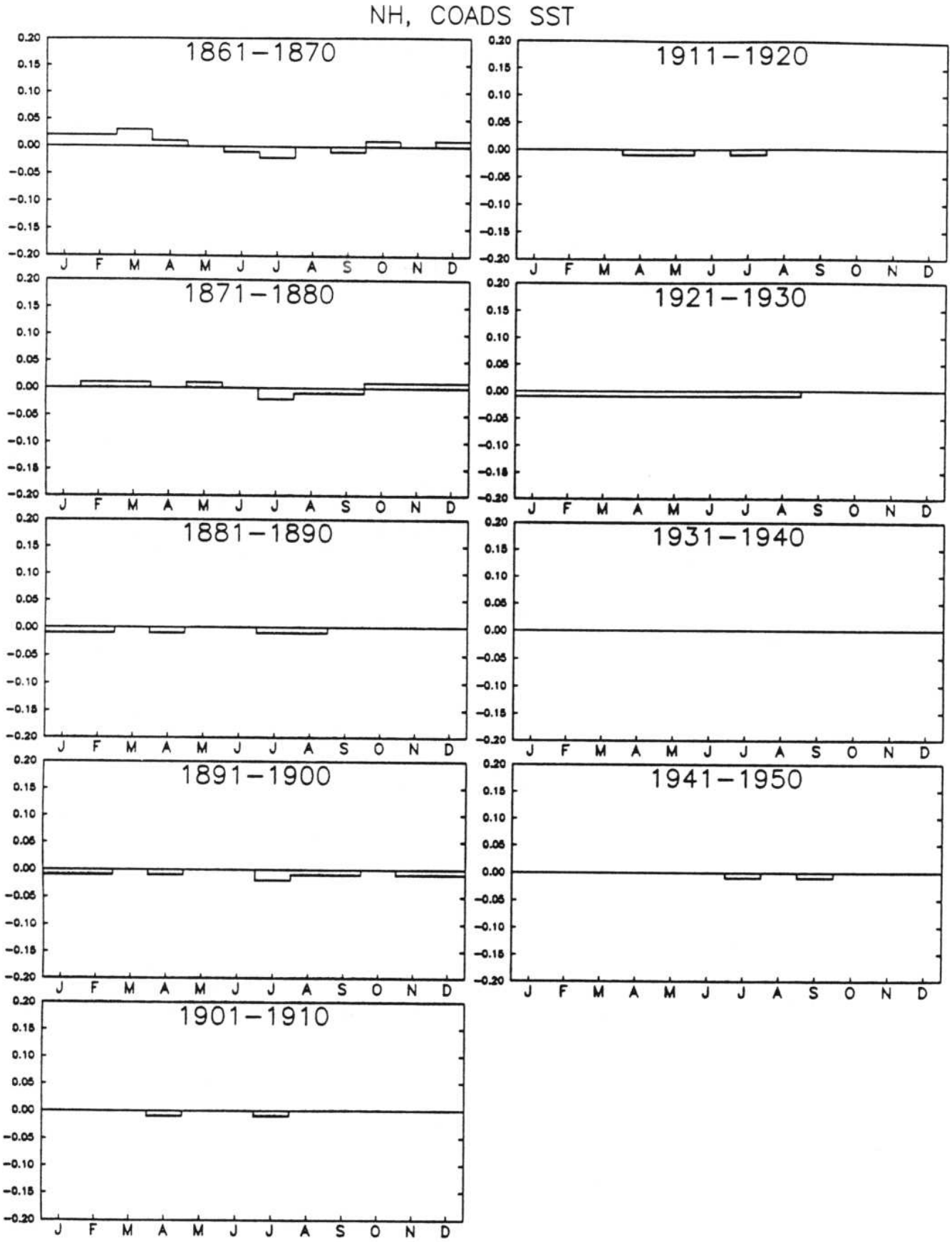

Fig. 3.10: Frozen grid analysis for NH COADS SST. Values are mean monthly anomalies for 1946-79 based on grids available in 1861-70, 1871-80 and so on.

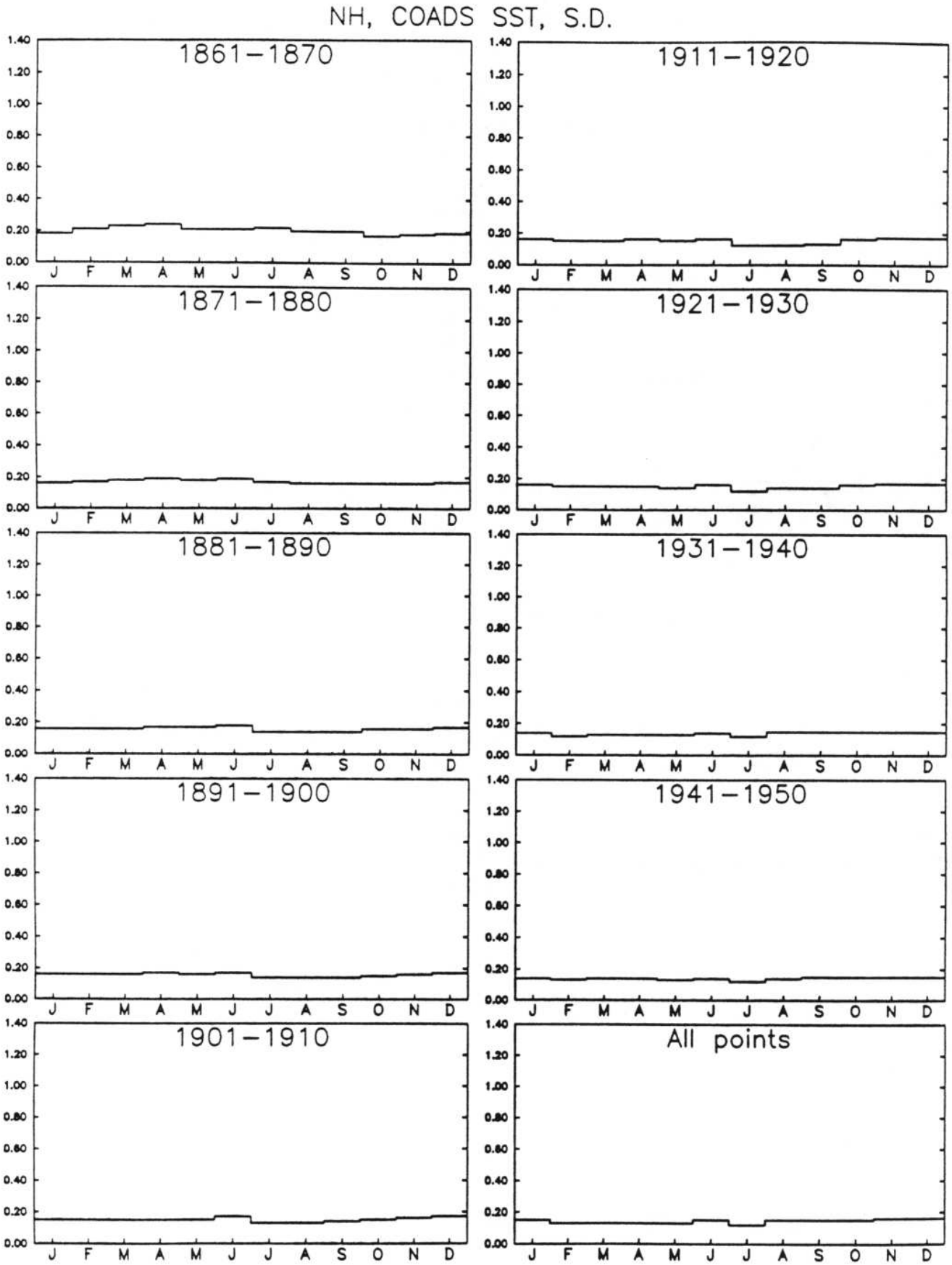

Fig. 3.11: Standard deviations of NH COADS SST decadal frozen grids.

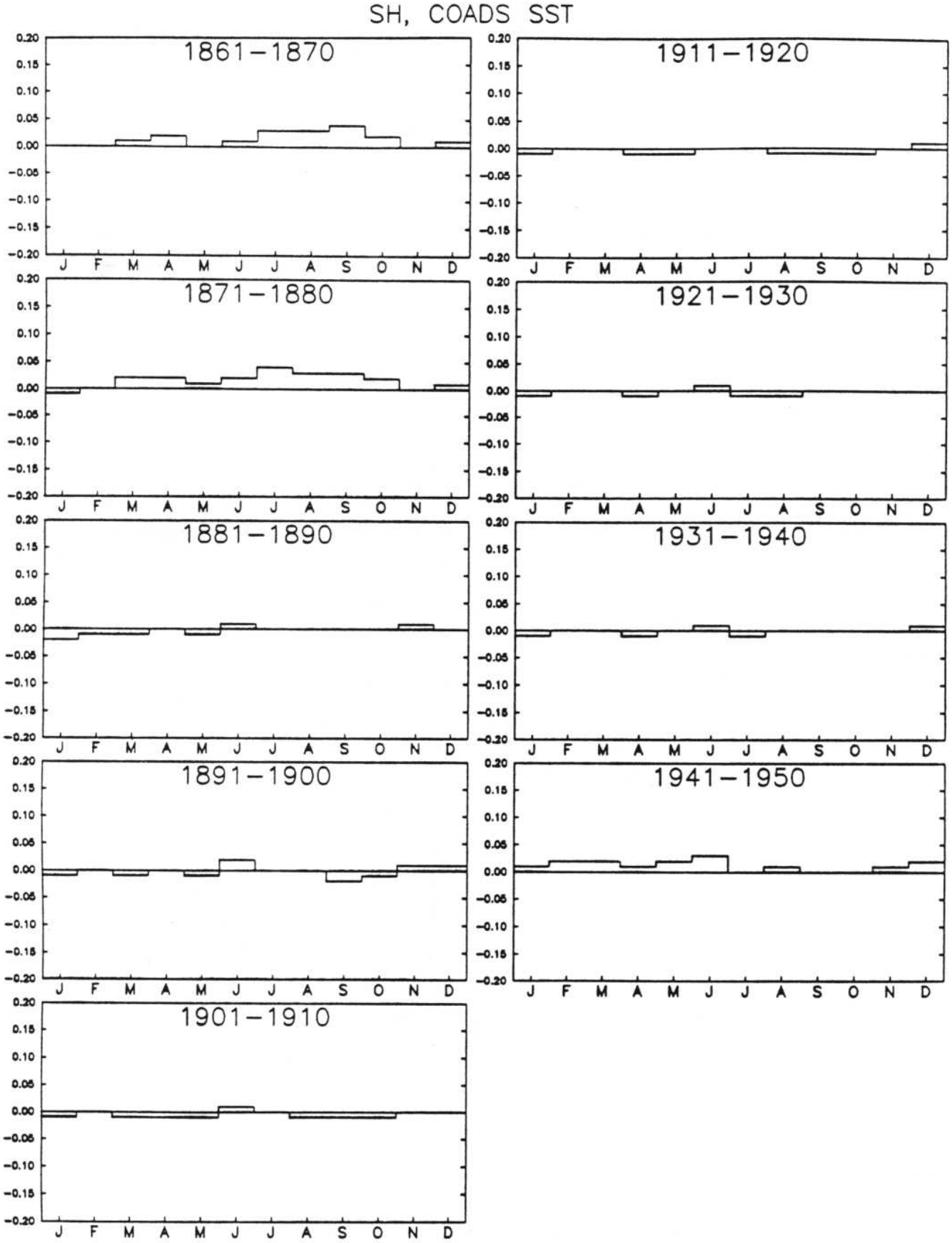

Fig. 3.12: Frozen grid analysis for SH COADS SST. Values are mean monthly anomalies for 1946-79 based on grids available in 1861-70, 1871-80 and so on.

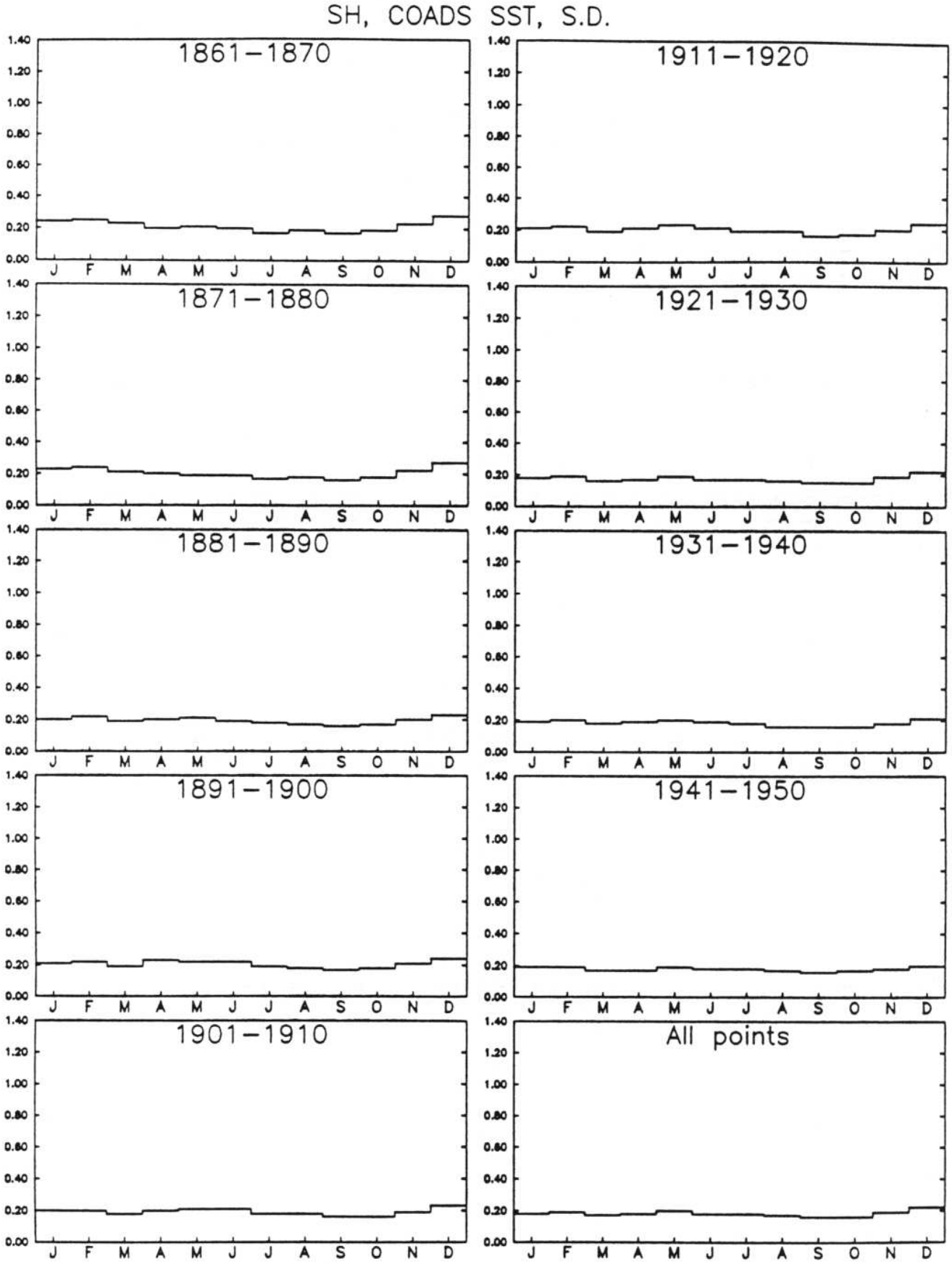

Fig. 3.13: Standard deviations of SH COADS SST decadal frozen grids.

are directly comparable with those based on land data (Figures 2.2 to 2.5). The area-averages of the marine data show no marked variations due to coverage changes, the maximum error in any one month being less than 0.05°C. Even the changes in inter-annual standard deviation of the monthly means due to coverage changes are small. These results for COADS confirm and complement those of Parker (1987) who found that estimates of trends of "global" and "hemispheric" mean NMAT and SST values were insensitive to the changes in geographical coverage that have occurred since 1860 in the UKMO data set.

3.5 Air temperature series: COADS/UKMO comparison

3.5.1 Hemispheric means

Figure 3.14 shows the hemispheric-mean UKMO NMAT values from 1856 to 1986 based on the raw data. Values are expressed as anomalies from the mean of the period 1951-80. Similar curves for COADS MAT are presented in Figure 3.15. The base period for COADS is 1950-79, a difference from UKMO which is of no practical significance.

Since the series in Figures 3.14 and 3.15 are based on the raw, uncorrected UKMO and COADS data, they contain trends and other features that result from both climatic and non-climatic influences. Most notable are the marked decline in temperatures between 1880 and 1910 and the warm peak in the early 1940s. The former almost certainly has a strong non-climatic component. The latter is largely non-climatic, although part of the apparent warmth of the early 1940s was related to the very strong El Niño/Southern Oscillation (ENSO) event in 1940-41. For comparison, note the warm peak in 1877-78 compared to the mean value for the 1870s and 1880s, a warming largely attributable to an exceptionally strong ENSO event.

Although both the UKMO and the COADS series are based on similar, overlapping data sources, there are important differences that are not

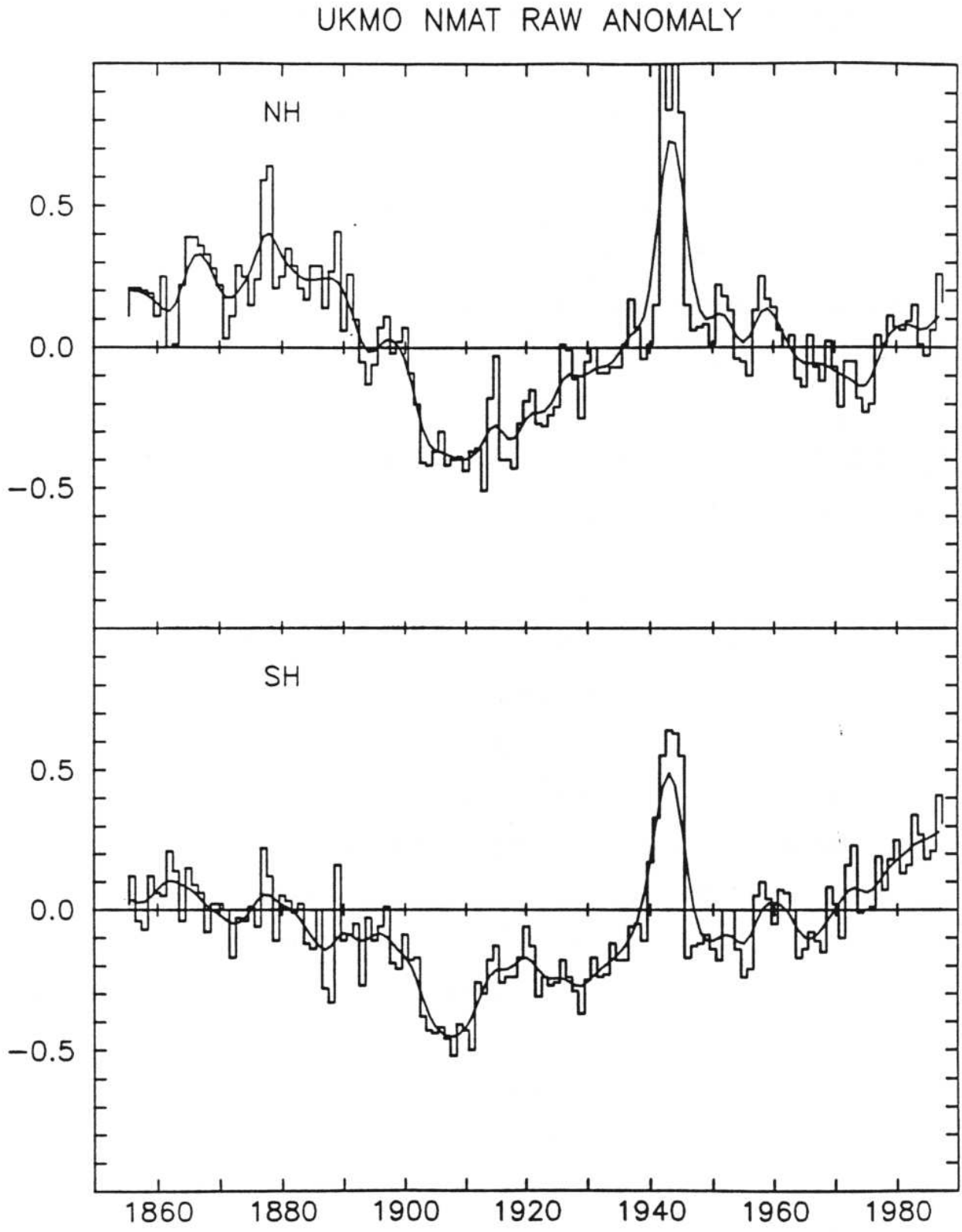

Fig. 3.14: Hemispheric annual time series of the raw UKMO NMAT data expressed as anomalies from the 1951-80 base period.

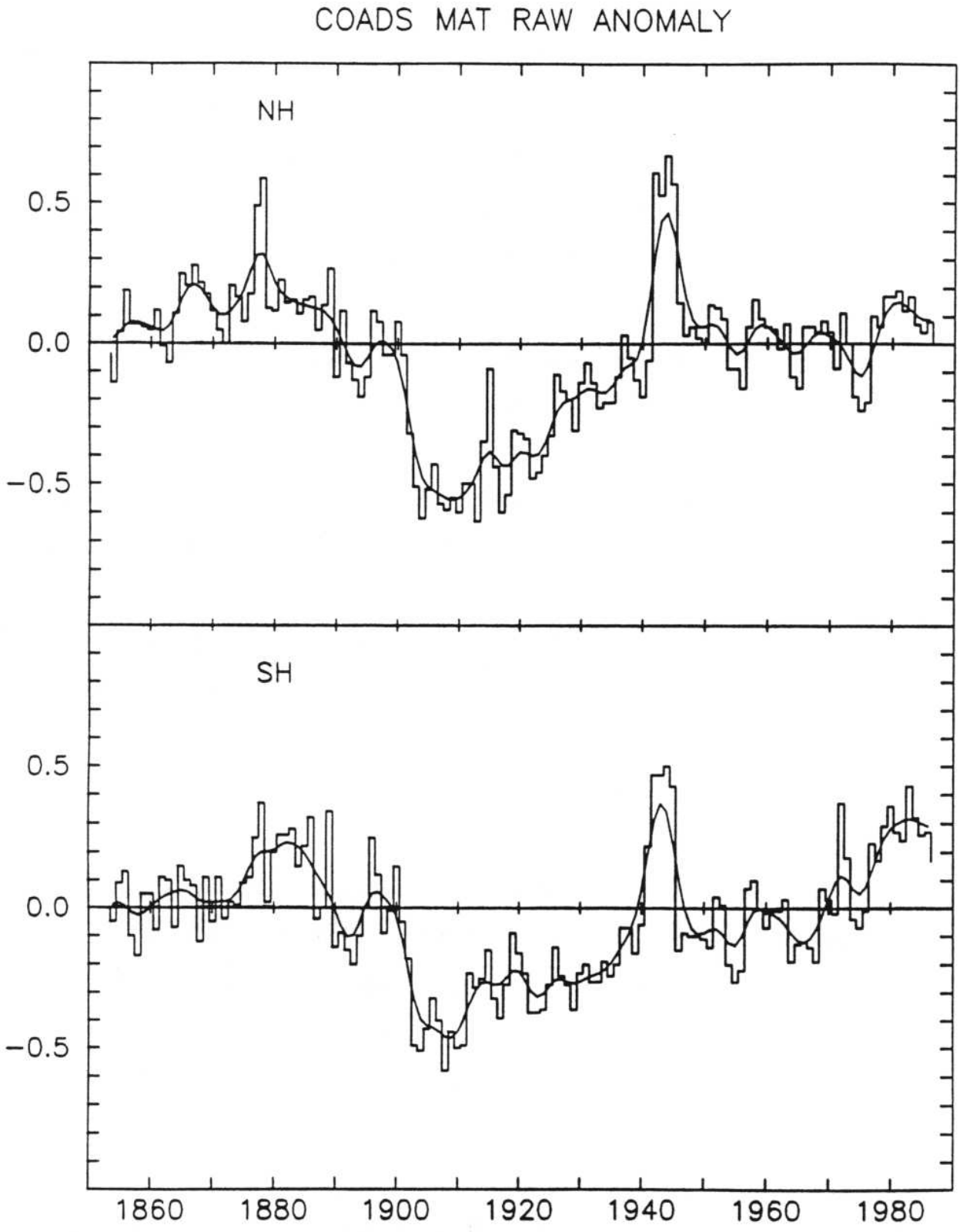

Fig. 3.15: Hemispheric annual time series of the raw COADS MAT data expressed as anomalies from the 1950-79 base period.

generally realized. To illustrate these differences, Figure 3.16 presents the difference (UKMO NMAT minus COADS MAT) on the hemispheric scale. For the NH, UKMO is consistently warmer than COADS by about 0.10-0.15°C up to 1940. Over the post-1950 period, UKMO is about 0.05°C warmer than COADS to 1960 and then generally cooler (by around 0.05-0.10°C) from 1961 to 1985.

The Southern Hemisphere shows a much more unusual pattern. From 1870 to 1890, UKMO becomes progressively cooler relative to COADS. After a warming of UKMO relative to COADS in the late 1880s, there is a second cooling excursion in the 1890s. Subsequently, the mean UKMO-COADS difference is near zero, but there are noticeable decadal and longer time scale excursions. In particular, UKMO cools by around 0.2°C relative to COADS over 1940-1980. For the individual series (Figures 3.14 and 3.15), UKMO NMAT for SH shows a general declining trend from 1856 to around 1910. COADS shows no trend over 1854-1900, followed by an almost step function cooling in the early 1900s. This change (spanning 1900-1904) is common to both UKMO and COADS air temperature data and is evident in both hemispheres. It is also apparent in the four SST series (Figures 3.25 and 3.26).

The differences in the raw data shown in Figure 3.16 may be partly attributable to the fact that the COADS data include day and night observations, whereas the UKMO are night-time only. This should be a relatively small effect because the data are anomalies rather than actual temperature values. However, differences may arise if the bias in either the day or night MAT observations varied with time (e.g. due to changing ship characteristics or observation practices), or if the mix of day and night temperatures in COADS varied with time, and/or if the UKMO NMAT data were contaminated with varying amounts of day-time data. The fact that the two data sets have different coverage (c.f. Figures 3.1 and 3.2) must also influence the area-averages, but, on the basis of the frozen grid analyses presented above, this should also be a relatively small effect. The

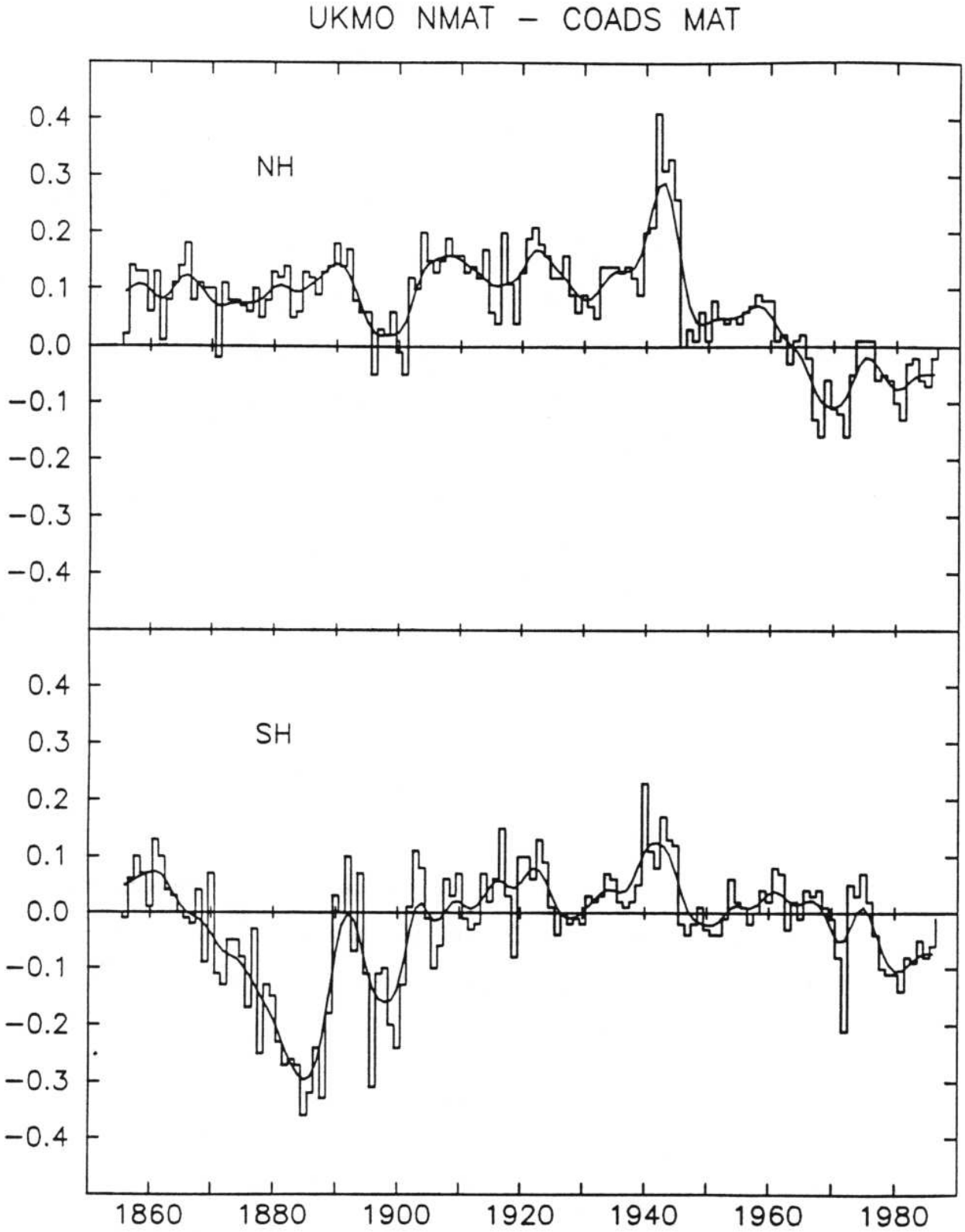

Fig. 3.16: Hemispheric, annual time series of UKMO NMAT minus COADS MAT using anomaly data. The marked differences are discussed in the text.

differences represent an important, and unexpected source of uncertainty in our knowledge of global-scale air temperature changes.

3.5.2 Zonal means

To obtain further insights, we now investigate the hemispheric UKMO-minus-COADS air temperature differences at the zonal scale. It would be possible to look at smaller scales, but, as the averaging-area decreases, inter-annual variability increases and masks the longer time scale fluctuations under study. Figure 3.17 gives zonal-mean series for annual UKMO NMAT minus annual COADS MAT for 1856-1986. The data shown are area-averages for ten degree latitude zones, 70-60°N, 60-50°N, and so on down to 40-50°S. For UKMO, the averages were obtained by averaging data from two 5° bands, e.g. 60-65°N and 65-70°N. For COADS, since the data are gridded on a 5° spacing rather than boxed, three bands were averaged, extending 2.5° latitude on each side of the UKMO zone.

Figure 3.16 (hemispheric data) shows UKMO to be around 0.1°C warmer than COADS for the Northern Hemisphere from the 1850s to 1940. Figure 3.17 (zonal data) shows that the effect is strongest, at around 0.2°C, over the mid-latitude zones of 10-40°N. The nineteenth century relative cooling feature in the Southern Hemisphere shown in Figure 3.16 is most prominent in the region 10-40°S. A further breakdown of Figure 3.17 into simple three-month seasonal series (Figures 3.18 to 3.21), shows the NH feature to be slightly weaker in April to June and the SH feature to be of roughly equal strength in all four seasons.

3.5.3 Land-marine comparison

Comparisons between land and marine data sets, to identify systematic differences, have been carried out using the Jones et al. land data and the COADS MAT data in Jones et al. (1986c). Figure 3.22 (from that work) shows the temperature difference between coastal land values and uncorrected

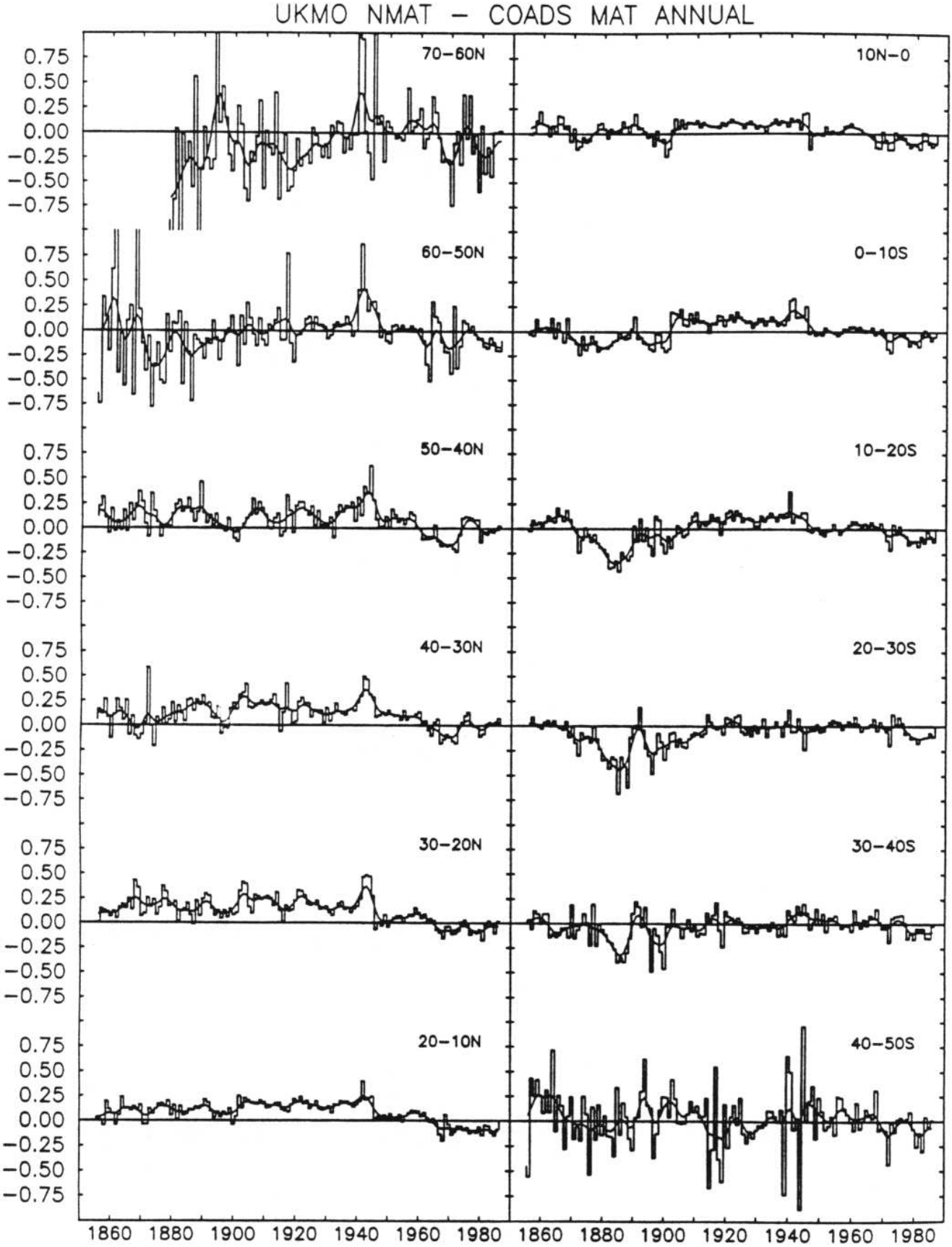

Fig. 3.17: Zonal (10° latitude band), annual time series of UKMO NMAT minus COADS MAT using anomaly data.

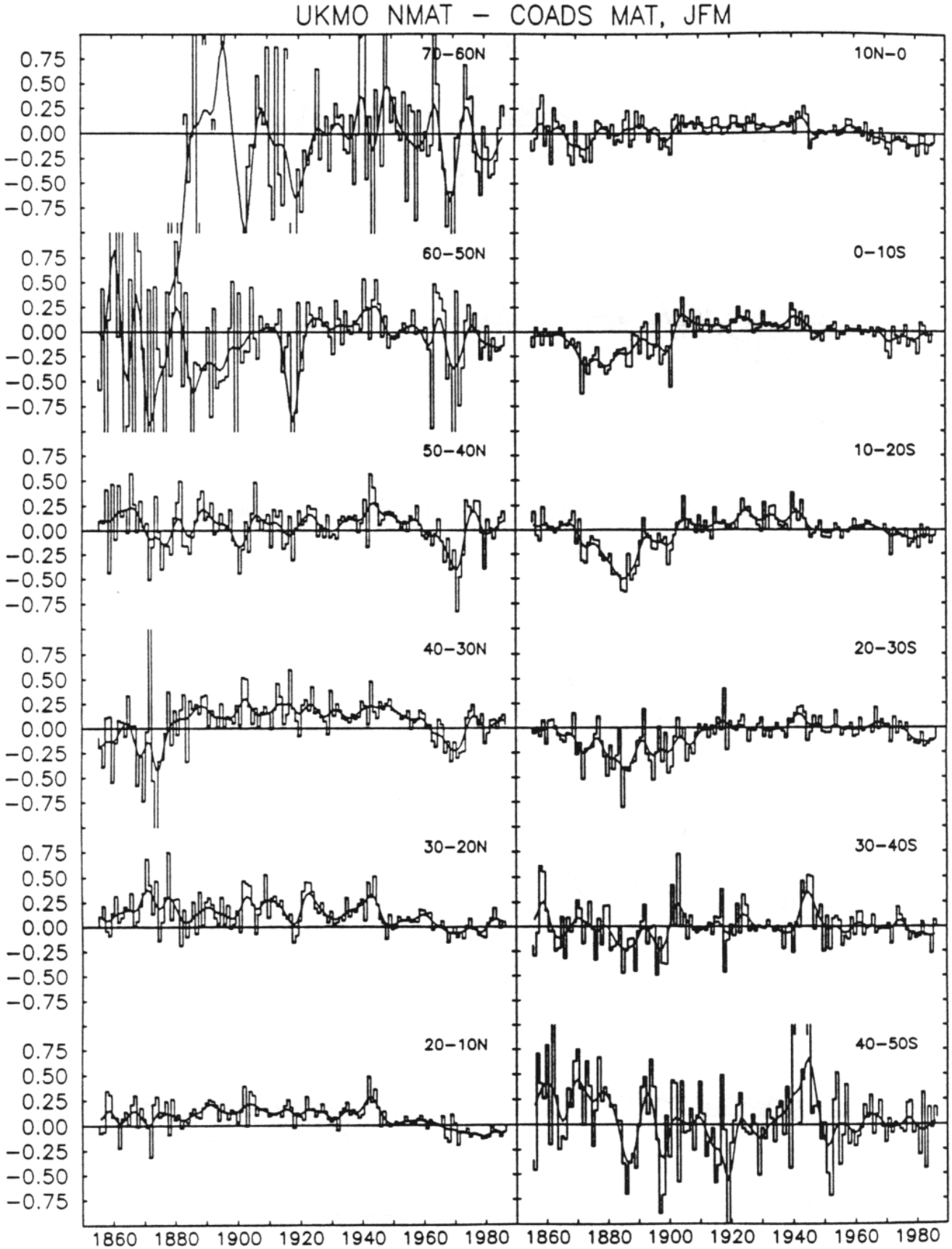

Fig. 3.18: Zonal, time series of UKMO NMAT minus COADS MAT using anomaly data for the January to March season.

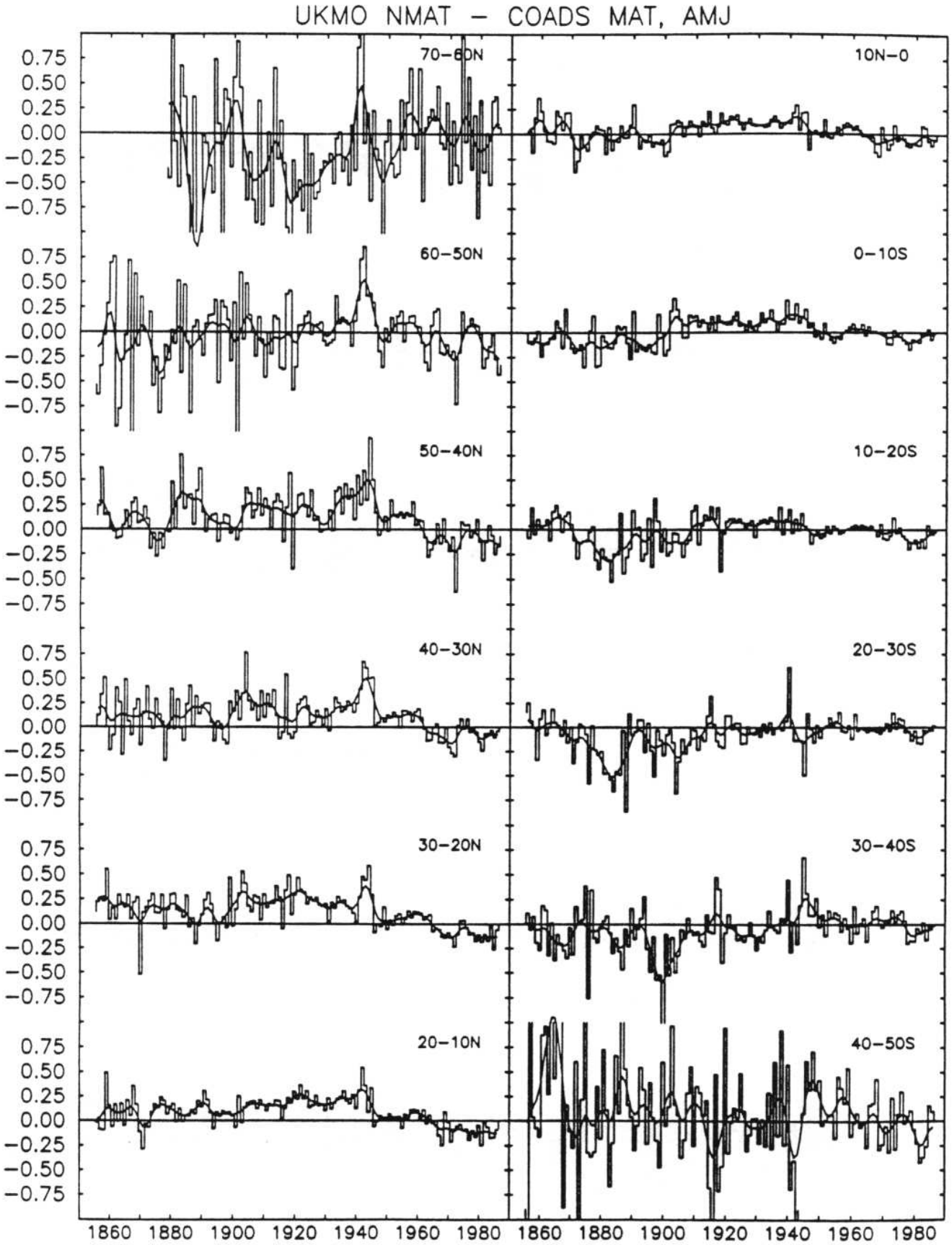

Fig. 3.19: Zonal time series of UKMO NMAT minus COADS MAT using anomaly data for the April to June season.

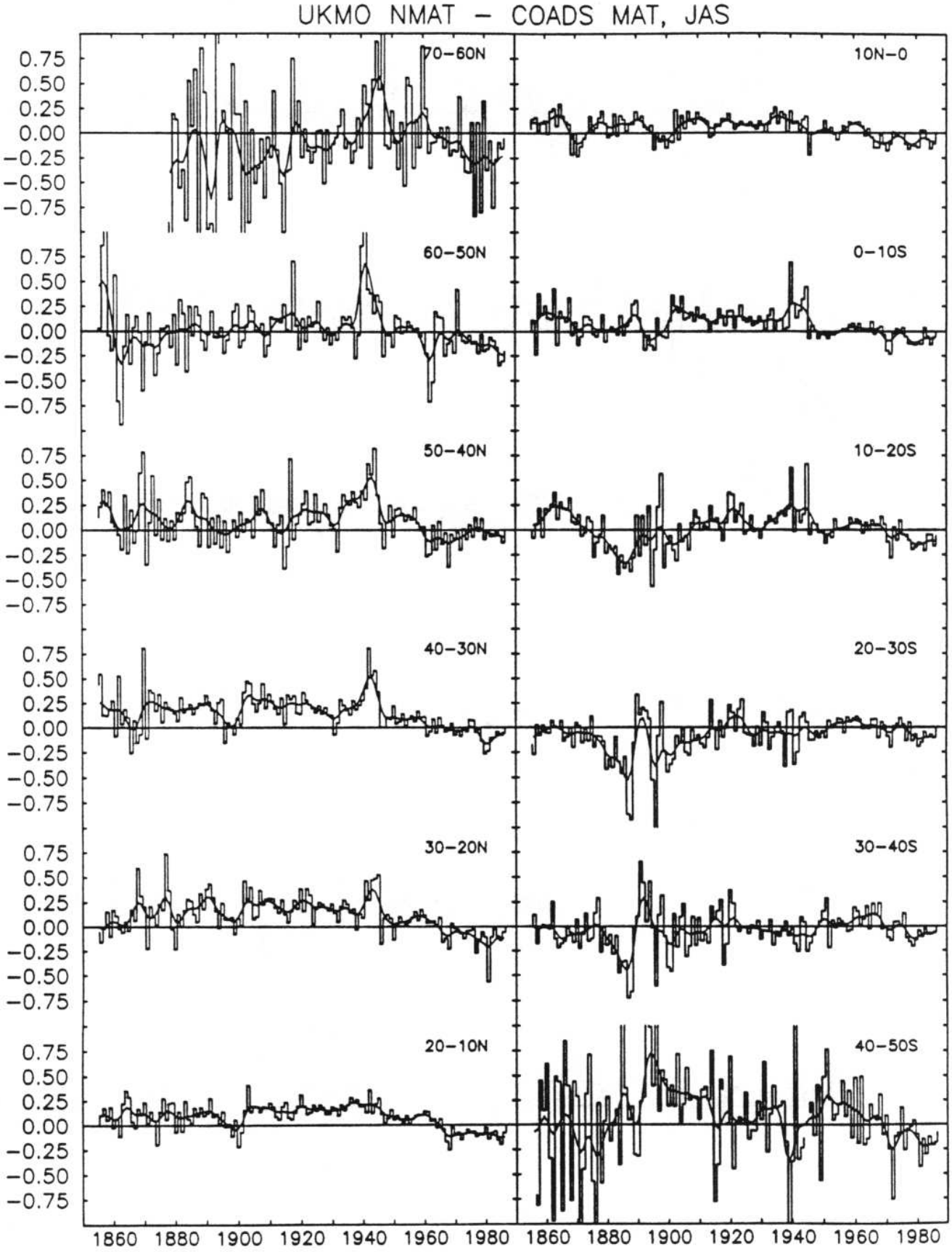

Fig. 3.20: Zonal time series of UKMO NMAT minus COADS MAT using anomaly data for the July to September season.

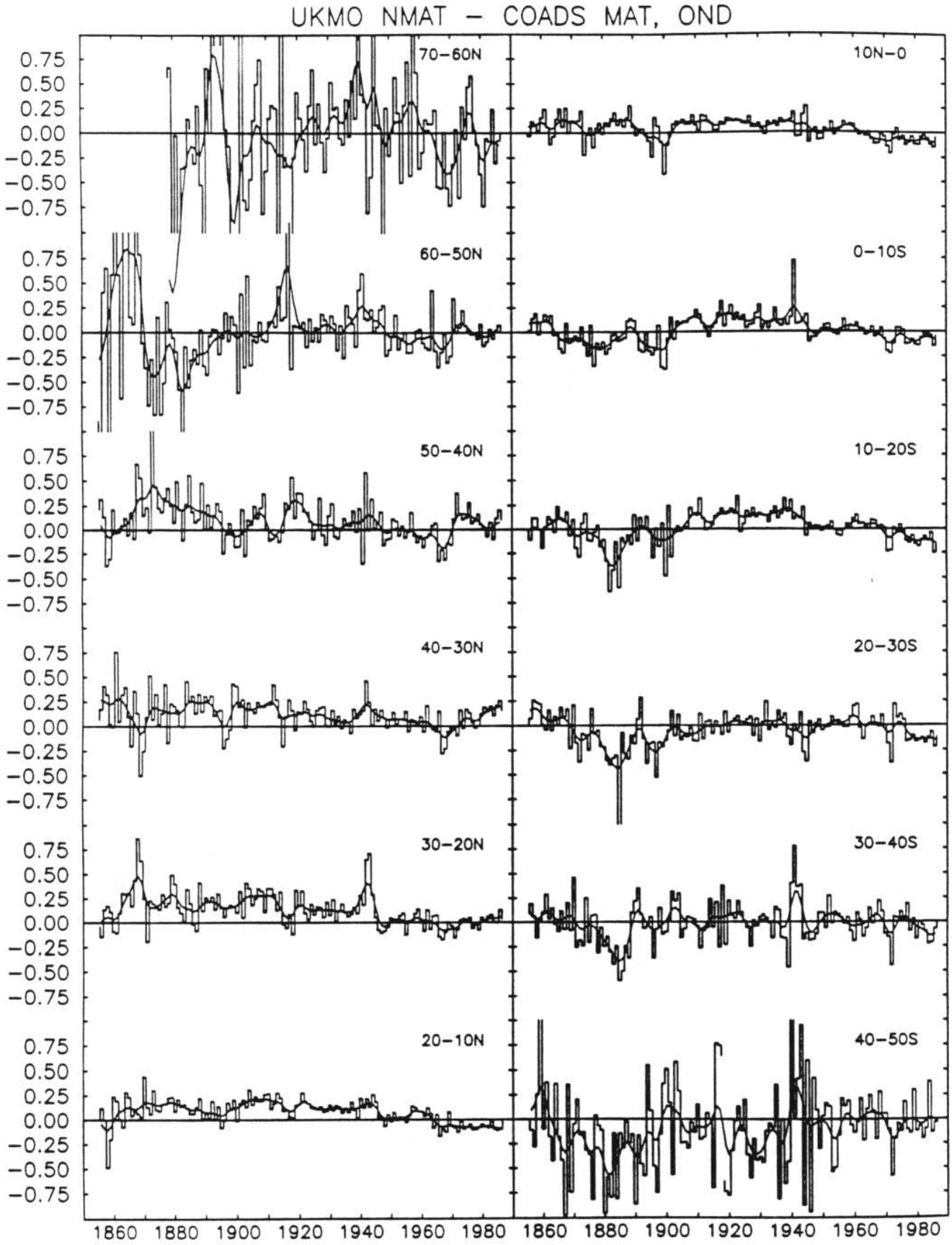

Fig. 3.21: Zonal time series of UKMO NMAT minus COADS MAT using anomaly data for the October to December season.

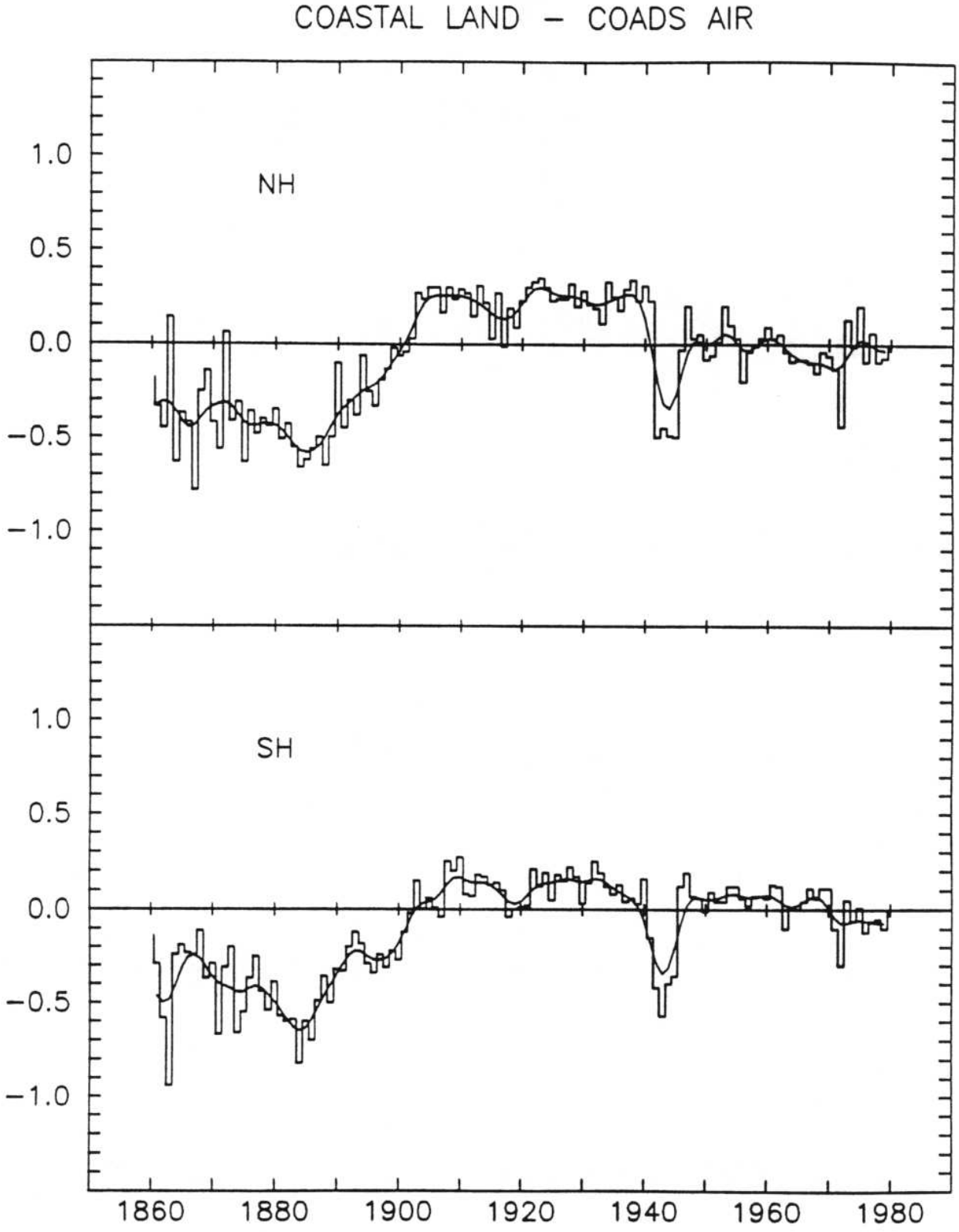

Fig. 3.22: Hemispheric, annual time series of coastal land temperatures minus raw COADS MAT, using anomaly data. (From Jones et al., 1986c)

COADS marine air temperatures.

Here we carry out similar comparisons using the UKMO data. A number of co-located grid boxes were identified which had data in both the land (islands) and UKMO NMAT data bases. The locations of the points, 35 in the NH and 24 in the SH, are shown in Figure 3.23. Time series of the annual land-minus-NMAT values, averaged over NH and SH boxes, are presented in Figure 3.24. (Note that, because only island grid points are used in the present analysis, there are not enough data to form the SH difference series until 1881.) As would be expected, given the differences between COADS MAT and UKMO NMAT (Figure 3.16) and the different array of comparison boxes (compare Figure 3.23 with Figure 1 in Jones et al., 1986c), there are some important differences between Figures 3.22 and 3.24. The most marked of these occur in the nineteenth century. Except in the first few decades of the NH record, these differences are due primarily to differences between the raw marine data rather than due to box location effects.

3.6 Sea surface temperature data: COADS/UKMO comparison

3.6.1 Hemispheric means

Figures 3.25 and 3.26 show hemispheric values of SST based on the raw, uncorrected anomaly data of UKMO and COADS. Differences (UKMO minus COADS) are shown in Figure 3.27. Up to 1880, the differences are small, although there is a cooling of UKMO relative to COADS in the Southern Hemisphere. From 1880 to the early 1960s, for both hemispheres, UKMO values are warmer than those of COADS, by 0.05-0.10^{o}C for the Northern Hemisphere and slightly less in the Southern Hemisphere. In the early 1960s there appears to be a step-like drop in the difference, making COADS warmer than UKMO in 1961, followed by a gradual rise back to the zero line by around 1970.

3.6.2 Zonal means

Zonal means for the UKMO data were based directly on the 5° by 5°

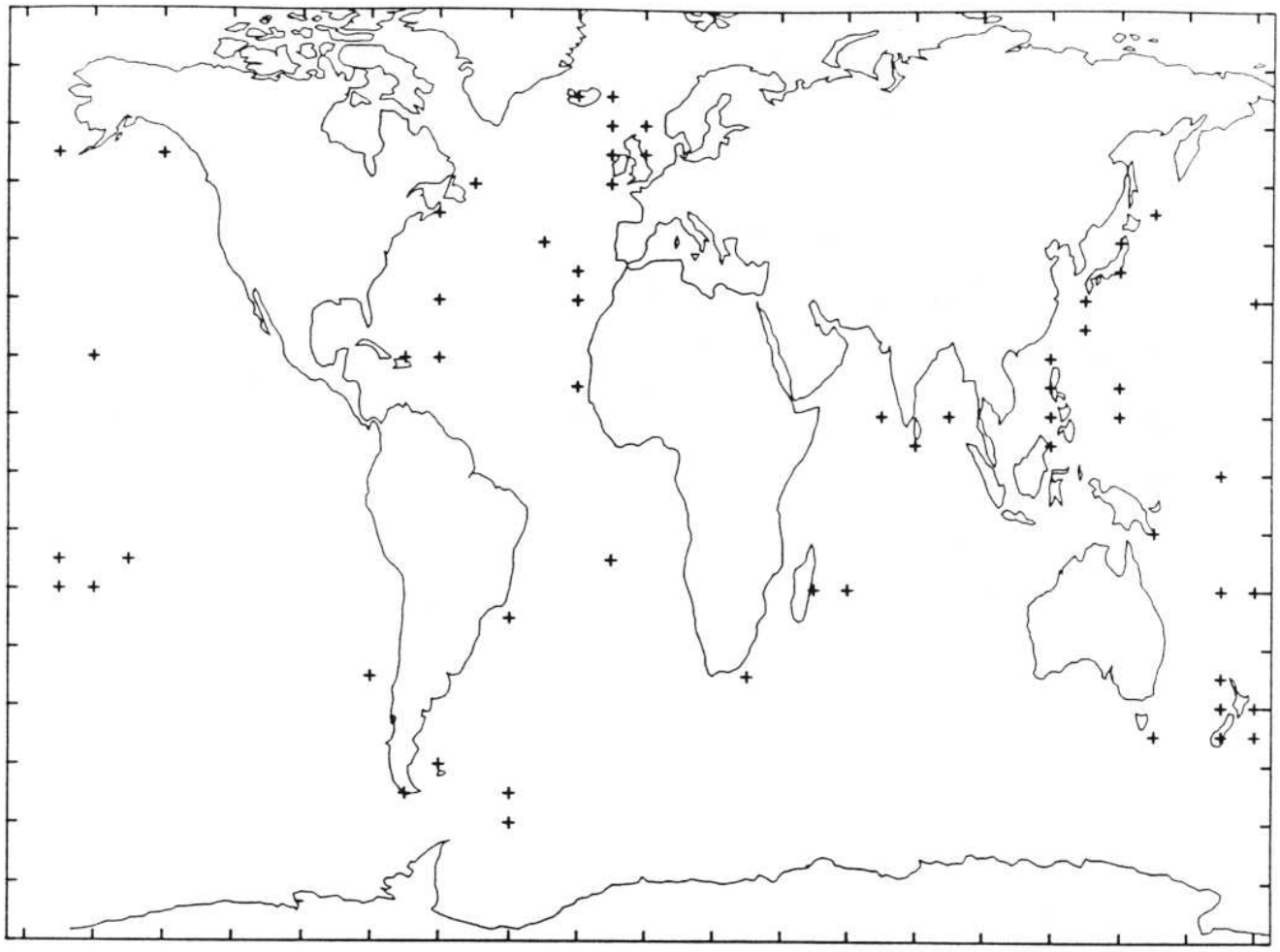

Fig. 3.23: Location of 35 grid points in NH and 24 in SH where island land temperatures and UKMO NMAT data are compared.

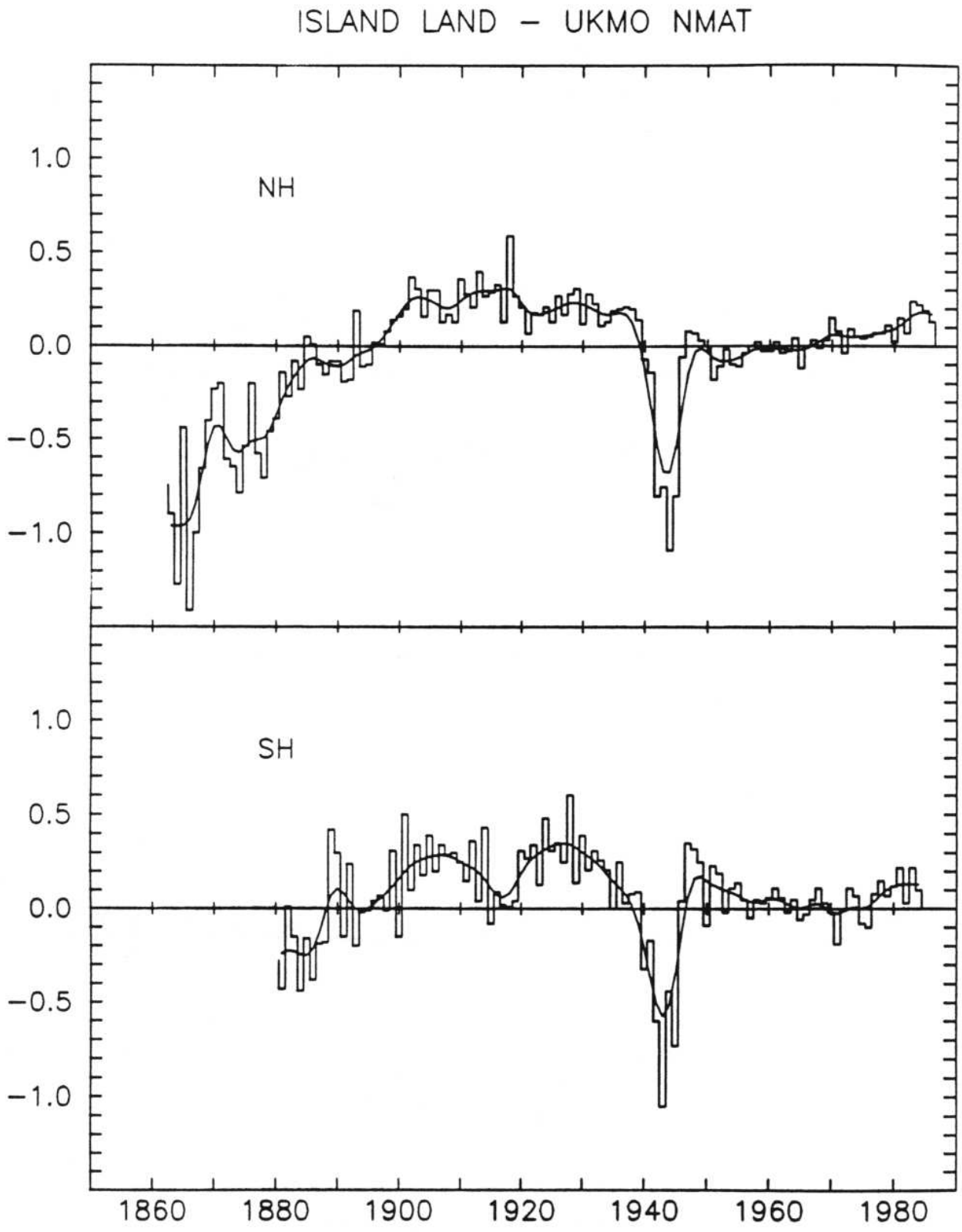

Fig. 3.24: Hemispheric, annual time series of island land minus UKMO NMAT anomaly temperatures.

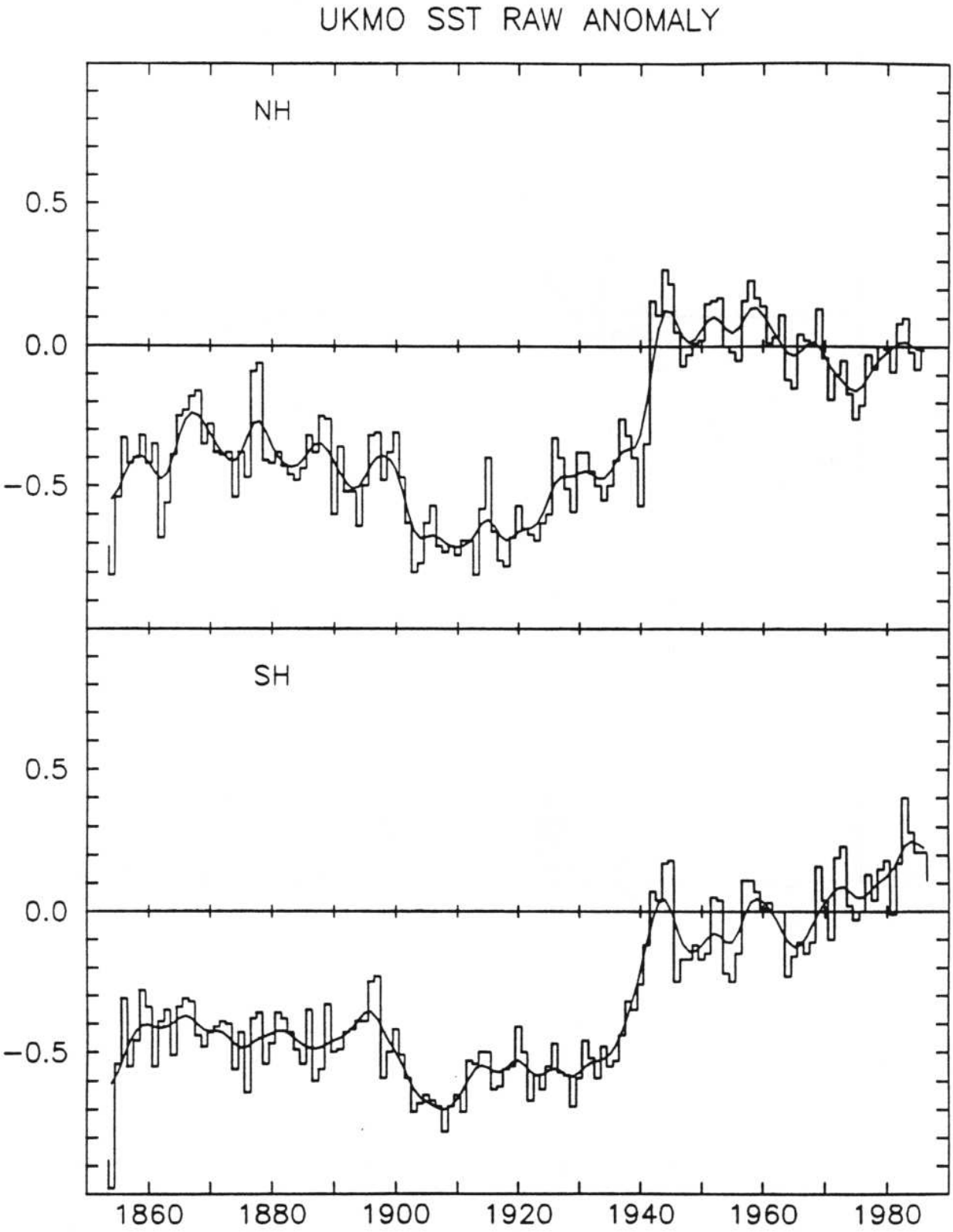

Fig. 3.25: Hemispheric, annual time series of UKMO SST data expressed as raw anomalies, 1854-1986.

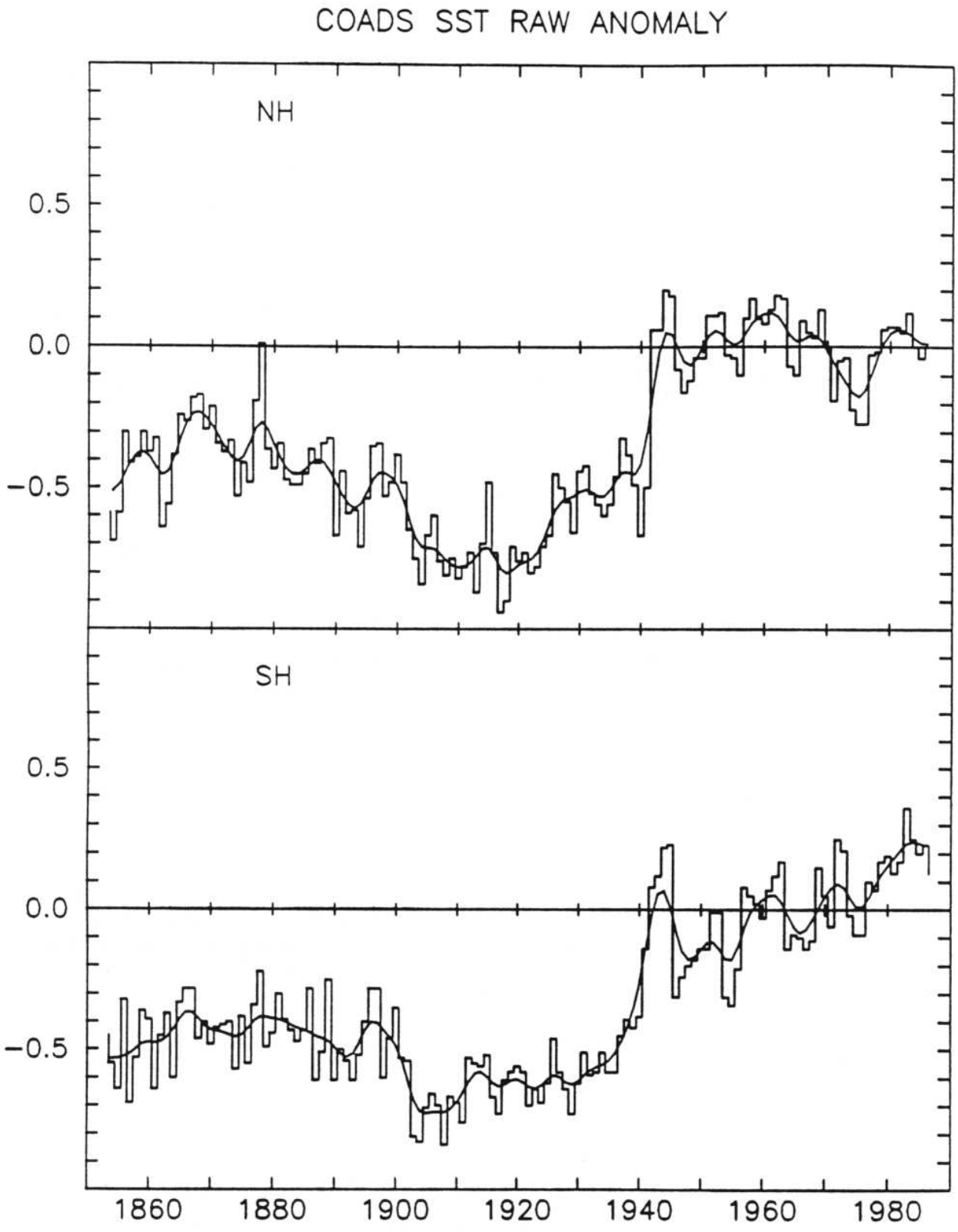

Fig. 3.26: Hemispheric, annual time series of COADS SST data expressed as raw anomalies, 1854-1986.

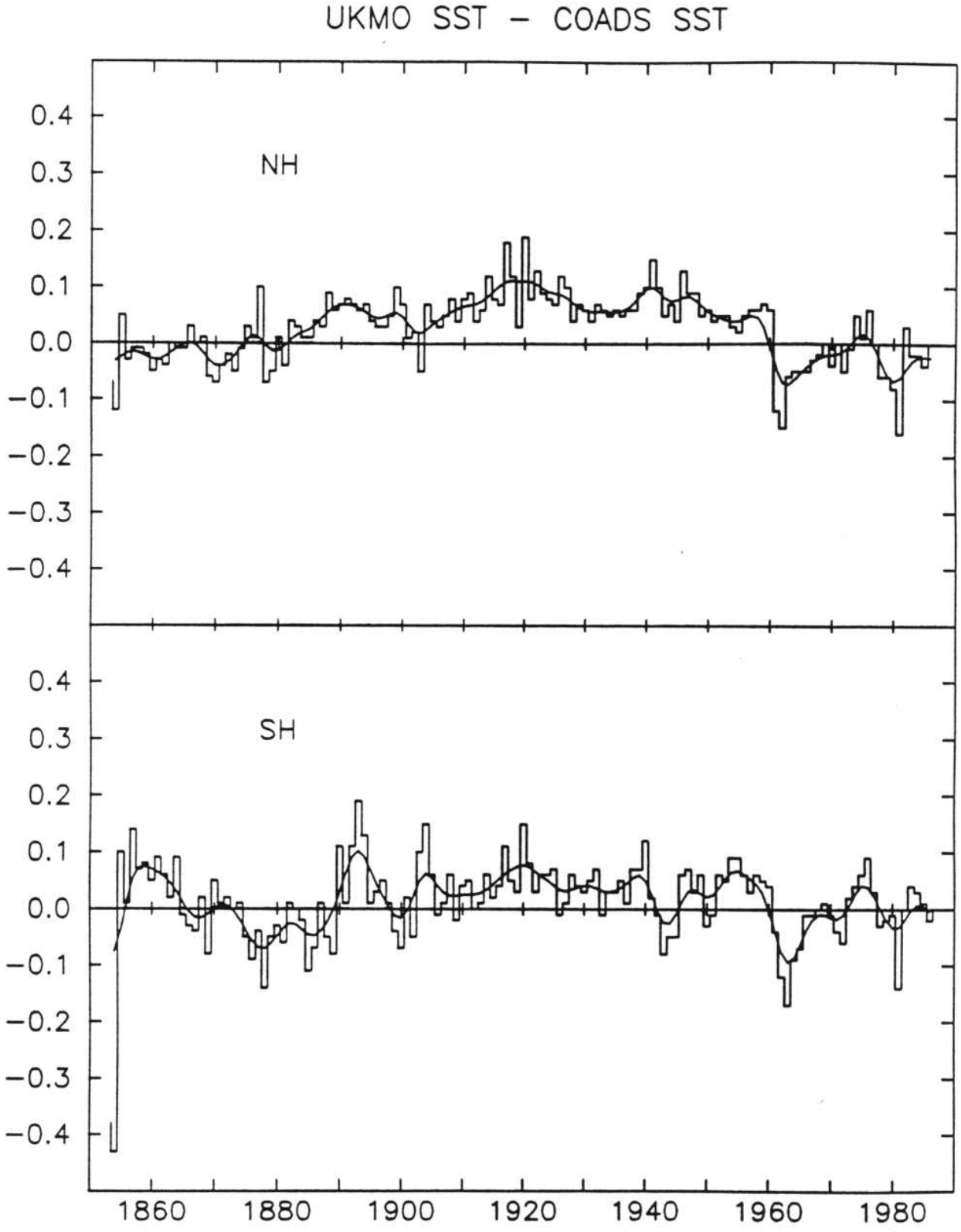

Fig. 3.27: Hemispheric, annual time series of UKMO SST minus COADS SST.

values. For COADS, it was necessary to average three 4° bands spanning the 10° zone. Annual time series of the SST differences (Figure 3.28) show much the same picture as at the hemispheric scale. The positive UKMO-minus-COADS difference over 1880-1960 arises mainly (in the Northern Hemisphere) from differences in the October to March half year in the zone 20-40°N (Figures 3.29 to 3.32). The smaller Southern Hemisphere difference appears to arise mainly in the zone 10-20°S. The drop around 1961 is strongest in 10-40°N and 20-40°S. It is evident in all seasons, although slightly stronger in the winter half-year.

The 1960/61 discontinuity requires further discussion. While it may be a real climatic feature (it falls within the post-war period when the data do not need to be corrected), it also occurs at a time when the UKMO data set has incorporated a large amount of Pacific Ocean data from MIT (see Section 3.3). In some months, the MIT data represent over 20% of the Northern Hemisphere area, around one third of the NH SST coverage. Moreover, the amount of incorporated MIT data drops throughout the 1970s, reaching zero by 1980. It is possible, therefore, that the MIT data are incompatible with the rest of the data set, and that they have introduced some spurious variations in the area averages. The issue is not clear cut, however, for two reasons. First, there are very few MIT data in the SH, yet the temperature discontinuity is also present in the SH. Second, according to Bottomley et al. (1989), the MIT data were subject to some form of quality control, with data excluded if the monthly value differed by more than 3°C from the average of the available adjacent 5° area values in the combined UKMO/MIT data set. This screening has not been entirely successful. For example, some MIT-based values in the tropical Pacific Ocean in December 1949 have anomaly values in excess of 10°C, values which are unlikely to be real.

It is likely, therefore, that the discontinuity has both climatic and non-climatic components. The MIT data, however, appear almost certainly to

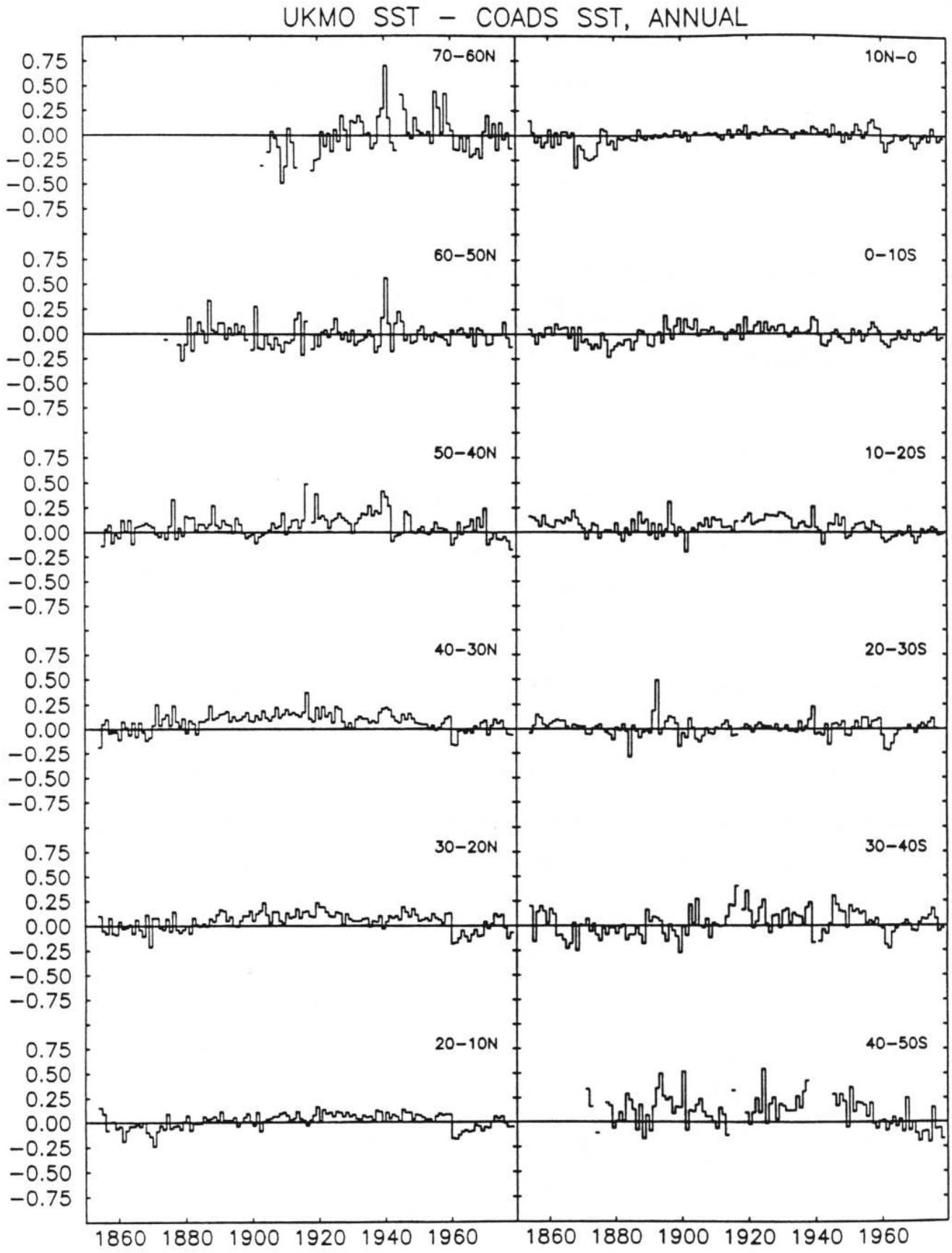

Fig. 3.28: Zonal, annual time series of UKMO SST minus COADS SST.

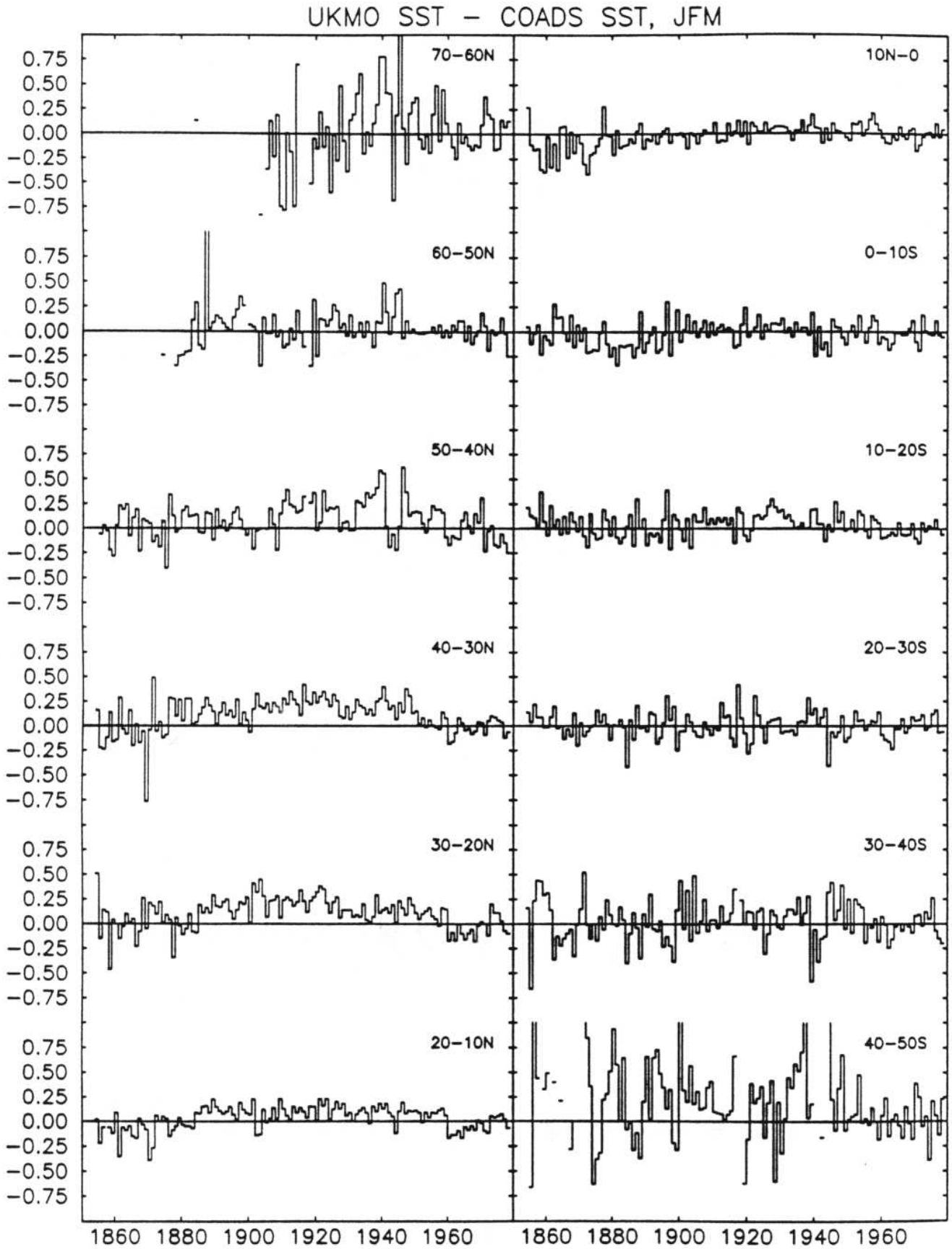

Fig. 3.29: Zonal time series of UKMO SST minus COADS SST, January to March season.

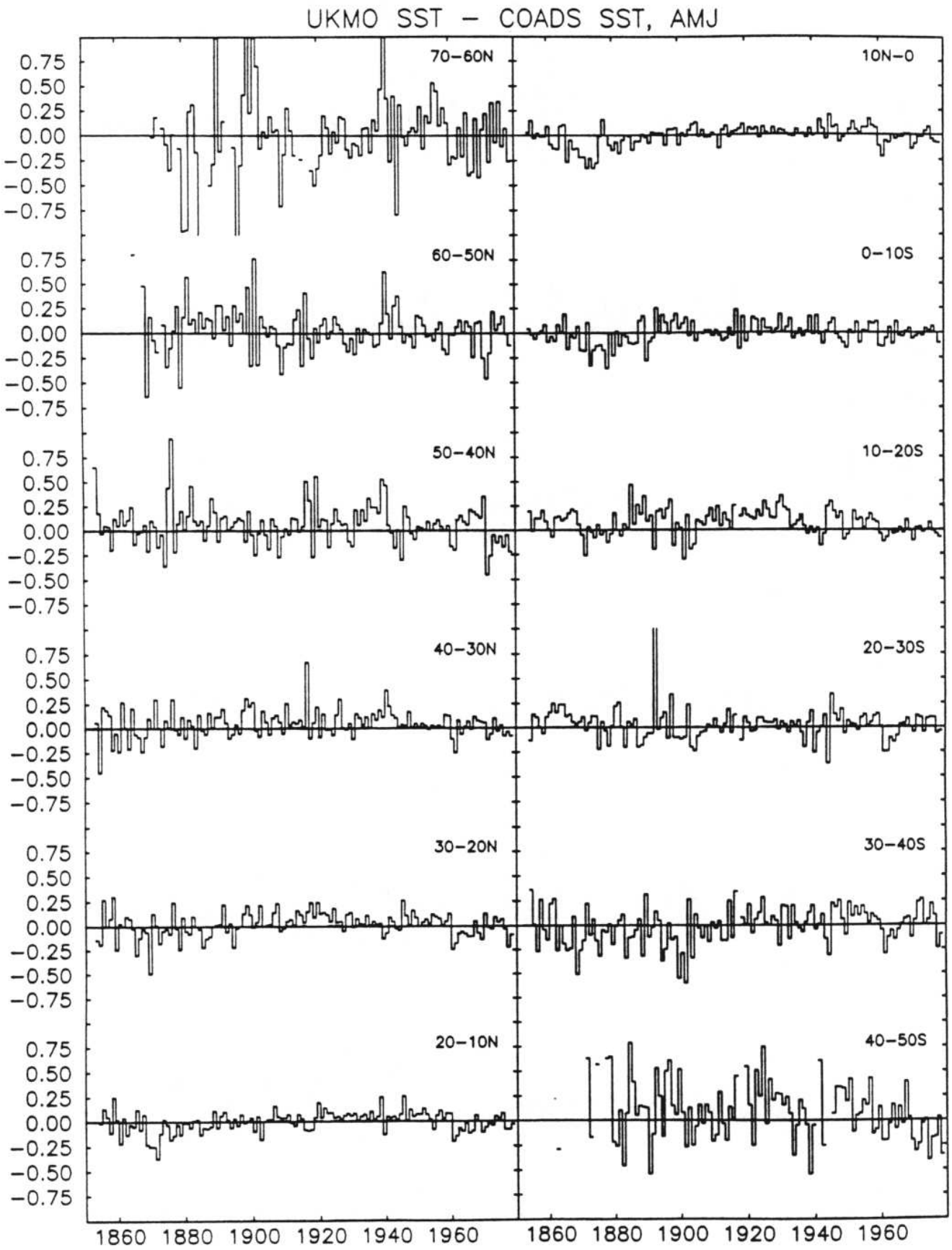

Fig. 3.30: Zonal time series of UKMO SST minus COADS SST, April to June season.

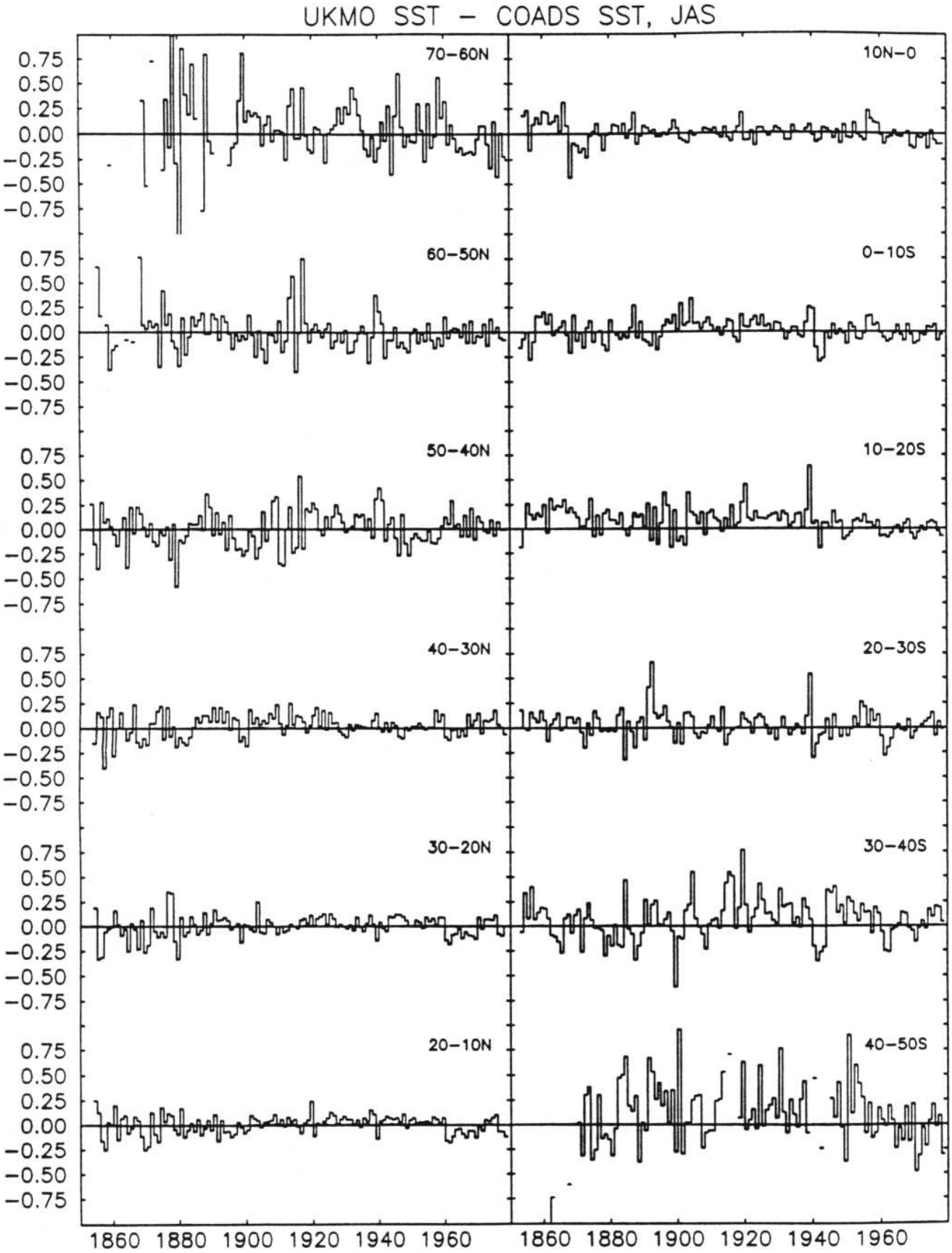

Fig. 3.31: Zonal time series of UKMO SST minus COADS SST, July to September season.

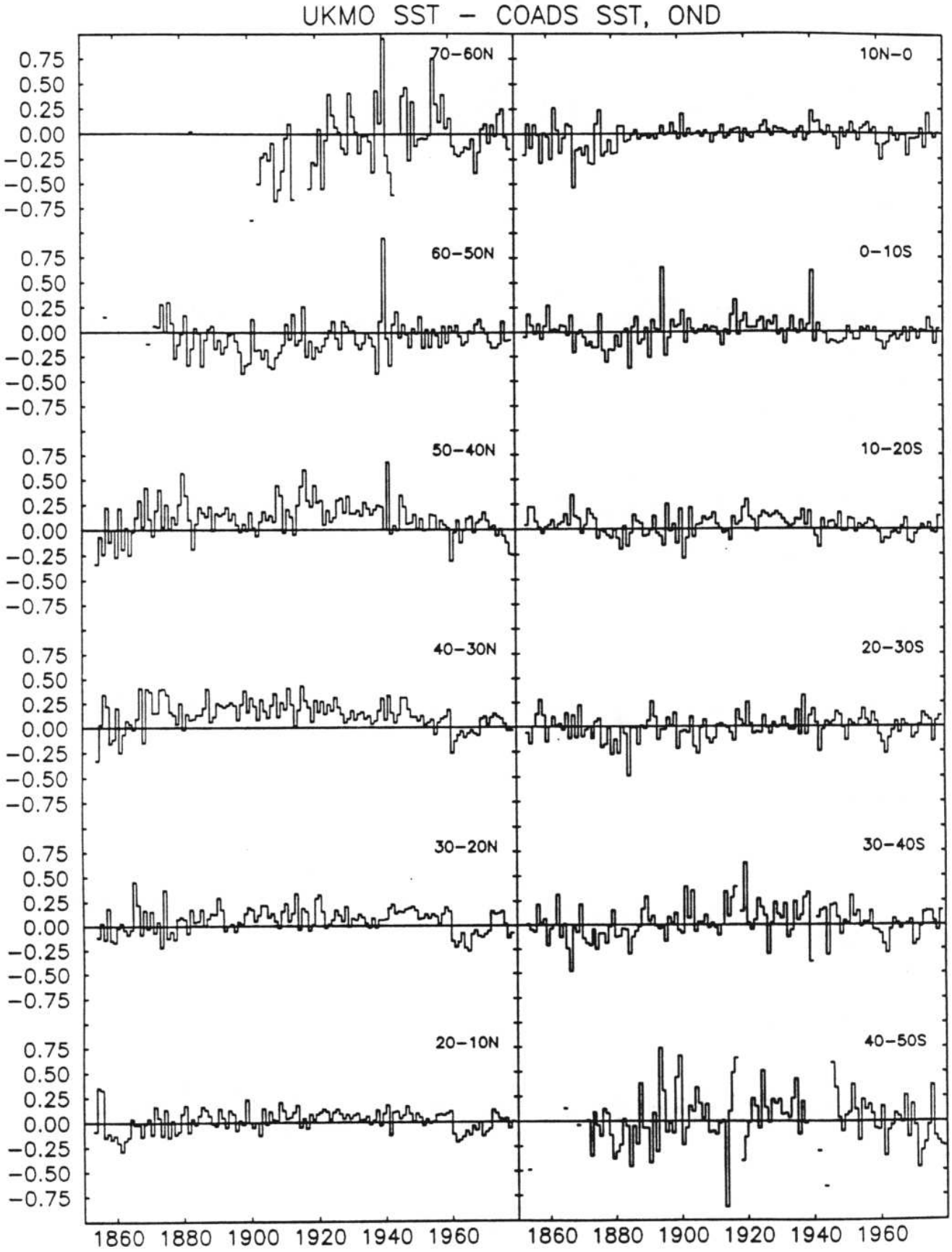

Fig. 3.32: Zonal time series of UKMO SST minus COADS SST, October to December season.

be of lesser quality than the basic UKMO and COADS data, and this must have distorted the UKMO averages to some degree.

3.7 Air-sea temperature differences

As a final comparison between the four data sets, we consider the difference between uncorrected air and SST values for both UKMO and COADS data sets. If instrumentation had remained constant, there should be little difference between air and SST temperatures, with no temporal change in the difference. That this is not the case is graphically demonstrated in Figures 3.33 (UKMO) and 3.34 (COADS). During the reference periods, differences should be near-zero and constant. The COADS data show larger excursions from this ideal than do the UKMO data. Prior to 1940, air temperature anomalies are significantly higher than SST anomalies in both data sets. From the 1850s to the 1890s the air is relatively warm by about 0.6°C in the NH and 0.45°C in the SH. This drops to around 0.4°C (NH) and 0.3°C (SH) from 1900 to 1940.

For the Northern Hemisphere, the UKMO and COADS air-sea difference curves are very similar, with the UKMO difference being consistently slightly greater. The greatest difference between the series comes in the SH over the period 1880 to 1900 where values for COADS MAT-minus-SST are much larger than those for UKMO NMAT-minus-SST. This disparity between the series is largely a function of the COADS/UKMO air temperature differences shown in Figure 3.16.

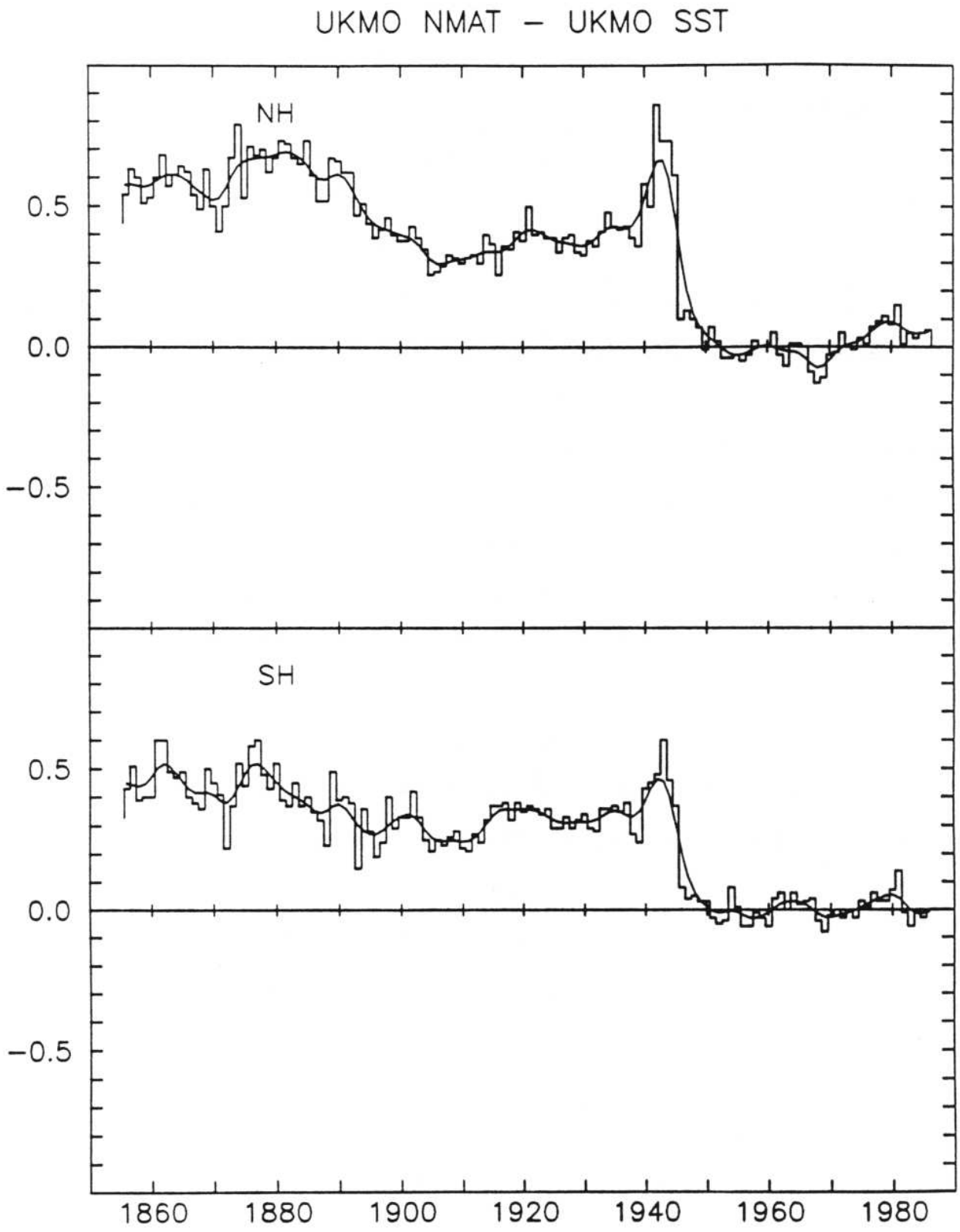

Fig. 3.33: Hemispheric, annual time series of UKMO NMAT minus UKMO SST.

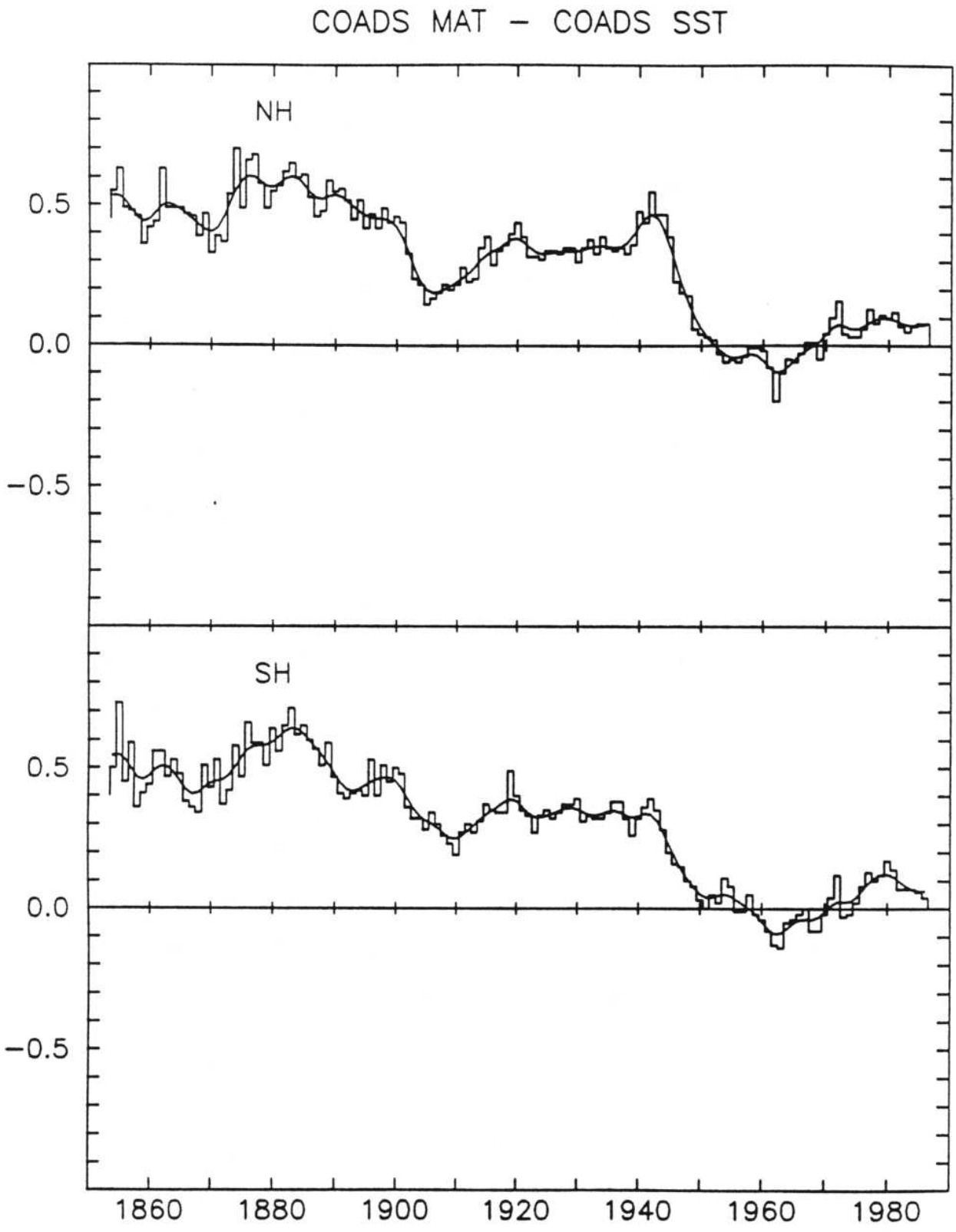

Fig. 3.34: Hemispheric annual time series of COADS MAT minus COADS SST.

4. *AN A PRIORI BUCKET MODEL APPROACH*

4.1 Introduction

Many factors can influence a sea surface temperature reading (Folland et al., 1984; Barnett, 1985; Jones et al., 1986c; Bottomley et al., 1989). Some of these introduce random errors while others result in systematic, non-cancelling errors. The most important factor is the method of collecting the sample, with the two basic methods being to haul a sample on deck with a bucket, or to measure the temperature of the intake water used for engine cooling. In this Section we are concerned with bucket measurements. These are affected by the kind of bucket used, the exposure of and physical conditions surrounding the bucket, how long the bucket was left before reading the thermometer, and ship speed.

In neither the UKMO nor the COADS data sets do we have detailed information concerning the methods of measurement, nor any indication of what method was used for the individual readings that make up the data. There is, nevertheless, strong evidence that readings before 1940 were predominantly bucket measurements, while those since 1945 were predominantly intake measurements. Furthermore, it is likely that the major difference between the data for these two periods is the non-climatic bias due to the evaporative cooling of the canvas bucket, an effect which would clearly cause pre-1940 data to be cooler than post-1945 data. (As discussed earlier, prior to about 1900 both wooden and canvas buckets were used.)

In order to derive correction factors for the bucket-derived temperatures, workers in the Meteorological Office have developed a computer model to estimate the cooling of an uninsulated canvas bucket (Folland and Hsiung, 1986; Bottomley et al., 1989). For this research project we have developed a similar bucket model and taken a different, though comparable approach to the estimation of the evaporative cooling effect. For the bucket model itself, the main difference between our work

and that of Folland and Hsiung (1986) is that we have solved the governing equations analytically. This makes application of the model less demanding computationally, and it allows us to perform a variety of sensitivity and related analyses, as described below.

4.2 The bucket model

4.2.1 Theory (following Folland and Hsiung, 1986)

Terminology:

b = $\partial e_{sA}/\partial T$
C = specific heat capacity of water
C_p = specific heat of air at constant pressure
e_A = vapour pressure of air
e_{sB} = saturation vapour pressure at T_B (e_{sA} similarly)
h = depth of water in bucket (approximately 15cm)
k_c = convective heat transfer coefficient
k_r = radiative heat transfer coefficient
$\hat{k}, k^*$ = water vapour mass transfer coefficients
L = latent heat of vaporization
p = atmospheric pressure
Q_B = shortwave radiation input adjusted for interception area
Q_H = heat transport away from bucket
r = bucket radius (approximately 9cm)
R = atmospheric relative humidity = e_A/e_{sA}
T_A = air temperature
T_B = bucket water temperature
T_S = sea surface temperature = $T_B(t=0)$
T_∞ = asymptotic bucket temperature
$\underline{U}$ = wind velocity in vicinity of bucket
$\underline{v}$ = ship velocity
$\underline{V}$ velocity of air flow past bucket = resultant of $\underline{v}$ and $\underline{U}$
Δ = correction = $T_S - T_B$
ρ = mean density of water plus bucket
θ = angle between $\underline{U}$ and $\underline{v}$
τ = relaxation time for evaporative cooling.

The equation for $T_B(t)$ derived by Folland and Hsiung (1986) is

$$r^2hC\frac{dT_B}{dt} = (2rh+r^2)[Q_B-Q_H] = (2rh+r^2)[(k_c+k_r)(T_A-T_B) + k^*L(e_A-e_{sB}) + Q_B] \quad \ldots(1)$$

This is simplified using the following (SI units)....

$$k_c = 2.34\sqrt{V/r} \qquad (Wm^{-2}K^{-1}) \qquad \ldots(1a)$$

$$k_r = 5.4 \qquad (Wm^{-2}K^{-1}) \qquad \ldots(1b)$$

$$k^* \approx (k_c+k_r)/AL \qquad (Wm^{-2}hPa^{-1}) \qquad \ldots(1c)$$

where A is the psychrometer coefficient ($\approx 0.7hPaK^{-1}$), together with the

above values of h and r to give

$$\frac{dT_B}{dt} \approx a\,[Q_B + (7.80\sqrt{V} + 5.4)(T_A - T_B + 1.4(e_A - e_{sB}))] \qquad ...(2)$$

where $a = 6.902\ 10^{-6}$ for t in seconds or $a = 4.141\ 10^{-4}$ for t in minutes. (Note that e must be in hPa.) Equation (2) involves the approximation (1c) which is neither strictly correct (k^* must be related to k_c alone, not to k_c+k_r) nor necessary. The correct result is given in Section 4.2.6. Nevertheless, equ. (2) is a very good approximation, and since it is the form used by Folland and Hsiung, we will retain it for the present.

The trick in solving equ. (2) is to note that $T_A \approx T_B$. This means that $e_{sB} \approx e_{sA} + b(T_B-T_A)$ where $b = \partial e_s/\partial T$ at T_A (strictly, at $(T_A+T_B)/2$, but the difference is negligible). If we write

$$u = 7.8\sqrt{V} + 5.4 \qquad ...(3)$$

then equ. (2) becomes

$$\frac{dT_B}{dt} + au(1+1.4b)(T_B-T_A) = a[Q_B - 1.4(1-R)ue_{sA}] \qquad ...(4)$$

The solution to this is

$$T_B = T_S - (T_S - T_\infty)(1 - \exp(-t/\tau)) \qquad ...(5)$$

where

$$T_\infty = T_A - (1.4(1-R)e_{sA} - Q_B/u)/(1+1.4b) \qquad ...(6)$$

is the asymptotic bucket-water temperature (i.e. an effective "wet bulb" temperature for the bucket) and

$$\tau = 2410/(u(1+1.4b)) \qquad ...(7)$$

is the time scale for relaxation of T_B towards T_∞ (in minutes).

4.2.2 Sensitivity analysis

In applying equ. (5), it must first be written explicitly in terms of the correction factor (Δ) to be applied to T_B ($T_S = T_B+\Delta$), viz.

$$\Delta = (T_B - T_\infty)(\exp(t/\tau) - 1) \qquad ...(5a)$$

Equ. (5a) is used to calculate Δ for various exposure times t, which are

then applied successively to the T_B anomaly values until the annual cycle is minimized. Since monthly and spatially averaged values are used, application of equ. (5a) is strictly valid only if $\bar{\Delta} = \Delta(\bar{T}_A, \bar{R}, \bar{Q}_B, \bar{u})$. Although this is clearly not correct, a linear form of equ. (5a) can be derived which is quite accurate, justifying the present application.

In general, $\tau \sim 30$ mins., so $t \ll \tau$. Hence, the exponential can be approximated using $\exp(t/\tau) \approx 1+t/\tau$ to give

$$\Delta \approx (T_B - T_\infty)t/\tau \qquad \ldots(5b)$$

or (using (6) and (7) and assuming $T_B - T_A \ll 0.7(1-R)e_{sA}$)

$$\Delta \approx (1.4(1-R)ue_{sA} - Q_B)t/2410 = \gamma t \qquad \ldots(5c)$$

This is non-linear in T_A (through e_{sA}) and V (which appears in u). However, the non-linear temperature effect is small because of the narrow range of marine temperatures observed at any site in any given month, while the V effect is minimized because it only appears as a square root and because of the constant term in u.

Analysis of the linear form equ. (5c), or logarithmic differentiation of equ. (5), shows that the calculated correction factor is relatively insensitive to errors in V, R or T_A. An error of $1 ms^{-1}$ in V gives an 8% error in Δ, a 5% error in R leads to a 25% error in Δ, while a 1^oC error in T_A gives a 17% error in Δ, using representative values of all the relevant parameters. Note that, since Δ depends roughly linearly on t, these figures also represent potential uncertainties in the value of t implied by a given Δ.

Direct sensitivity to V, R and T_A is, however, not the most important issue. Rather, we need to know whether or not the t value which minimizes the seasonal cycle in corrected T_B values is sensitive to uncertainties in V, R and T_A. This is something which cannot be determined analytically. Instead, one must perturb the parameters by reasonable amounts and see whether or not the implied t value changes. When this is done, the results are found to be robust to input uncertainties. The sensitivity to V is

perhaps the most important issue because V depends partly on ship speed which has varied with time, and because of the considerable uncertainty involved in translating available wind speed data to values appropriate to the vicinity of the bucket. The effects of these variations are considered further below.

Even an error in estimating t may not matter, since the key question is errors in the eventual correction factor. Suppose one or more of V, R and T_A is in error. This will produce erroneous Δ and t results. When individual (i.e. seasonally- and spatially-specific) corrections are then made using a single, biased t value, this bias will act to offset any errors in the individual corrections caused by "local" V, R and T_A errors. This is a consequence of the near-linearity in V, R and T_A of the basic evaporative cooling equation. The net effect, through compensating errors, is that the final corrected results should show only minimal sensitivity to data input uncertainties. The primary checks on the model are on the spatial consistency of the calculated exposure times, and on the realism of the average exposure time. As will be shown below, the results are both spatially consistent and realistic.

4.2.3 Effect of bucket/intake mix and different bucket types

For virtually all of the period of record, the data come from a mixture of observation techniques. Because of this, the inferred exposure time is actually an effective exposure time. To show this, suppose that the fraction of uninsulated buckets is f, the fraction of insulated buckets is g, and the remainder (1-f-g) are intake measurements. Suppose also that all data are to be corrected to intake measurements (we could equally well suppose that correction was to some standard mix of instruments). Insulated buckets give temperatures very similar to intake measurements, so this distinction could be omitted. However, early "insulated" buckets (such as wooden buckets) may have been poorly insulated. For these, the

correction factor would be of the form

$$\Delta_i = \xi \Delta_u \qquad \ldots(8)$$

where $\xi < 1$ and subscripts i and u refer to insulated and uninsulated buckets. The mean correction is therefore

$$\bar{\Delta} = 0 + f\Delta_u + g\Delta_i = (f+\xi g)\Delta_u \qquad \ldots(9)$$

If t is the true exposure time and t^* is the exposure time implied by $\bar{\Delta}$ assuming 100% uninsulated buckets, then, using equ. (5c), we have

$$\gamma t^* = (f+\xi g)\gamma t$$

so that

$$t^* = (f+\xi g)t \qquad \ldots(10)$$

In other words, if f and g are approximately constant, then the implied exposure time will simply be a constant multiple of the true exposure time. When t^* is used to make corrections, the resulting correction will be the correctly weighted value which automatically accounts for the bucket/intake mix.

4.2.4 The ship speed effect

The value of $\underline{V}$ used above is the resultant of the wind velocity $\underline{U}$ and the ship velocity $\underline{v}$, so that

$$V = (a + b\cos\theta)^{1/2} \qquad \ldots(11)$$

where

θ is the angle between $\underline{U}$ and $\underline{v}$

$a = v^2 + U^2$

$b = 2vU$

Since θ is unknown, it may be considered a uniform random variable on $(0,2\pi)$. The mean value of V is therefore

$$\bar{V} = \frac{1}{\pi}\int_0^{\pi} (a + b\cos\phi)^{\frac{1}{2}}\, d\phi$$

i.e.

$$\bar{V} = \frac{2}{\pi} (v+U) E(m) \qquad ...(12)$$

where

$$m = 2b/(a+b) = 4vU/(v+U)^2$$

and E is the complete Elliptic Integral of the Second Kind (for solution see Abramowitz and Stegun, 1965).

If β is the ship speed expressed in terms of the wind speed, i.e.

$$v = \beta U \qquad ...(13)$$

then the ship speed effectively inflates the wind speed by a factor

$$\bar{V} = \alpha U \qquad ...(14)$$

where α varies from 1 when $\beta = 0$, through $4/\pi$ (=1.2732...) for $\beta = 1$, upwards, with α tending to β for large β. Variations of α as a function of β are shown in Table 4.1.

Table 4.1: Variations in $\alpha = \bar{V}/U$ as a function of $\beta = v/U$.

β	0.0	0.1	0.2	0.3	0.4	0.5	0.6	0.7	0.8	0.9
α	1	1.0003	1.0100	1.0226	1.0404	1.0635	1.0922	1.1268	1.1678	1.2160
β	1.0	1.2	1.5	2.0	2.5	3.0	4.0	5.0	7.0	10.0
α	1.2732	1.4196	1.6719	2.1271	2.6010	3.0839	4.0627	5.0501	7.0358	10.025

Variations in ship speed through time, therefore, can only have an appreciable effect if ship speed, v, noticeably exceeds wind speed, U. Over the period for which data exist, average ship speed has increased from around $4ms^{-1}$ (≈8kt) to $7ms^{-1}$ (≈14kt). Mean wind speed at ship deck height is probably around $5ms^{-1}$, so that V has changed from $5.8ms^{-1}$ to $7.9ms^{-1}$ implying a 17% change in Δ. As noted above, however, the crucial question is whether or not the implied t value which minimizes the seasonal anomaly cycle has changed, or, more importantly, whether the final "local"

correction factors are in error. For the latter, compensating errors operate, as noted above. For the former, calculations of t using ship speeds of $4ms^{-1}$ and $7ms^{-1}$ confirm that the ship speed effect is minor.

4.2.5 The effect of bucket size and shape

The geometry of the bucket affects the cooling magnitude at time t through the term a in equ. (2), and, to a lesser degree, through the ratio of short-wave interception area to total surface area which is included in the Q_B term. The former effect operates just like the effect of bucket/intake mix in that it simply scales the time. If a cooling Δ occurs after time t with bucket dimensions (r,h), then, for dimensions (r_1,h_1), Δ occurs after time

$$t^* = t \frac{r_1 \; h_1 \; (2h+r)}{r \; h \; (2h_1 + r_1)}$$

Thus, just as for bucket/intake mix, if bucket geometry has changed with time, this would be manifest as a change in the optimum exposure time. As a corollary, such changes can be incorporated in any correction strategy simply by changing the exposure time. Of course, if the changes are not known a priori, then, by hypothesizing such changes, one may introduce a tunable parameter into the analysis.

4.2.6 A more correct bucket equation

In Folland and Hsiung's (1986) development of the bucket model, they employ a relationship between the heat and mass transfer coefficients which is only approximate. We have followed their method above, but it is worth noting the correct version. Equ. (1) involves sensible, radiative and latent heat transport terms which we combine here as Q_H

$$Q_H = (k_c + k_r)(T_B - T_A) - k^*L(e_A - e_{sB}) \qquad \ldots(15)$$

Folland and Hsiung simplify this using the approximate relationship $Lk^* \approx (k_c + k_r)/A$ where A is the psychrometer coefficient and L is latent heat. The correct way to do this is to relate k^* and k_c. This requires

writing Q_H in terms of specific humidity

$$Q_H = (k_c + k_r)(T_B - T_A) - \tilde{k}\, L(q_A - q_{sB}) \qquad \ldots(16)$$

In this form, the mass transfer coefficient is related to the convective heat transfer coefficient by

$$\tilde{k} = k_c\, Le^{2/3}/C_p \qquad \ldots(17)$$

where Le is the Lewis number (i.e. Prandtl number divided by Schmidt number) and C_p is the specific heat of moist air at constant pressure (Spalding, 1963). For moist air, Le $\approx$ 1.2. Since $q \approx \epsilon\, e/p$ where $\epsilon = 0.622$ and p is atmospheric pressure, equ. (17) implies

$$k^* = \frac{\epsilon}{pC_p}\,(Le)^{2/3}\, k_c = k_c/A^* \qquad \ldots(18)$$

where $A^* = 0.58$.

If we now use the approximation employed in Section 4.2.1, $e_{sB} \approx e_{sA} + b(T_B - T_A)$ where $b = \partial e_s/\partial T$, together with the k_c and k_r expressions given by Folland and Hsiung, equ. (15) becomes

$$Q_H = (T_B - T_A)[u + \frac{b}{A^*}(u-5.4)] + \frac{e_{sA}}{A^*}(u-5.4)(1-R) \qquad \ldots(19)$$

where $u = 7.80\sqrt{V} + 5.4$. This should be compared with the previous result which is equivalent to

$$Q_H = (T_B - T_A)[u + \frac{b}{A}u] + \frac{e_{sA}}{A}(u)(1-R) \qquad \ldots(20)$$

The difference lies solely in the terms involving A^* or A. To go from equ. (19) to equ. (20) requires replacing $(u-5.4)/A^*$ by u/A. These two terms have quite similar magnitudes (they are identical for $V = 11.2\,ms^{-1}$), confirming that the Folland and Hsiung equation is a reasonable approximation. The solution given by equ. (5) and its variants is unaltered except that T_∞ and τ become

$$T_\infty = T_A - \frac{(u-5.4)(1-R)e_{sA} - A^* Q_B}{A^* u + b(u-5.4)} \qquad \ldots(21)$$

$$\tau = \frac{2410\ A^*}{A^* u + b(u-5.4)} \qquad \ldots(22)$$

If the relaxation times and asymptotic temperatures of the approximate and correct solutions are compared, one finds that, for $V < 11.2 ms^{-1}$, τ(correct) < τ(approx.) and T_∞ (correct) > T_∞ (approx.). The differences, for all practical cases, are less than 5% (expressing the T_∞ difference in terms of $T_S - T_\infty$). For small exposure times ($t \lesssim 8$ minutes) the two solutions differ by only a few hundredths of a degree Celsius for most situations.

In all calculations that follow, we have employed the correct solution (i.e. equ. (5a) together with equs. (21) and (22)) rather than the Folland and Hsiung formulation.

4.3 Application of the bucket model

4.3.1 Model input data

Application of the bucket model (equ. (5a)) requires knowledge of T_B, T_A, R, V (and its components U and v) and Q_B. (e_{sA} and $b = \partial e_{sA}/\partial T$ values were calculated from T_A using the formula of Murray, 1967.) For R, U, T_B and T_A we used climatological values derived for the period 1950-79 from COADS: R and U values were derived by A.H. Oort (personal communication), while for T_B and T_A we derived our own 1950-79 climatology. Representative ship speeds were taken from the shipping literature (e.g. Kirkaldy, 1919) and are the same as suggested by Folland and Hsiung (1986), and Q_B values were as used by Folland and Hsiung (1986) and supplied by D.E. Parker (personal communication, 1989). The use of climatological values is justified by the sensitivity analysis given above. As a further justification, note that we are concerned here primarily with isolating the spatial and seasonal variations in evaporative cooling, variations whose range far exceeds the

range of temporal variations at any one point on the monthly to inter-annual time scale.

There is one aspect of the use of climatological values that requires further comment. With climatological T_A, this means that T_B relaxes towards a climatological 'bucket wet-bulb' temperature, which is clearly incorrect. Nevertheless, because T_A at any grid point for any given month varies only slightly, and because $t \ll \tau$ in general, it is a reasonable approximation. To test it, we replaced T_A by $T_A \pm 2\sigma$ where σ is the standard deviation of monthly-mean T_A values. The results showed only minor differences from the T_A results.

4.3.2 Seasonal cycles in the uncorrected data

The gridded COADS (UKMO) SST data are expressed as anomalies from the appropriate 1950-79 (1951-80) monthly-mean field. This means that, for the base period, virtually the whole of the seasonal cycle of SST at each grid point has been removed. If the intra-annual variations at a grid point are examined for any period prior to 1941, however, there will be a seasonal cycle, due partly to natural variability in the seasonal cycle and partly to the fact that instrumentally introduced "errors" also have a seasonal cycle.

To measure the magnitude of the seasonal cycle we fitted equations of the form

$$T = A \sin(\pi m/6 - \phi)$$

where m is the month number (1, 2, 3....12) and A and ϕ are the best-fit values of the amplitude and phase of the annual cycle in the anomaly data obtained using standard harmonic analysis methods. These analyses were carried out using mean values over the periods 1860-79 and 1905-40, periods during which we expect the correction factors to be roughly constant.

Figure 4.1 gives zonal means for the amplitude of the annual cycle for COADS anomaly data over 1950-79, the base period. The zonal bands were derived by averaging three 4-degree bands to produce slightly overlapping

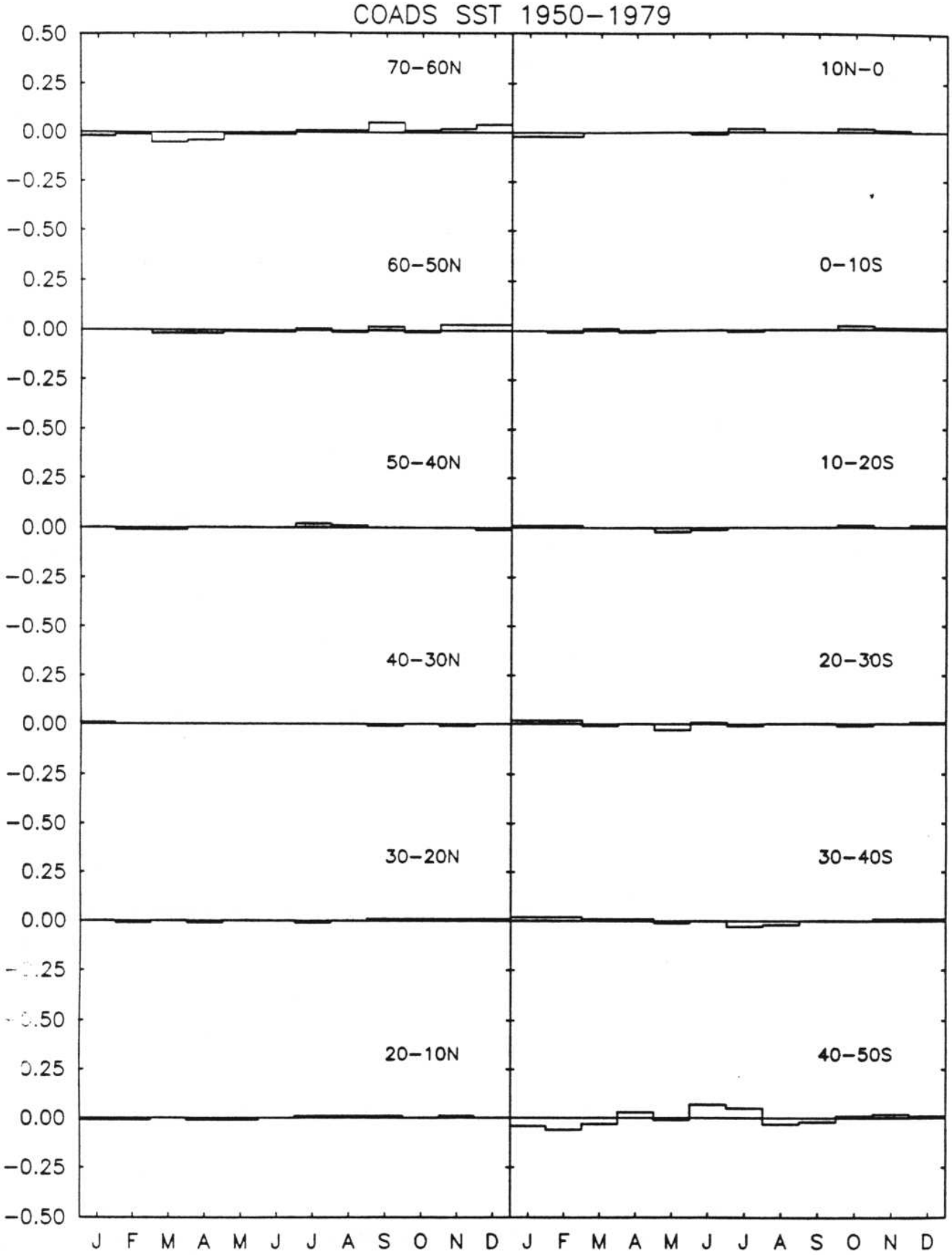

Fig. 4.1: The mean residual annual cycle in the COADS SST data over the period 1950-1979. COADS SST data are anomalies from 1950-1979.

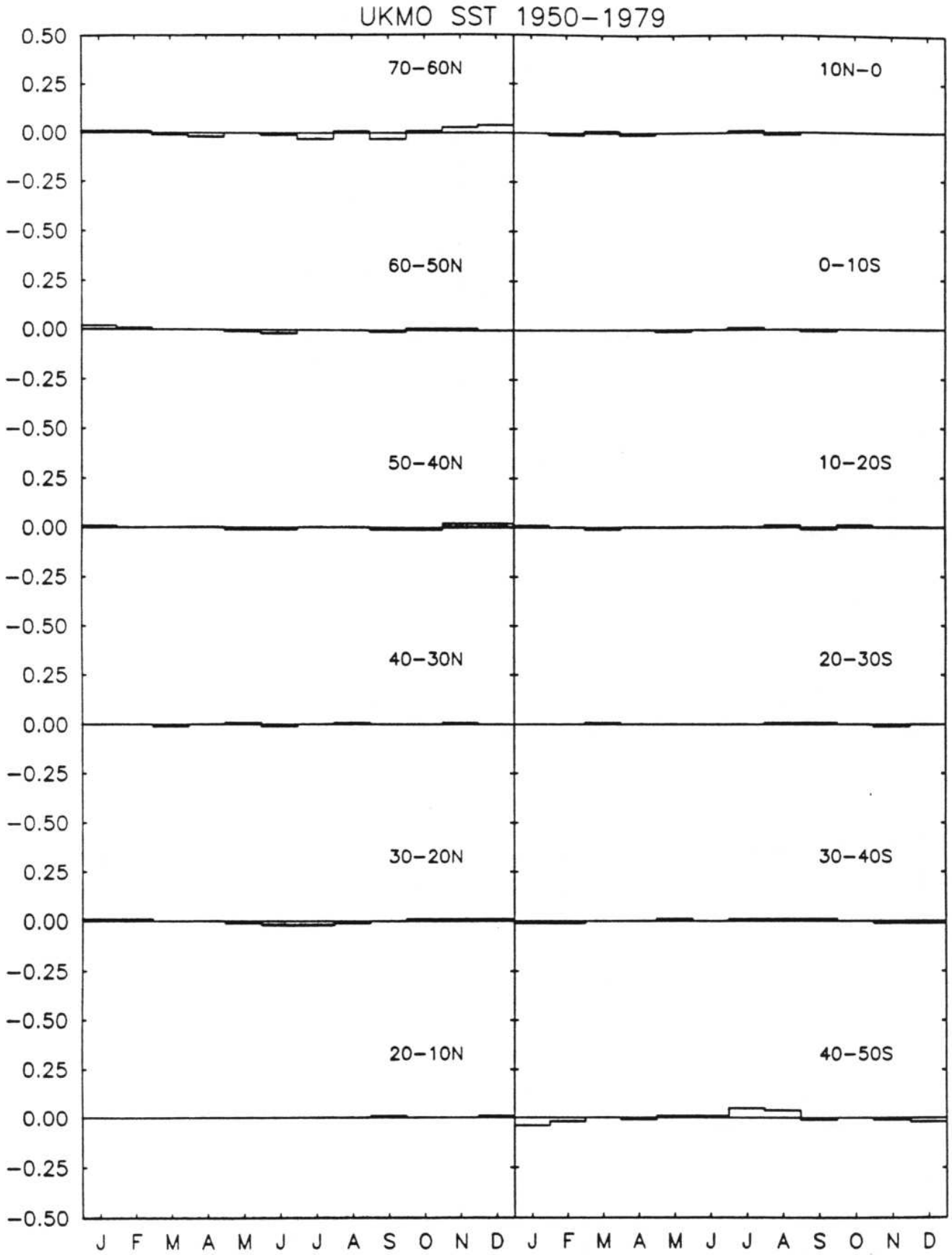

Fig. 4.2: The mean residual cycle in the UKMO SST data over the period 1950-1979. UKMO SSt data are anomalies from 1951-1980.

twelve degree bands. Figure 4.2 shows equivalent results for the UKMO data, based on ten degree bands. As expected, there is very little residual cycle in any of the latitude zones of Figures 4.1 and 4.2.

In Figures 4.3 and 4.4 we show the results of a similar analysis for the period 1905-40. For this period, there is a strong residual cycle in the mid-latitude NH zones, around 20-50°N. The cycle is stronger in COADS than in UKMO. It is this kind of spurious, instrument-based cycle that the temperature corrections have to remove, or, at least, minimize (remembering, of course, that some fraction of the cycle may be due to natural climatic change).

Similar analyses over the period 1860-79 (Figures 4.5 and 4.6) also show residual annual cycles. Once again they are better defined in COADS than in UKMO and they are strongest in the band 20-50°N. (In this early period there are not enough data in the 60-70°N band to undertake the analysis.)

4.3.3 Minimizing the spurious cycle

The bucket model is now used to estimate correction factors, grid point by grid point, for a variety of exposure times up to 8 minutes. The data are then corrected and, for each exposure time, residual annual cycles are calculated. The amplitude of the residual annual cycle will depend on the assumed exposure time.

In Section 4.2 we noted that the most important source of uncertainty in calculating correction factors lies in the V term. To account for this uncertainty, we repeated all our analyses four times using four different sets of V values. Since V depends on ship speed, this was taken to be either $4ms^{-1}$ or $7ms^{-1}$, roughly equivalent to sail and steam ship speeds respectively. The other parameter varied was the proportionality constant relating anemometer wind speed to wind speed around the bucket. These will differ substantially due to wind speed variations with height, and because

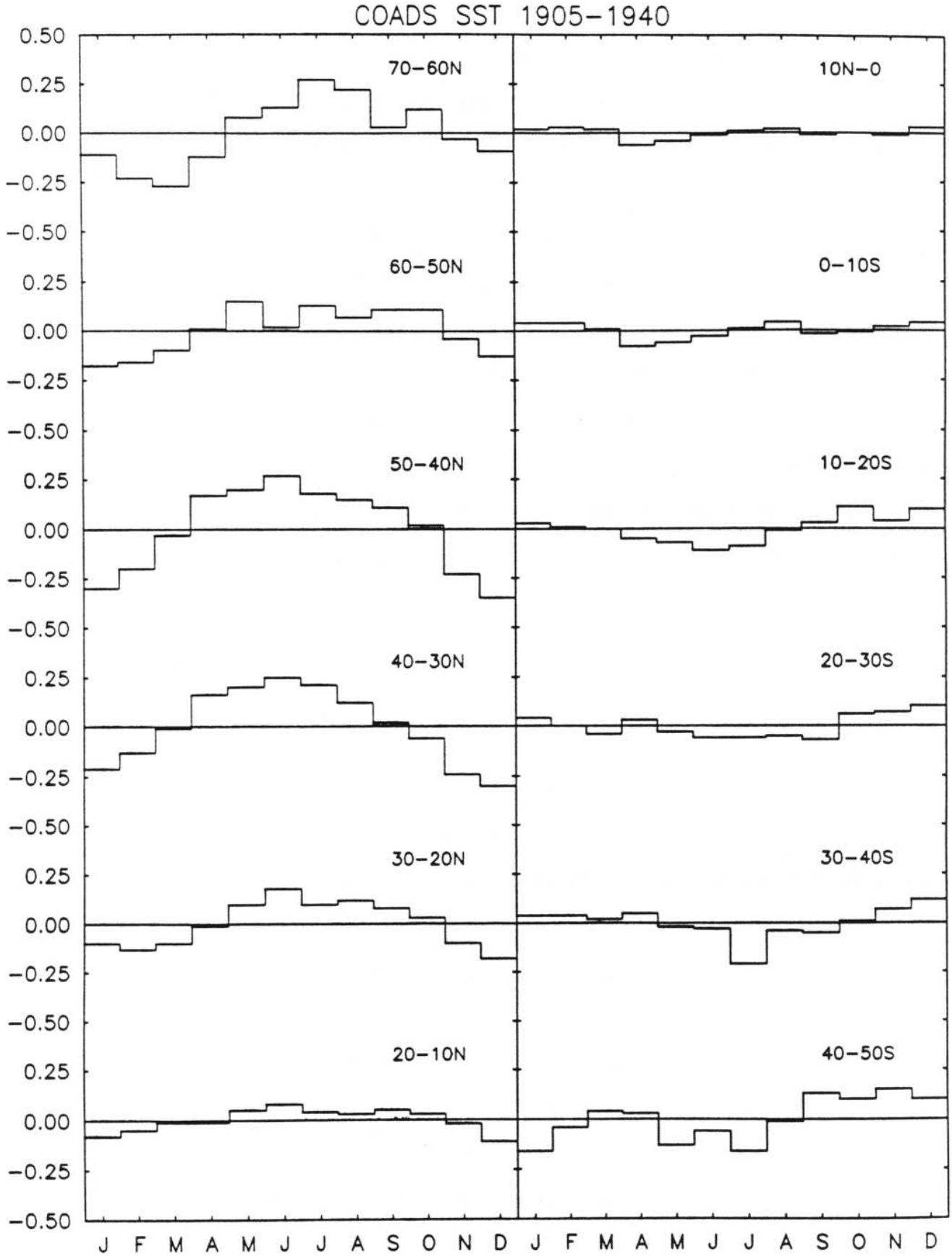

Fig. 4.3: Mean residual annual cycle for COADS SST data over 1905-1940.

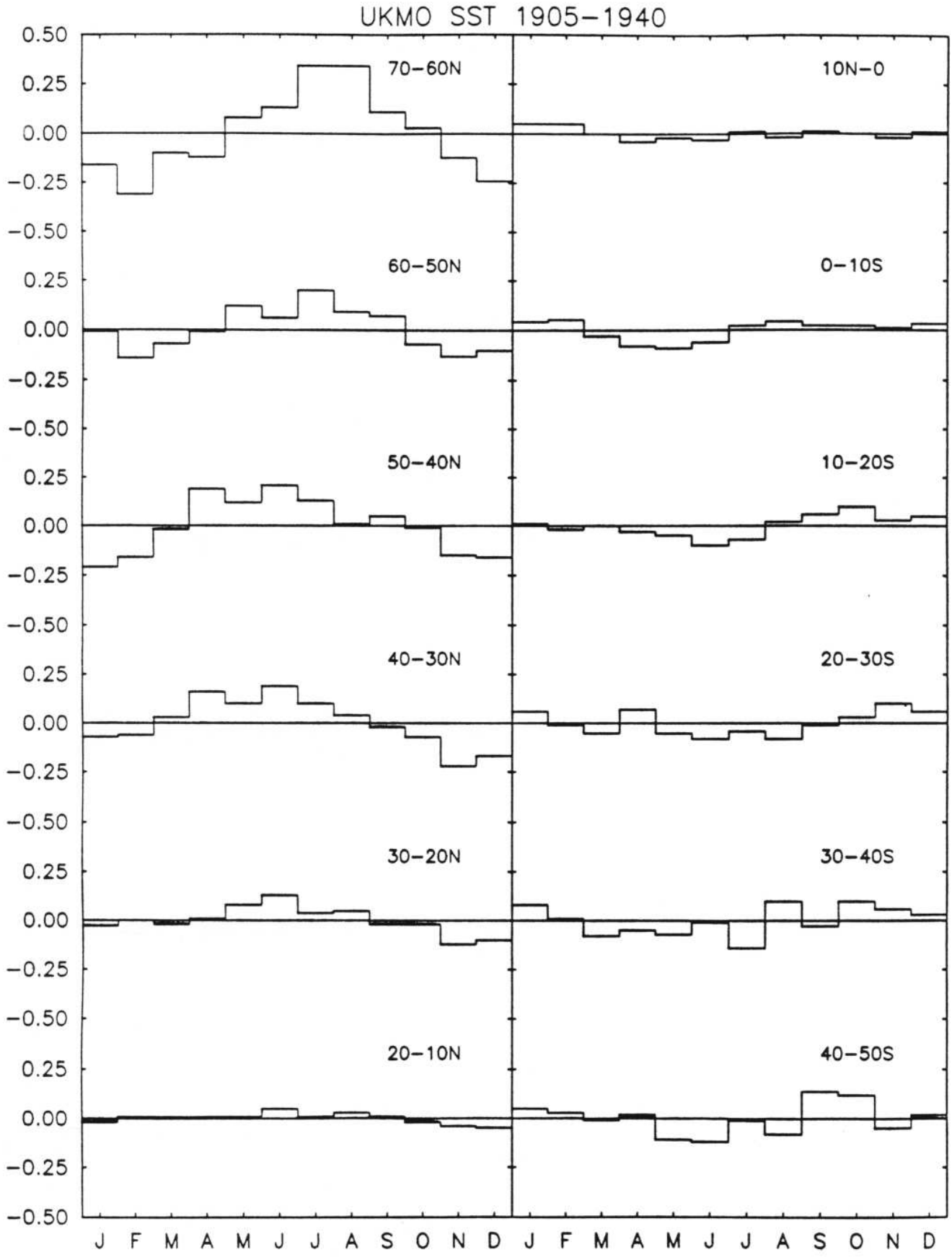

Fig. 4.4: Mean residual annual cycle for UKMO SST data over 1905-1940.

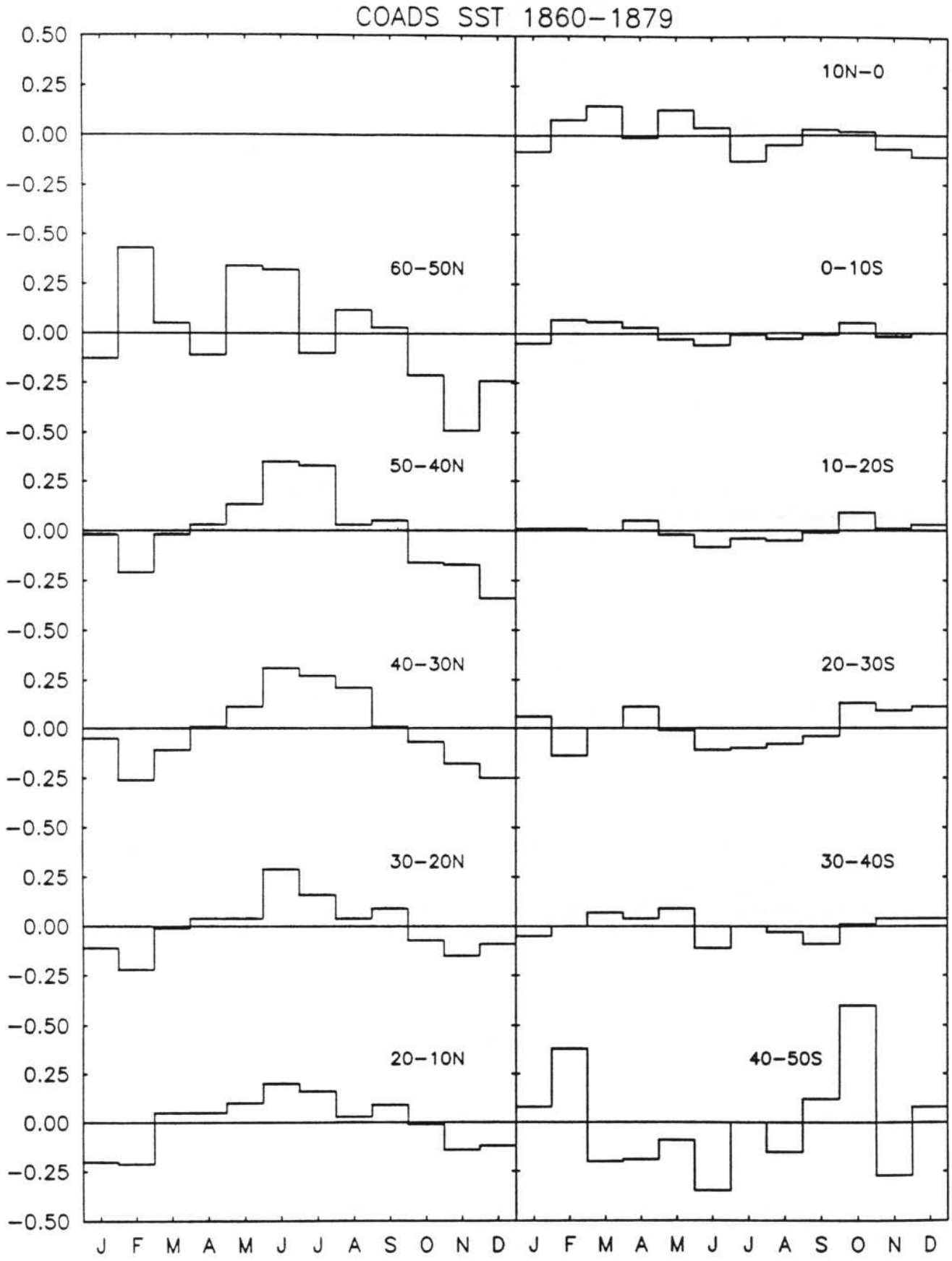

Fig. 4.5: Mean residual annual cycle for COADS SST data over 1860-1879.

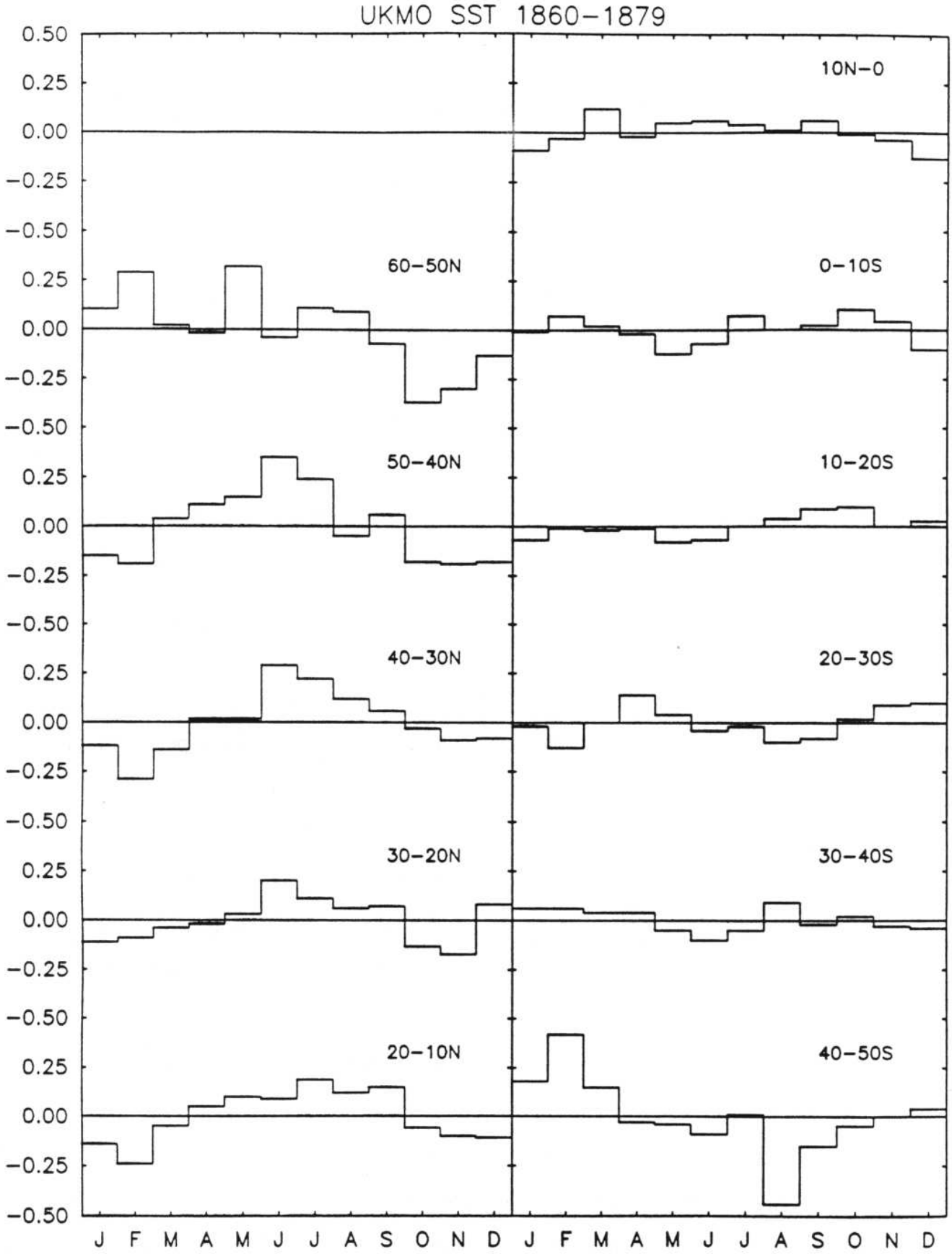

Fig. 4.6: Mean residual annual cycle for UKMO SST data over 1860-1879.

the bucket is likely to be somewhat sheltered both when being hauled up on deck and when standing on deck. Folland and Hsiung (1986) use different proportions while the bucket is hauled to the deck, and when the bucket is standing on the deck. Our analytical approach does not allow us to make such fine distinctions (which will have only a negligible effect on the final results in any event), and we have used either 40% or 60% of the mean anemometer wind speed for the whole of the exposure time.

Figures 4.7 to 4.10 show results for COADS for 1905-40. Some of these show a clear minimum in the residual seasonal cycle, representing the optimum exposure time for that combination of ship speed, wind speed fraction and latitude band. There is little effect in the equatorial bands of 10°N to 10°S, but the seasonal cycles are weak in these regions to begin with.

In Figures 4.3 and 4.4 we saw that the strongest residual cycles were in the northern mid and high latitudes. If a single exposure time is to be chosen, should, therefore, greater weight be given to this region? The answer to this question is "no" because it is likely that natural variability in the seasonal cycle is also large here, making isolation of the non-climatic effect more difficult, and probably leading to a spuriously high value for the exposure time. Allowing, subjectively, for this problem, the exposure time suggested by Figures 4.7 to 4.10 would be 3-6 minutes. The effect of ship speed on this judgement, and on the positions of the minima, is negligible; as can be seen by comparing Figures 4.7 with 4.9, and 4.8 with 4.10. Using a higher percentage wind speed produces exposure times which are a minute or less shorter than those based on the lower percentage, and the minima tend to be a little better defined for the higher percentage cases: compare Figure 4.7 with 4.8, and 4.9 with 4.10.

Applying this method to earlier SST data (1860-79) is somewhat more complicated because of possible changes in bucket type. To account for

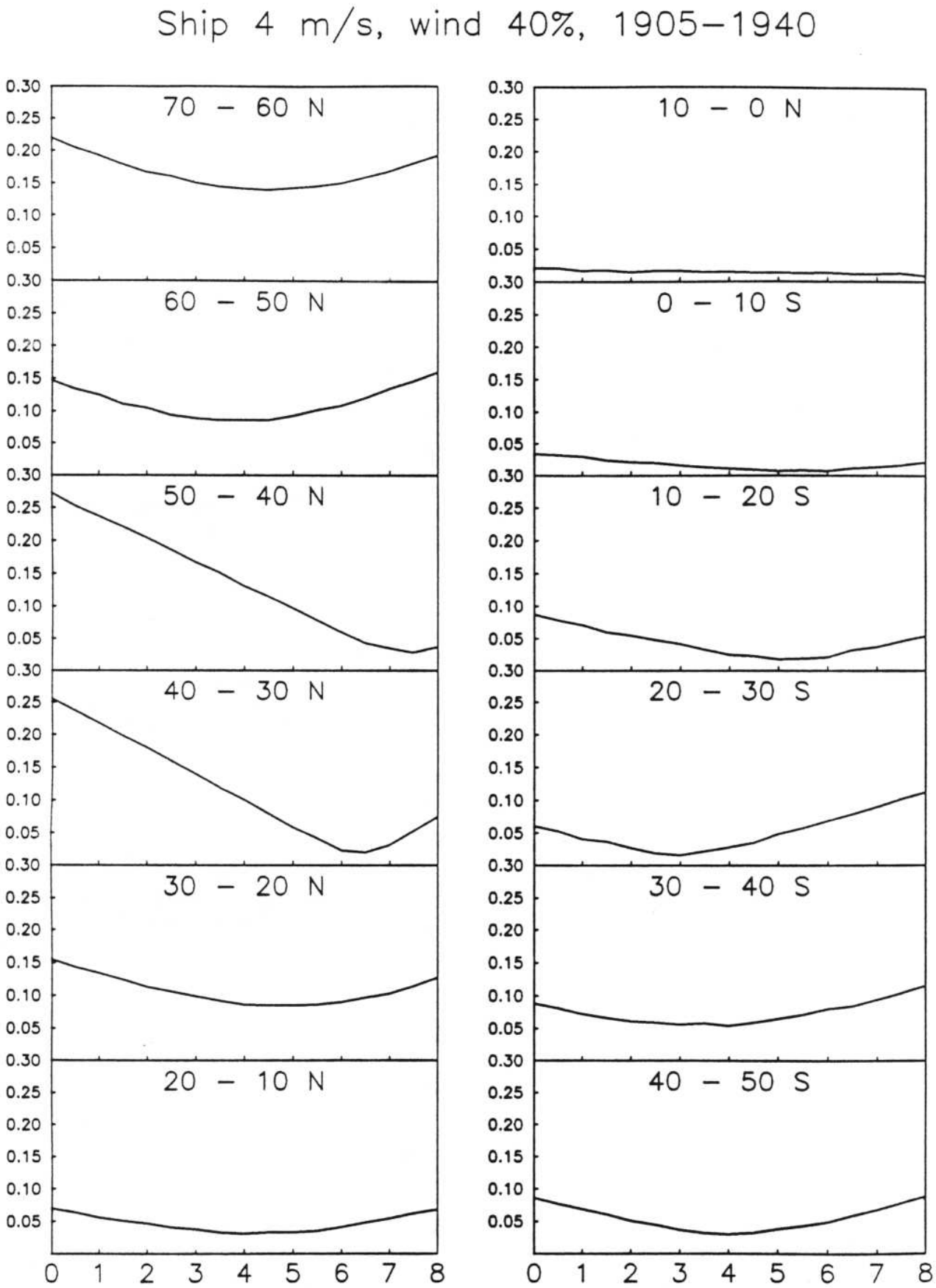

Fig. 4.7: Minimizing the spurious cycle. Zonal averages for the period 1905-40 using a ship speed of $4ms^{-1}$, 40% mean anemometer wind speed. Calculated exposure times are from 0 to 8 minutes in 0.5 minute steps.

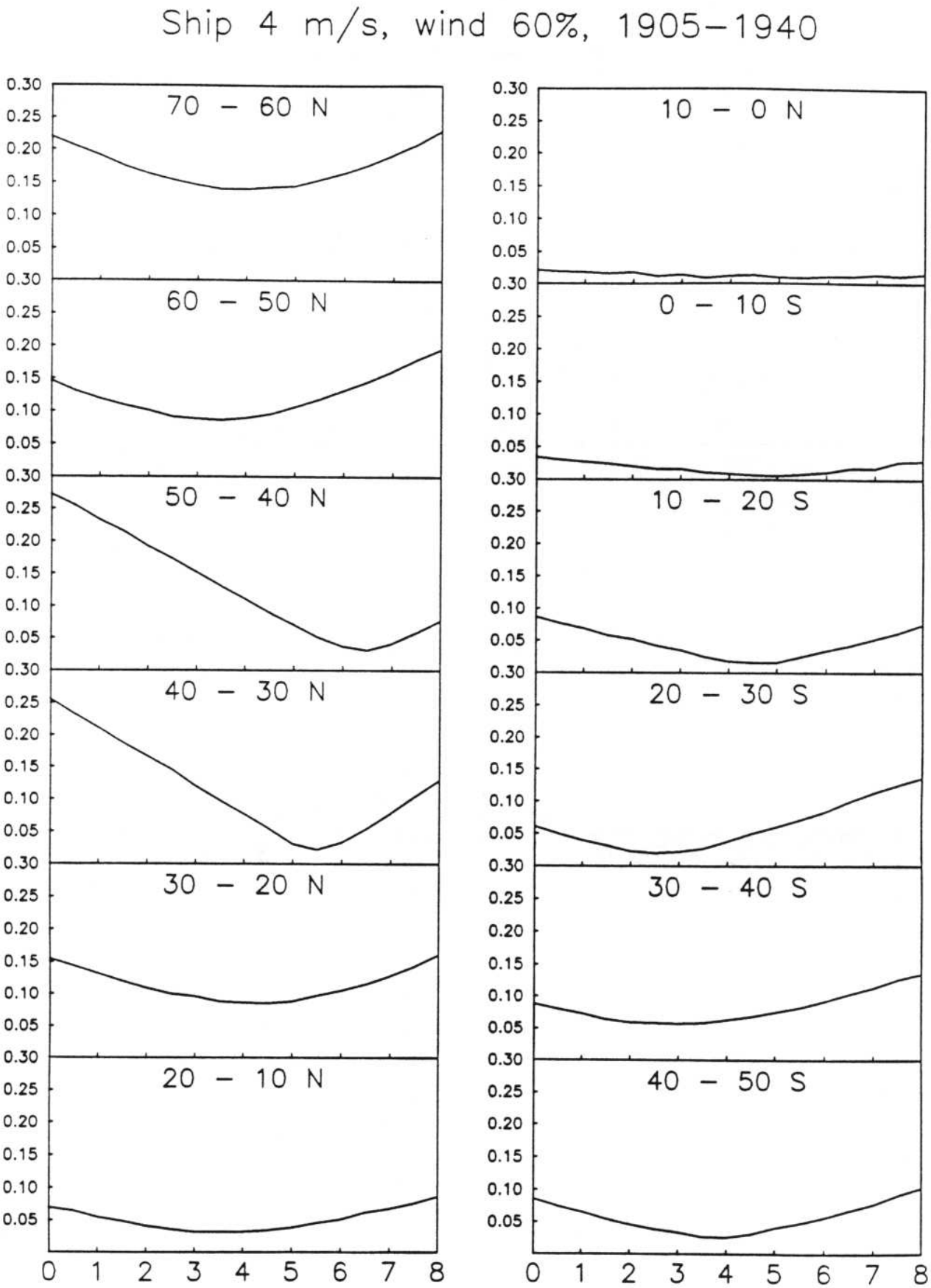

Fig. 4.8: Minimizing the spurious cycle. Zonal averages for the period 1905-40 using a ship speed of $4ms^{-1}$, 60% mean anemometer wind speed. Calculated exposure times are from 0 to 8 minutes in 0.5 minute steps.

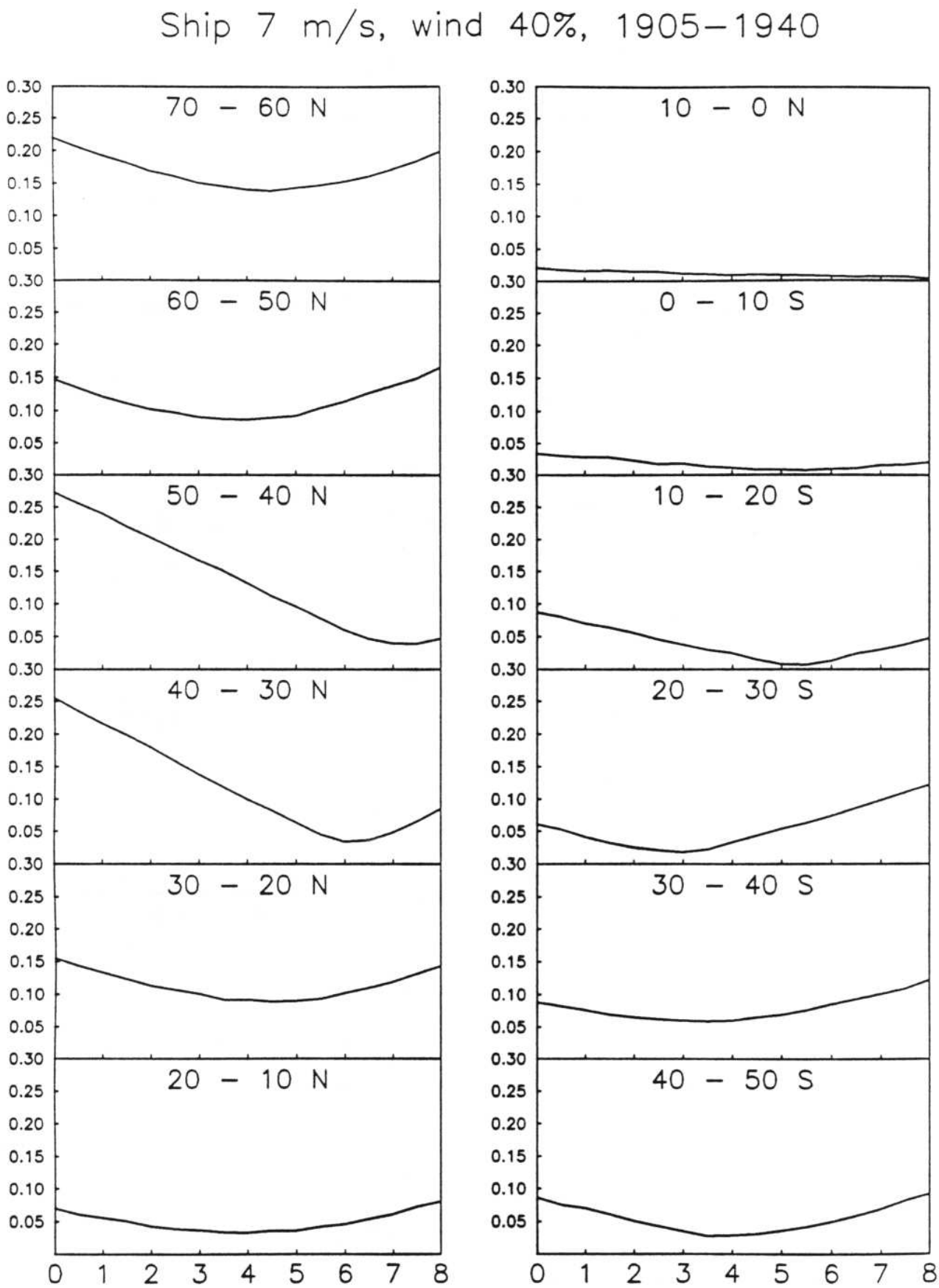

Fig. 4.9: Minimizing the spurious cycle. Zonal averages for the period 1905-40 using a ship speed of $7ms^{-1}$, 40% mean anemometer wind speed. Calculated exposure times are from 0 to 8 minutes in 0.5 minute steps.

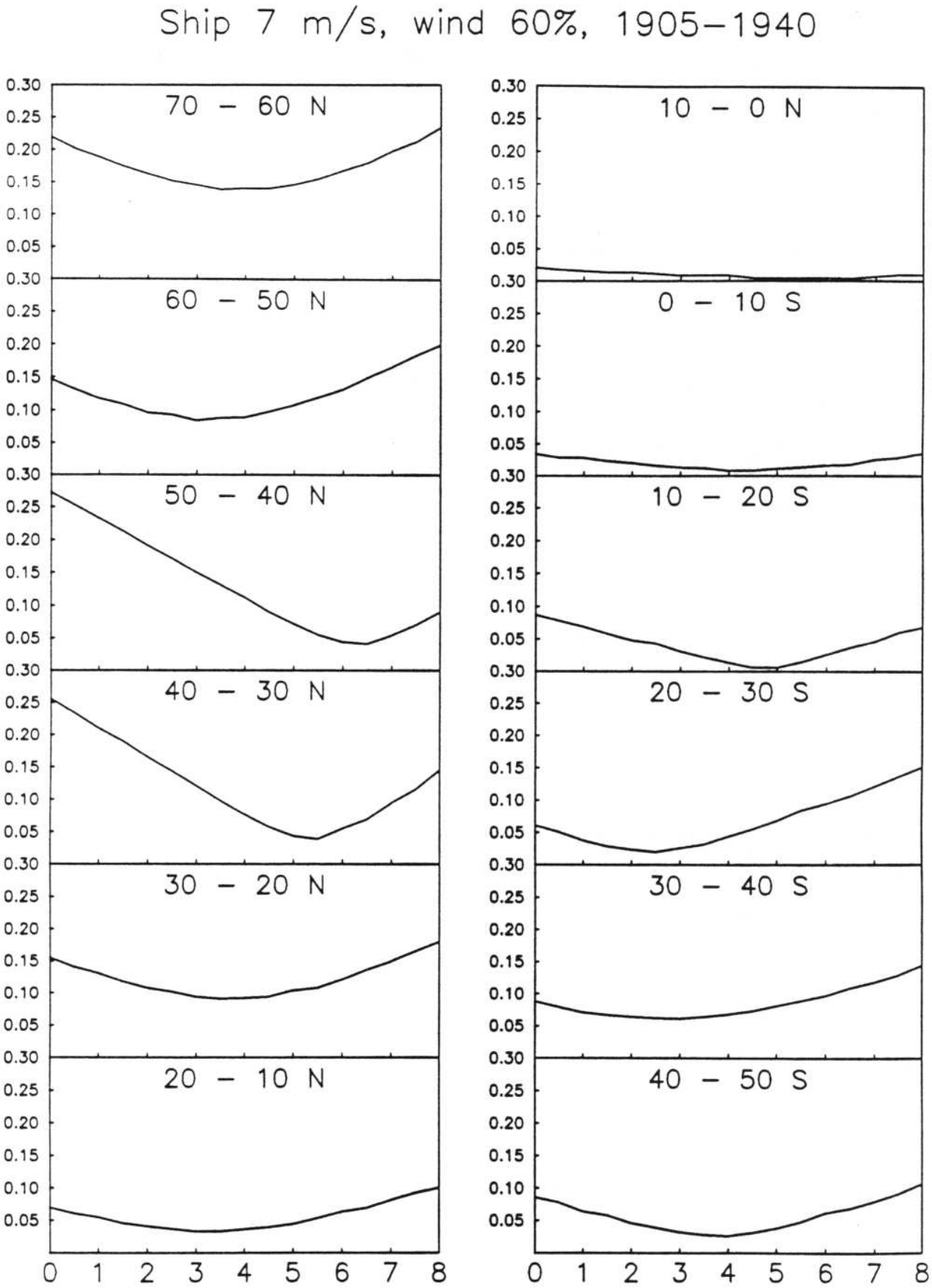

Fig. 4.10: Minimizing the spurious cycle. Zonal averages for the period 1905-40 using a ship speed of $7ms^{-1}$, 60% mean anemometer wind speed. Calculated exposure times are from 0 to 8 minutes in 0.5 minute steps.

this we have assumed various fractions of uninsulated bucket, 1/4, 1/2, 3/4 and 1 (see section 4.2.3), and repeated the 1905-40 calculations for the period 1860-79. The results, four times as many as for 1905-40, are shown in Figures 4.11 to 4.26. They differ markedly from the 1905-40 results in a number of ways. Firstly, the tropical bands generally show a higher residual cycle amplitude in the raw data (i.e. zero minutes exposure time), suggesting, in accord with expectations, that the fraction of natural variability in the 1860-79 seasonal cycle anomalies relative to 1950-79 is greater than for 1905-40. Secondly, compared with 1905-40 there is less difference between the Figures for any given uninsulated bucket fraction, suggesting that the effect of ship speed and percentage wind speed is minimal. Although it is difficult to draw any firm conclusions from this result, it is consistent with our earlier suggestion that evaporative cooling is not the main cause of the seasonal cycle anomalies. Thirdly, there is greater spatial variability in the positions of the minima, with much lower exposure times suggested for the SH than for the NH. This result is incompatible with the idea of a significant evaporative cooling effect; although it could also be an indication that noise due to data uncertainties and natural climatic variability is masking the cooling effect.

If results for different uninsulated bucket fractions are compared, we note that lower bucket fraction gives a later minimum. For the Southern Hemisphere, a low bucket fraction is required to produce results consistent with those for 1905-40. For the Northern Hemisphere, the reverse is true. We suspect, however, that there were larger natural changes in the amplitude of the seasonal cycle in the Northern Hemisphere than in the Southern Hemisphere. What the bucket model is therefore trying to do, is remove not only any spurious annual cycle in the data, but also the real annual cycle changes. If natural changes were in the same direction as the spurious cycle, then this would mean that the optimum exposure time would be inflated. While arguments like this can explain the results obtained

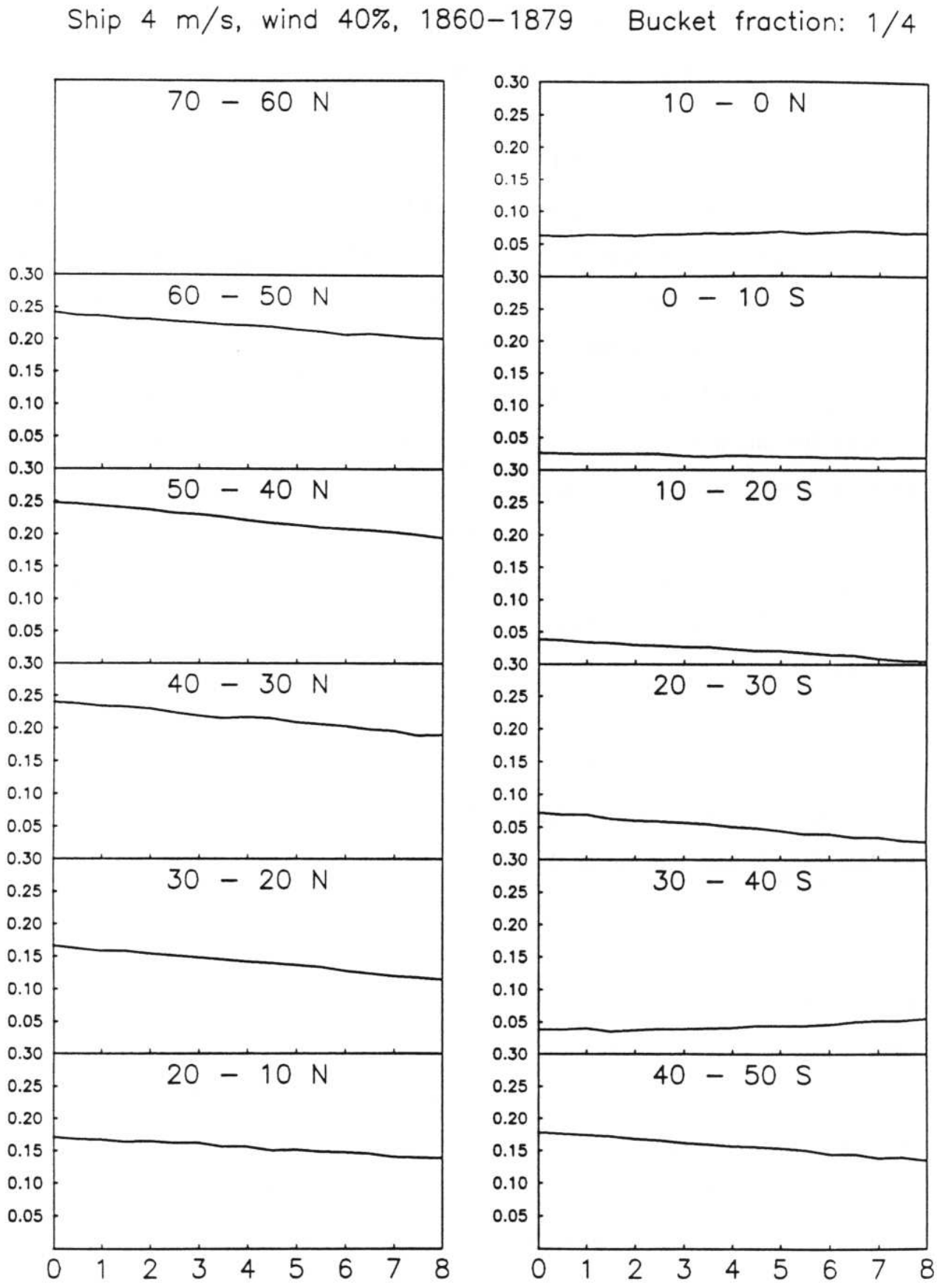

Fig. 4.11: Minimizing the spurious annual cycle with the addition of a bucket fraction i.e. the assumed fraction of canvas buckets in use. The period for Figures 4.11 to 4.26 is 1860-79. This figure shows a ship speed of $4ms^{-1}$, 40% mean anemometer wind speed and a bucket fraction of 0.25.

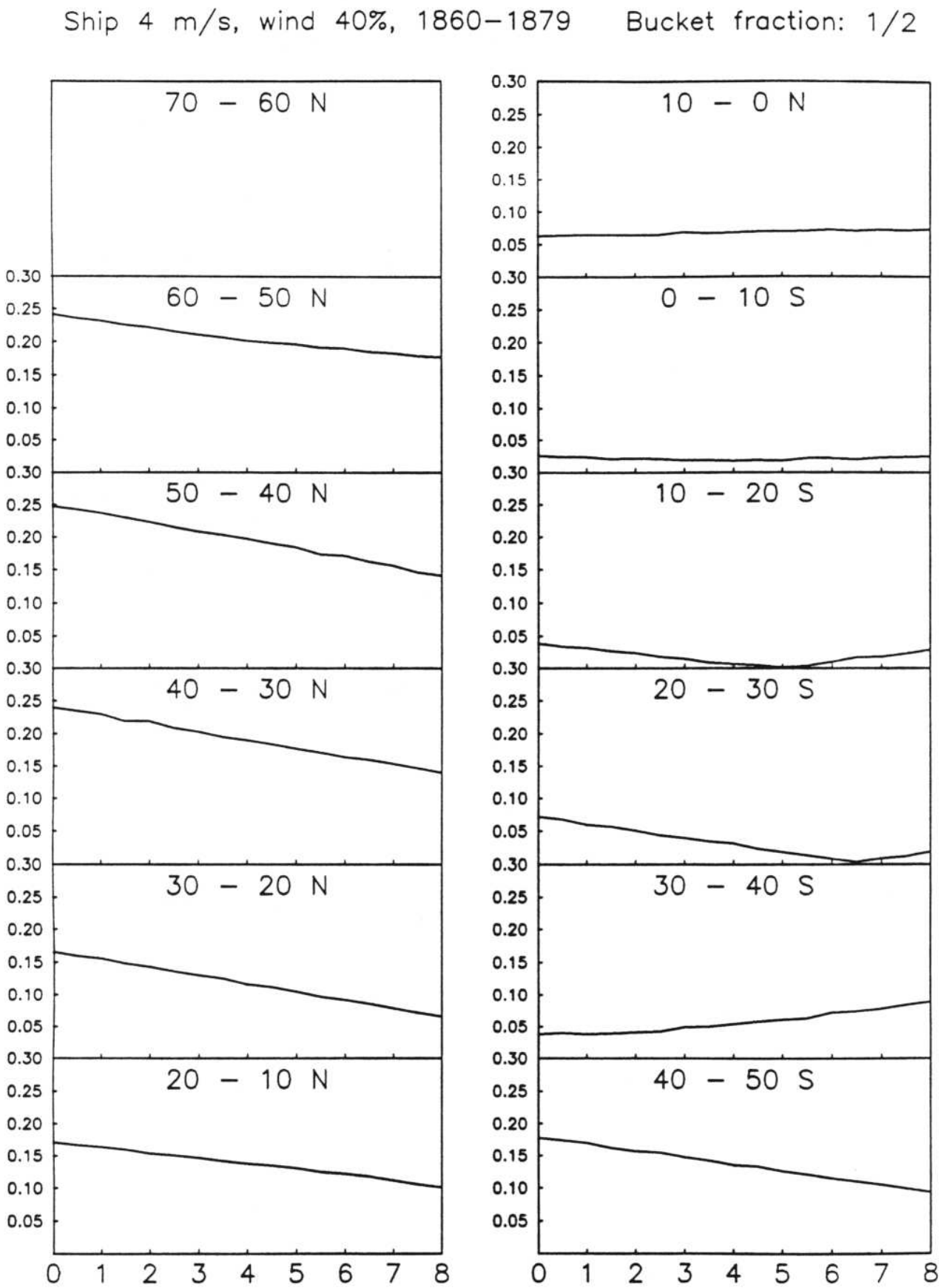

Fig. 4.12: Minimizing the spurious annual cycle with the addition of a bucket fraction i.e. the assumed fraction of canvas buckets in use. The period for Figures 4.11 to 4.26 is 1860-79. This figure shows a ship speed of $4ms^{-1}$, 40% mean anemometer wind speed and a bucket fraction of 0.5.

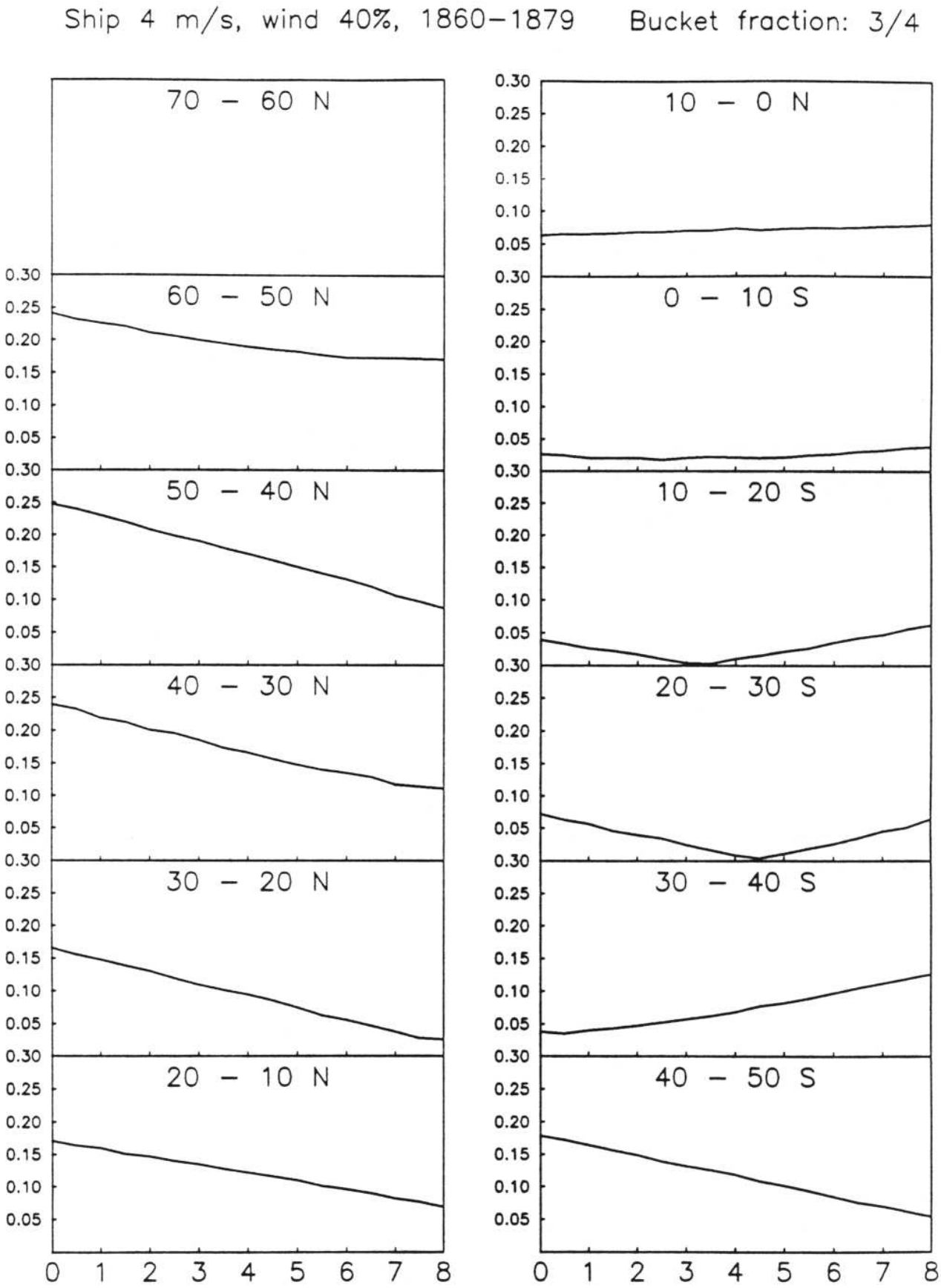

Fig. 4.13: Minimizing the spurious annual cycle with the addition of a bucket fraction i.e. the assumed fraction of canvas buckets in use. The period for Figures 4.11 to 4.26 is 1860-79. This figure shows a ship speed of $4ms^{-1}$, 40% mean anemometer wind speed and a bucket fraction of 0.75.

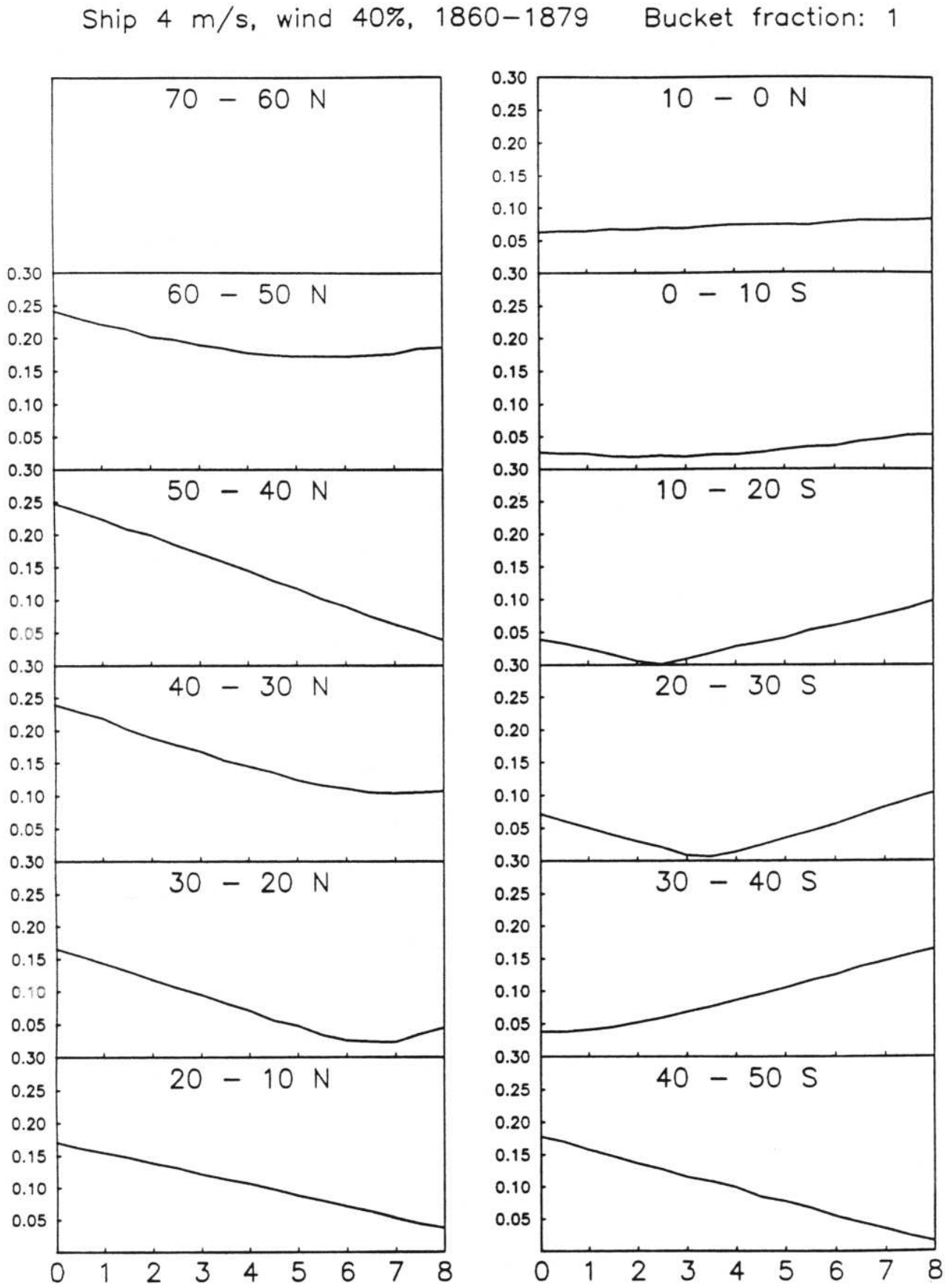

Fig. 4.14: Minimizing the spurious annual cycle with the addition of a bucket fraction i.e. the assumed fraction of canvas buckets in use. The period for Figures 4.11 to 4.26 is 1860-79. This figure shows a ship speed of $4ms^{-1}$, 40% mean anemometer wind speed and a bucket fraction of 1.0.

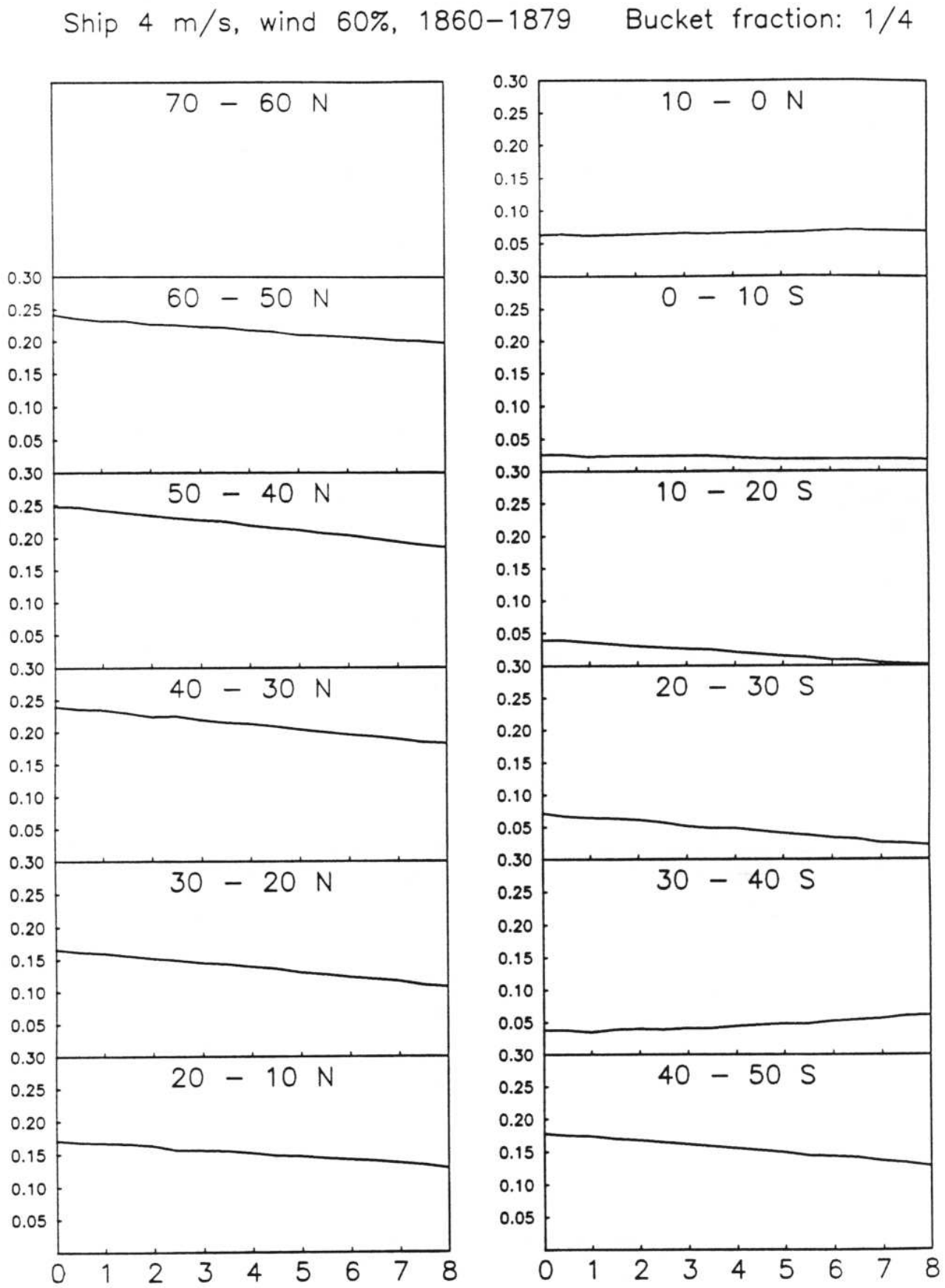

Fig. 4.15: Minimizing the spurious annual cycle with the addition of a bucket fraction i.e. the assumed fraction of canvas buckets in use. The period for Figures 4.11 to 4.26 is 1860-79. This figure shows a ship speed of $4ms^{-1}$, 60% mean anemometer wind speed and a bucket fraction of 0.25.

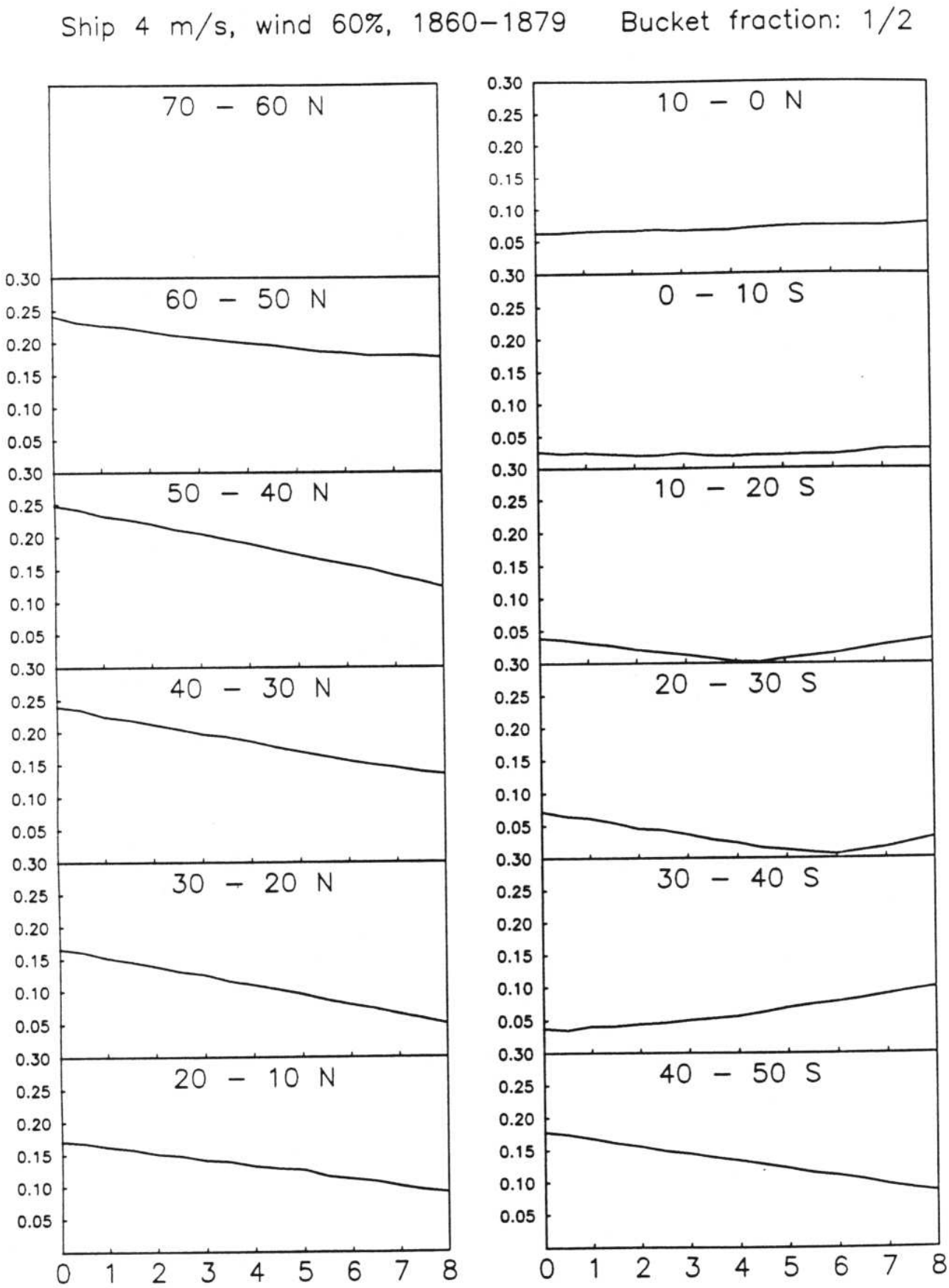

Fig. 4.16: Minimizing the spurious annual cycle with the addition of a bucket fraction i.e. the assumed fraction of canvas buckets in use. The period for Figures 4.11 to 4.26 is 1860-79. This figure shows a ship speed of $4ms^{-1}$, 60% mean anemometer wind speed and a bucket fraction of 0.5.

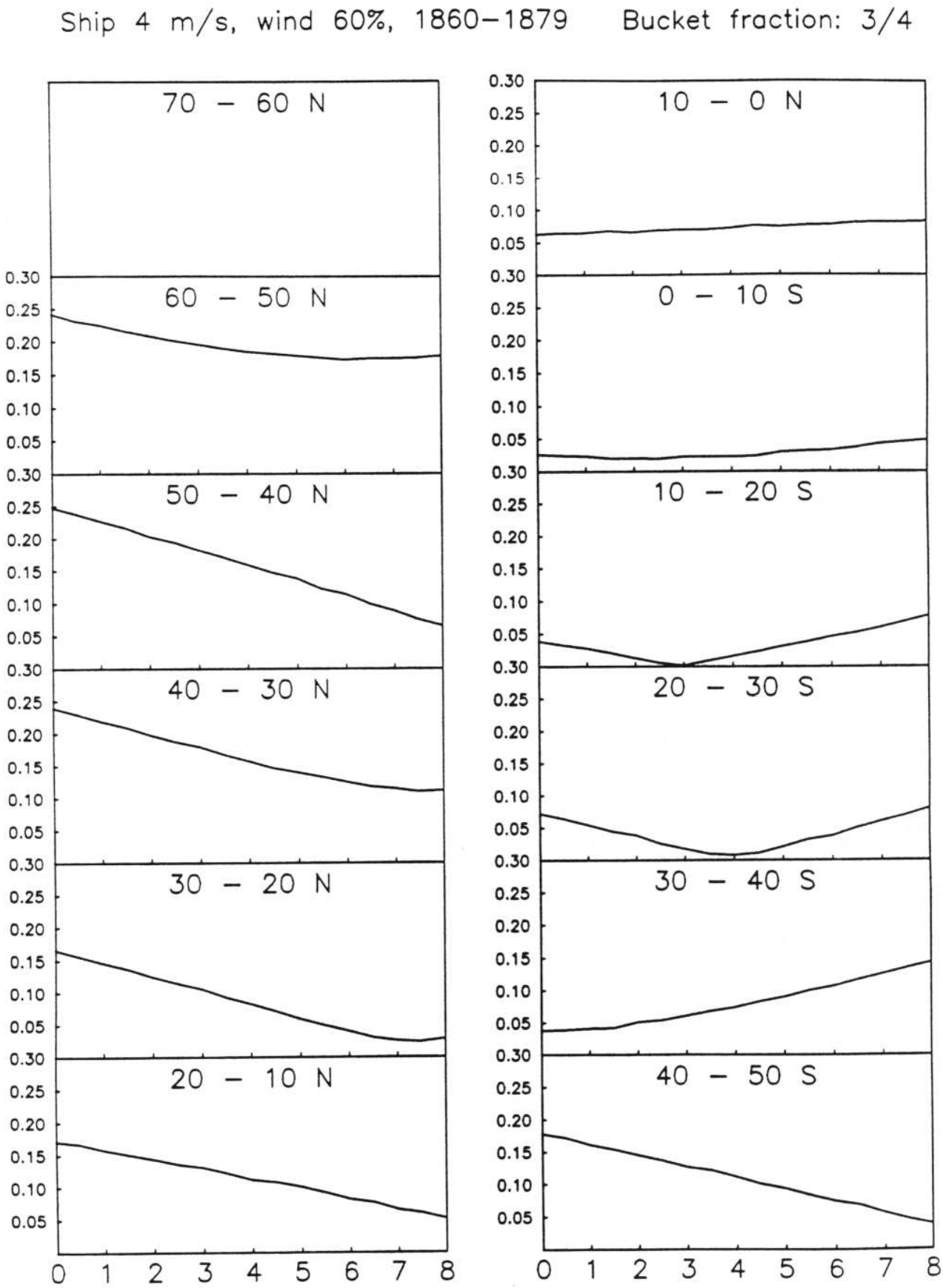

Fig. 4.17: Minimizing the spurious annual cycle with the addition of a bucket fraction i.e. the assumed fraction of canvas buckets in use. The period for Figures 4.11 to 4.26 is 1860-79. This figure shows a ship speed of $4ms^{-1}$, 60% mean anemometer wind speed and a bucket fraction of 0.75.

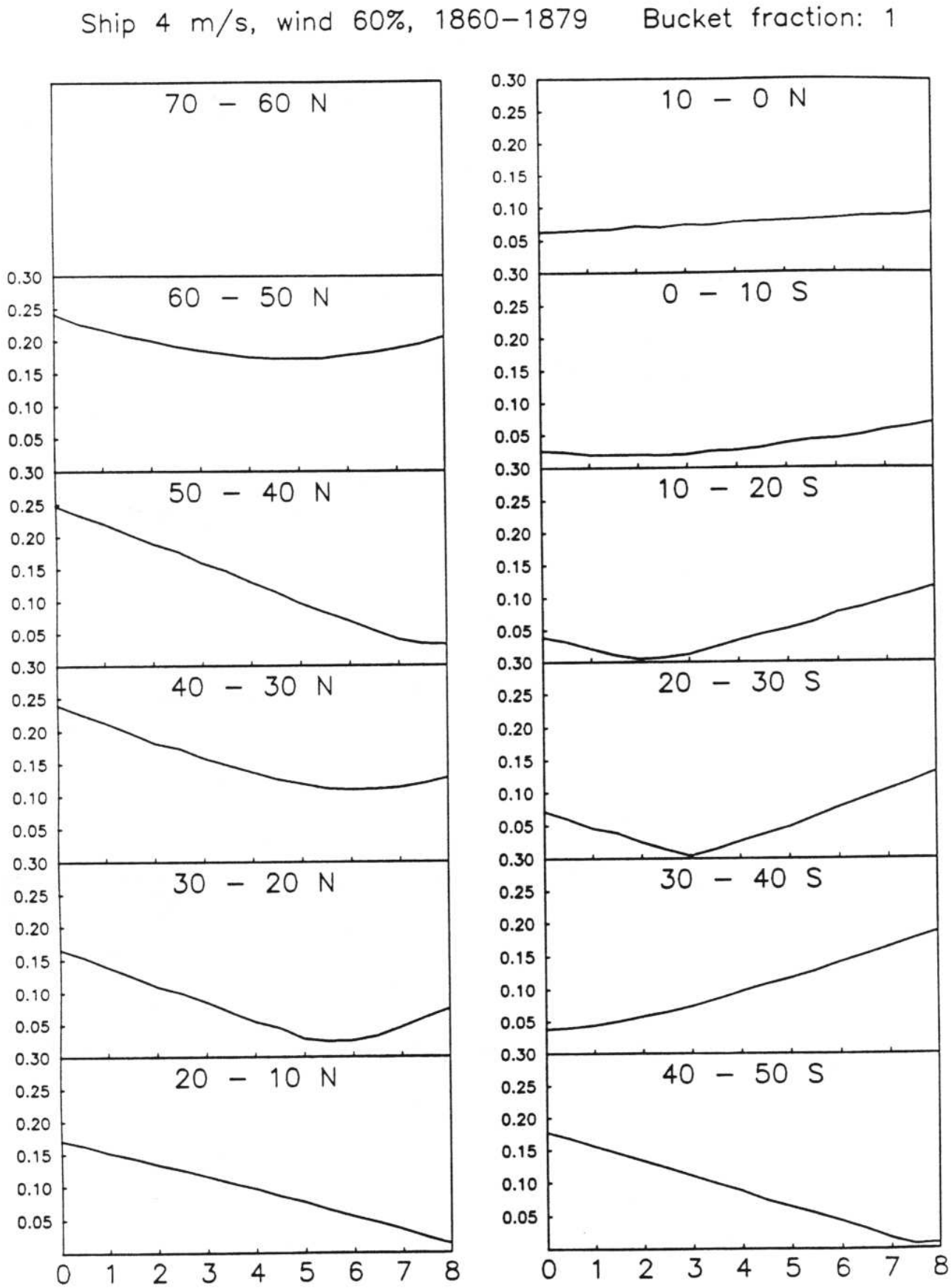

Fig. 4.18: Minimizing the spurious annual cycle with the addition of a bucket fraction i.e. the assumed fraction of canvas buckets in use. The period for Figures 4.11 to 4.26 is 1860-79. This figure shows a ship speed of $4ms^{-1}$, 60% mean anemometer wind speed and a bucket fraction of 1.0.

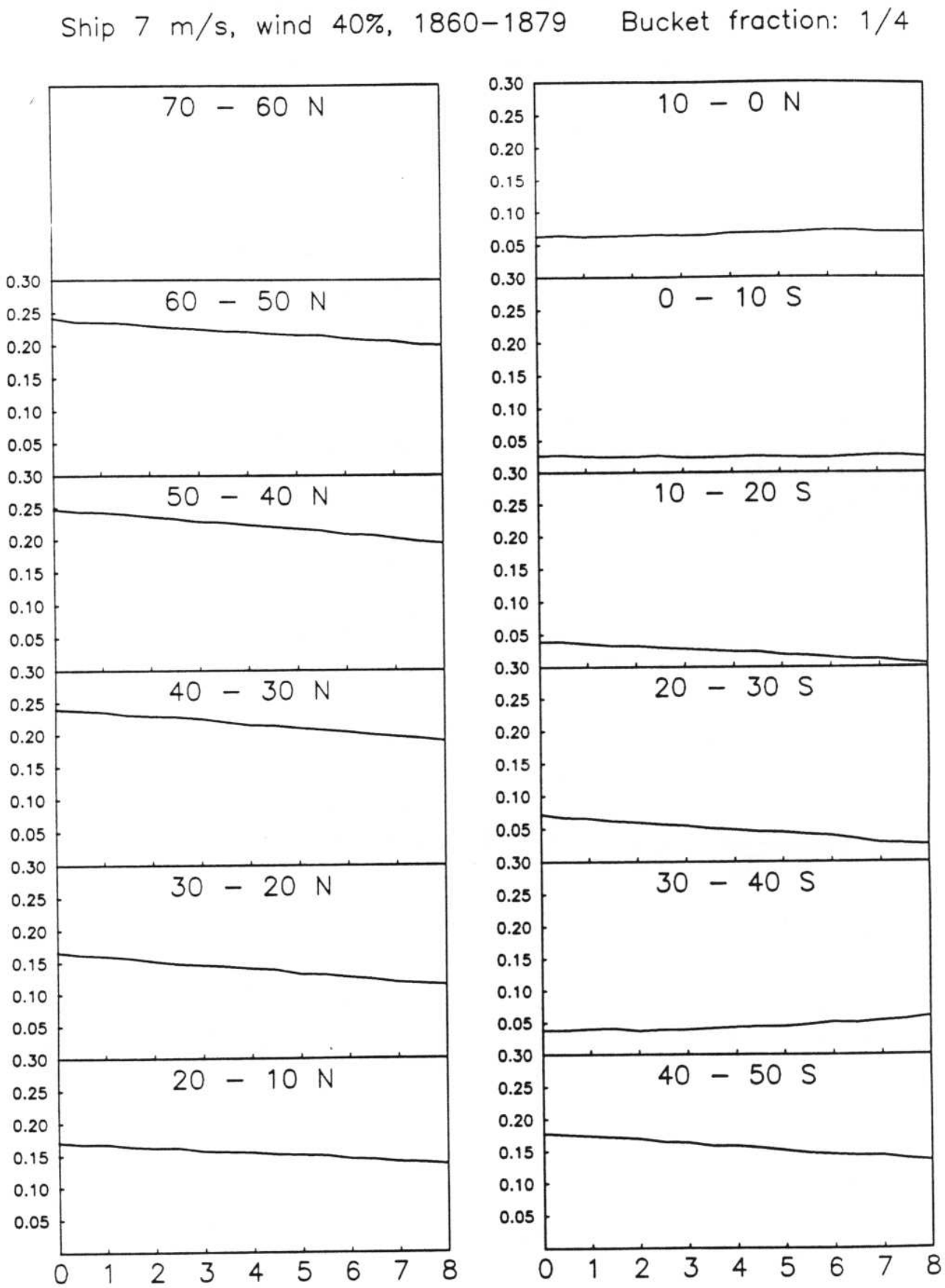

Fig. 4.19: Minimizing the spurious annual cycle with the addition of a bucket fraction i.e. the assumed fraction of canvas buckets in use. The period for Figures 4.11 to 4.26 is 1860-79. This figure shows a ship speed of $7ms^{-1}$, 40% mean anemometer wind speed and a bucket fraction of 0.25.

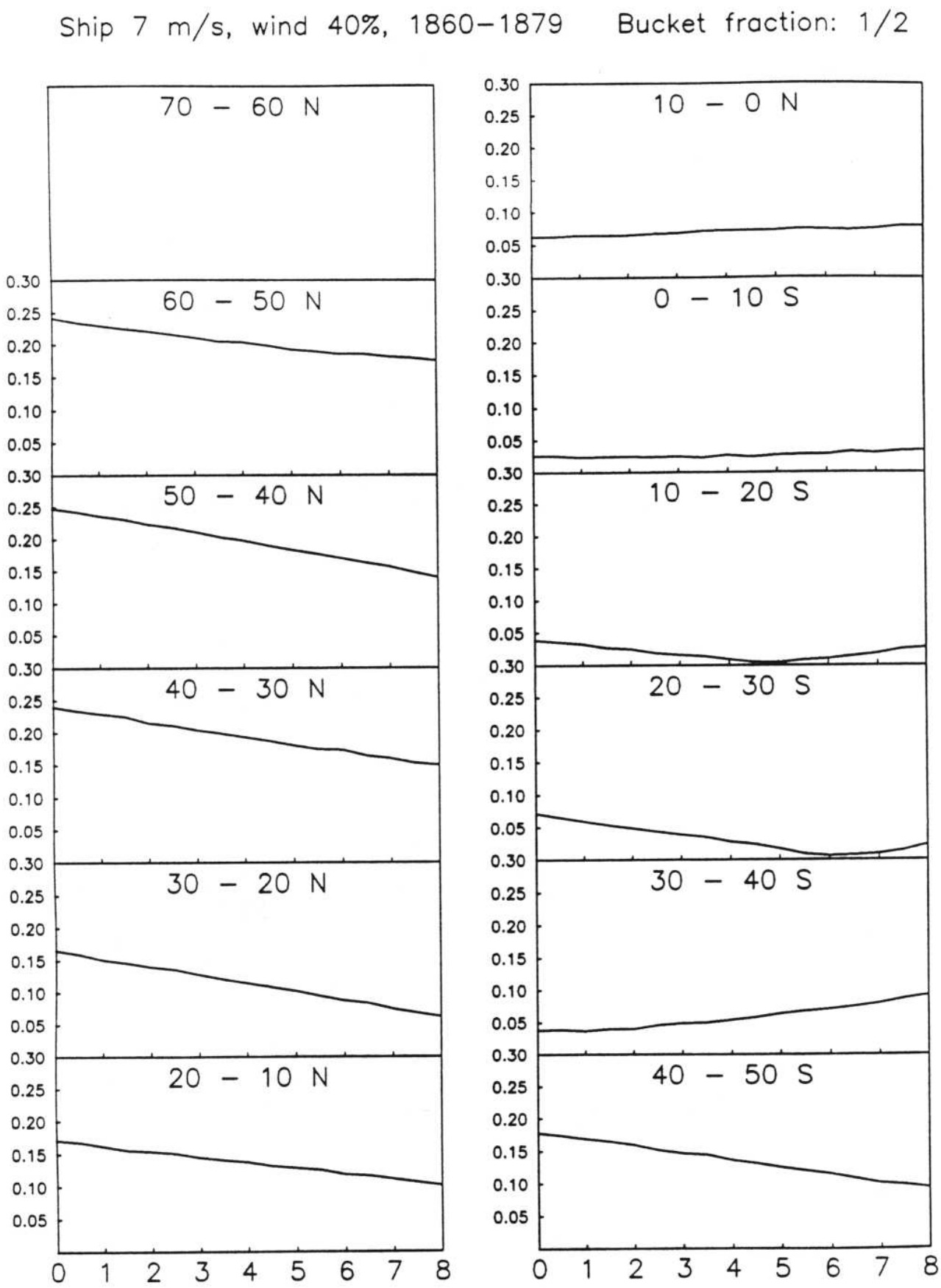

Fig. 4.20: Minimizing the spurious annual cycle with the addition of a bucket fraction i.e. the assumed fraction of canvas buckets in use. The period for Figures 4.11 to 4.26 is 1860-79. This figure shows a ship speed of $7ms^{-1}$, 40% mean anemometer wind speed and a bucket fraction of 0.5.

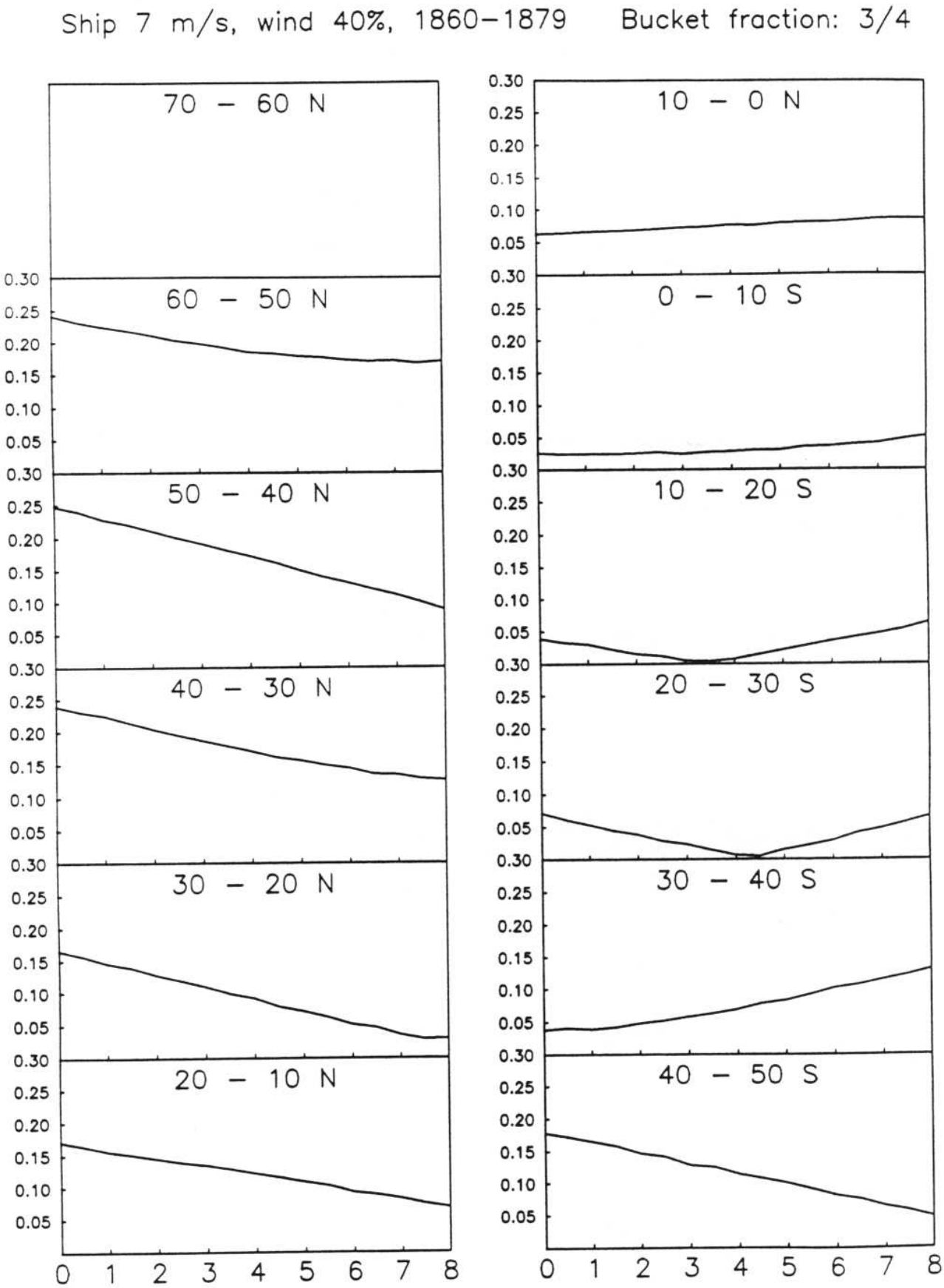

Fig. 4.21: Minimizing the spurious annual cycle with the addition of a bucket fraction i.e. the assumed fraction of canvas buckets in use. The period for Figures 4.11 to 4.26 is 1860-79. This figure shows a ship speed of $7ms^{-1}$, 40% mean anemometer wind speed and a bucket fraction of 0.75.

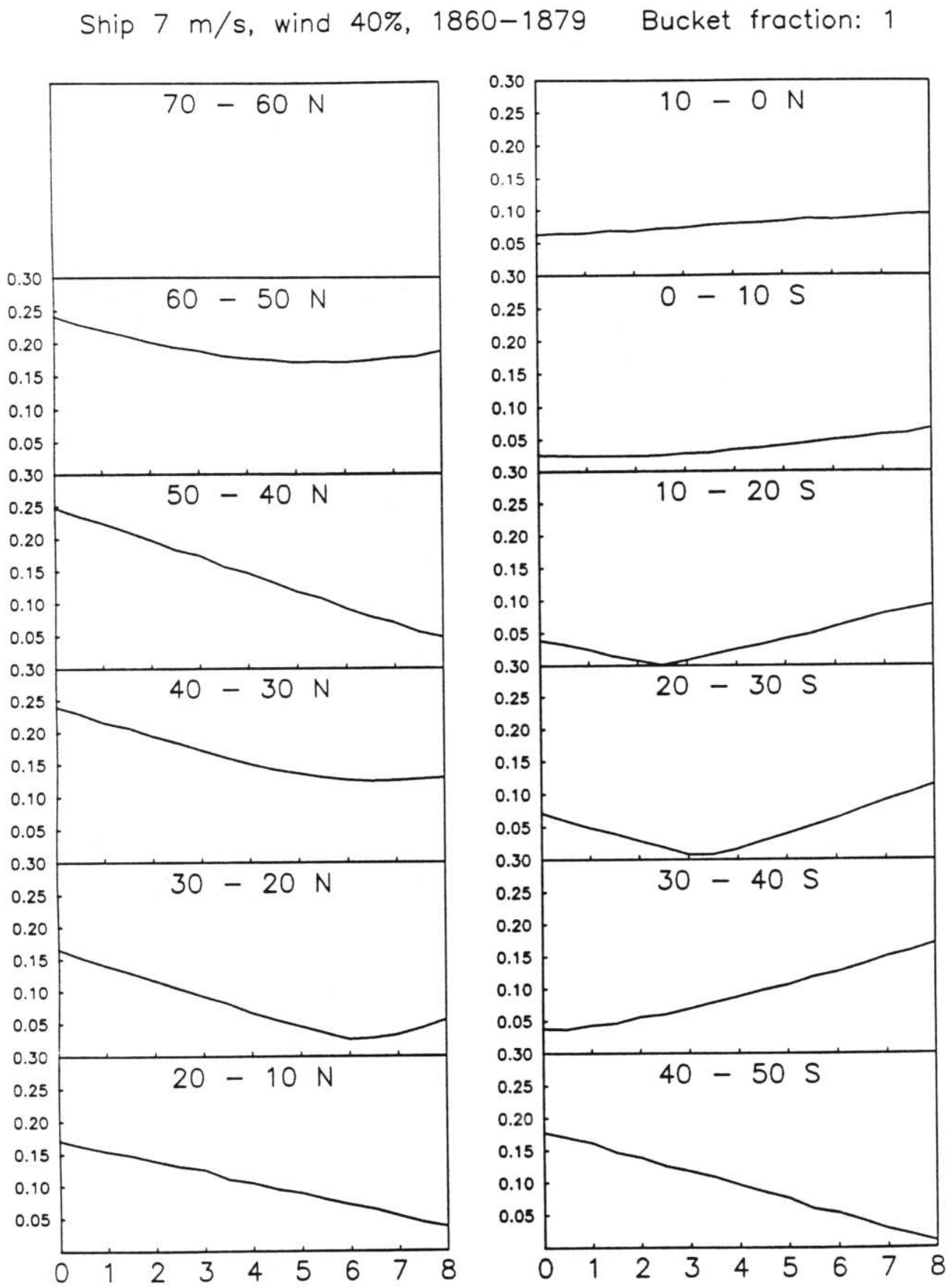

Fig. 4.22: Minimizing the spurious annual cycle with the addition of a bucket fraction i.e. the assumed fraction of canvas buckets in use. The period for Figures 4.11 to 4.26 is 1860-79. This figure shows a ship speed of $7ms^{-1}$, 40% mean anemometer wind speed and a bucket fraction of 1.0.

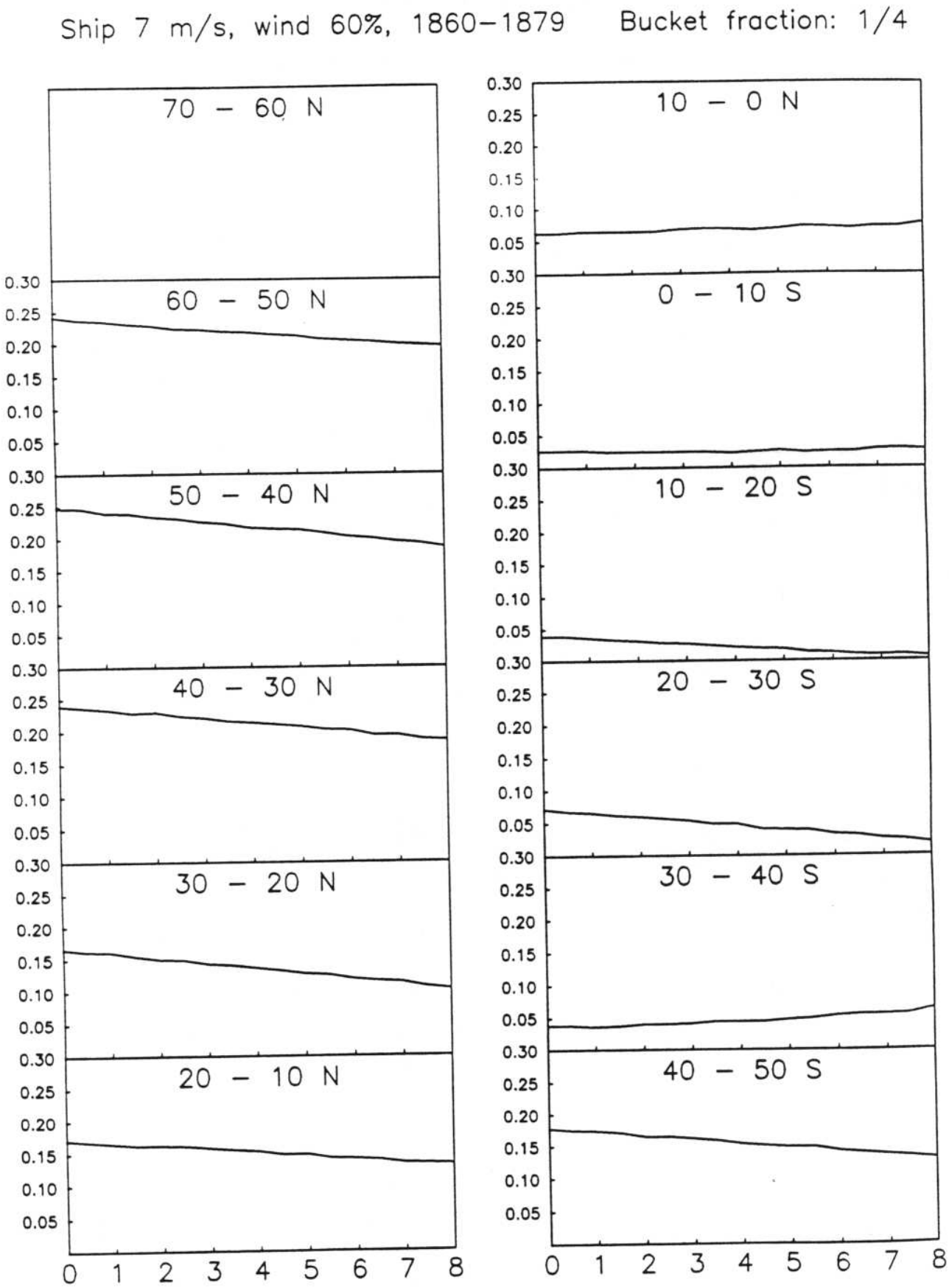

Fig. 4.23: Minimizing the spurious annual cycle with the addition of a bucket fraction i.e. the assumed fraction of canvas buckets in use. The period for Figures 4.11 to 4.26 is 1860-79. This figure shows a ship speed of $7ms^{-1}$, 60% mean anemometer wind speed and a bucket fraction of 0.25.

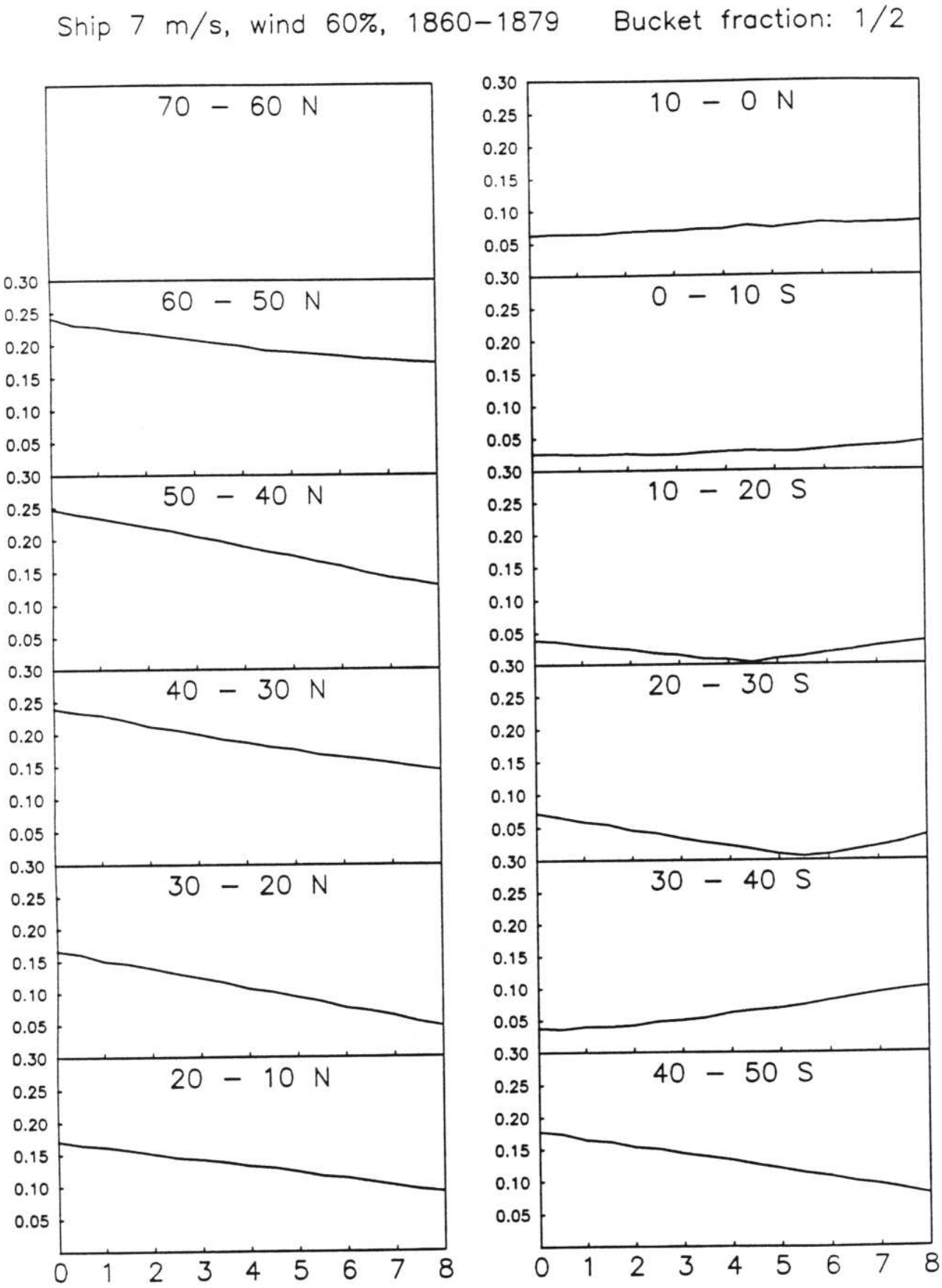

Fig. 4.24: Minimizing the spurious annual cycle with the addition of a bucket fraction i.e. the assumed fraction of canvas buckets in use. The period for Figures 4.11 to 4.26 is 1860-79. This figure shows a ship speed of $7ms^{-1}$, 60% mean anemometer wind speed and a bucket fraction of 0.5.

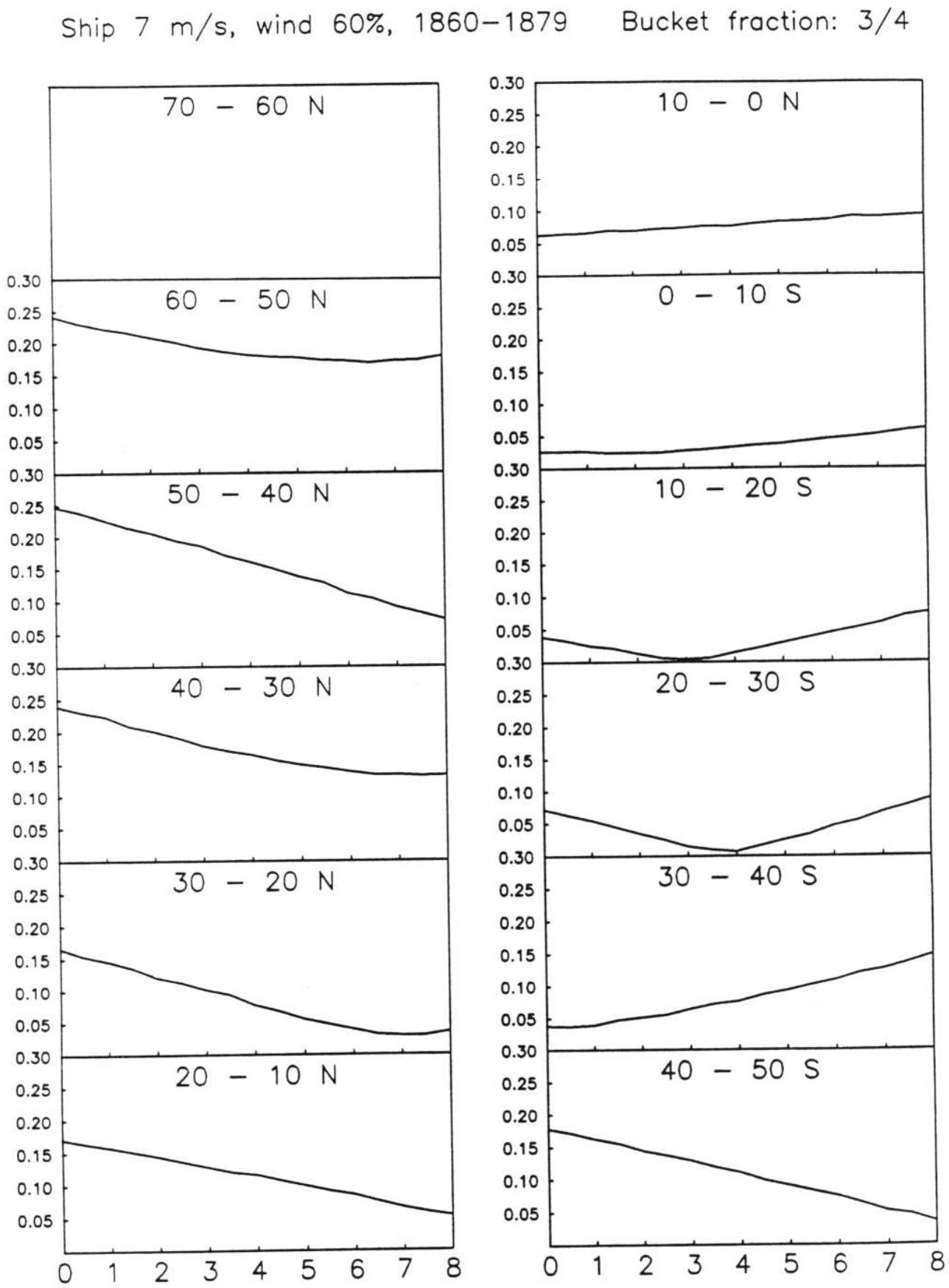

Fig. 4.25: Minimizing the spurious annual cycle with the addition of a bucket fraction i.e. the assumed fraction of canvas buckets in use. The period for Figures 4.11 to 4.26 is 1860-79. This figure shows a ship speed of $7ms^{-1}$, 60% mean anemometer wind speed and a bucket fraction of 0.75.

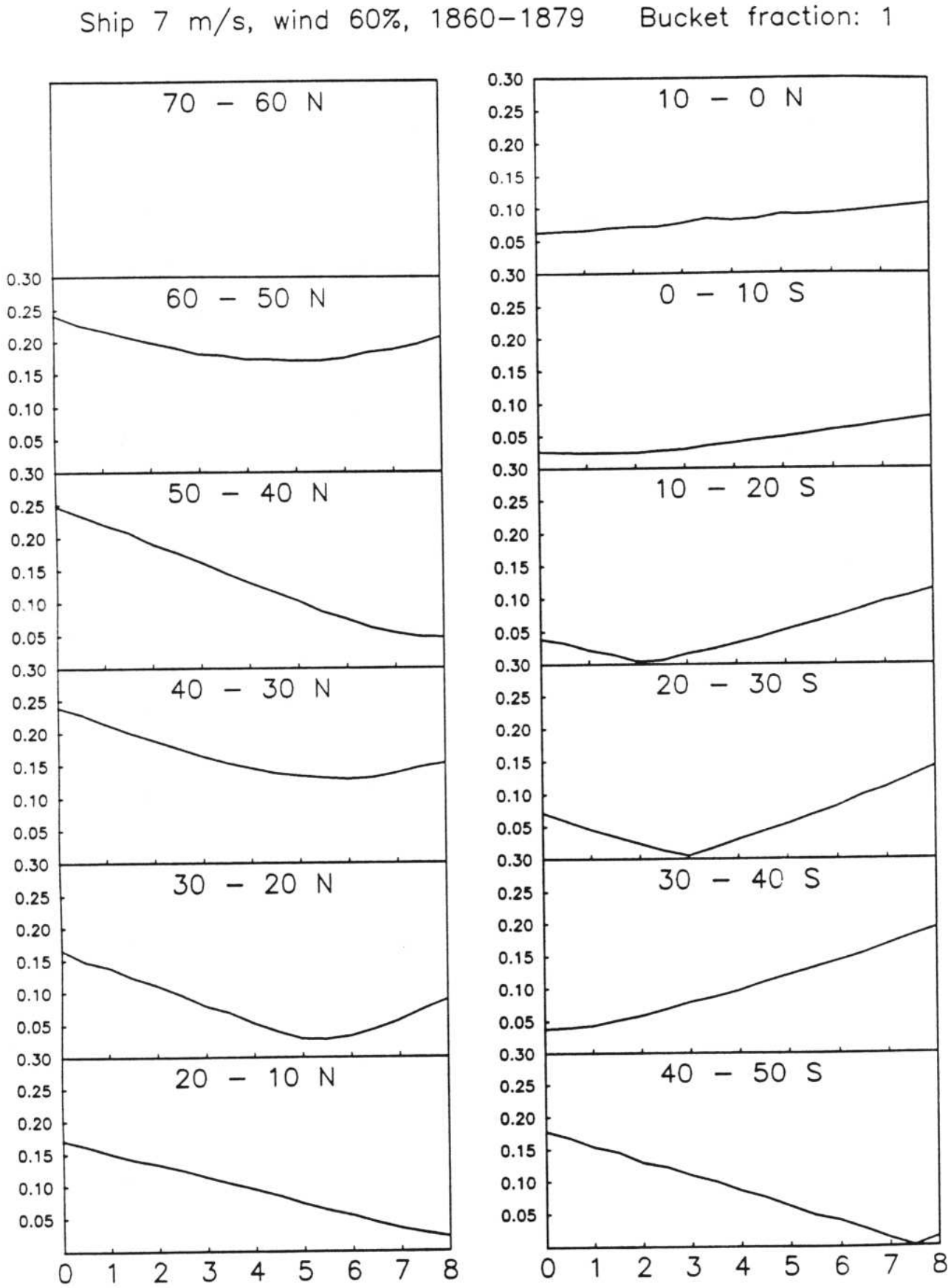

Fig. 4.26: Minimizing the spurious annual cycle with the addition of a bucket fraction i.e. the assumed fraction of canvas buckets in use. The period for Figures 4.11 to 4.26 is 1860-79. This figure shows a ship speed of $7ms^{-1}$, 60% mean anemometer wind speed and a bucket fraction of 1.0.

here, they are essentially speculative. Given natural variability, and the greater "noisiness" of the nineteenth century data, it is virtually impossible to derive a single optimum exposure time and a particular bucket fraction with any reliability based solely on the type of analysis used here. In total, however, these results tend to support the idea that evaporative cooling is not the main cause of the seasonal cycle anomalies for 1860-79. Although this conclusion is somewhat equivocal, it is consistent with the suggestion made earlier that uninsulated/canvas buckets were not the main bucket type.

5. *SPATIAL ASPECTS OF SST DATA AND CORRECTION FACTORS*

5.1 Introduction

The discussion so far has centred on zonal and hemispheric averages. In the previous chapter, we saw that, for the period 1905-40, correction factors based on a bucket model with an exposure time of 3-6 minutes would give a satisfactory reduction in the residual seasonal cycle of SST data, at the zonal scale. Before proceeding further on the subject of an optimum exposure time, we present more detail on the spatial variability in both the raw SST data and the correction factors.

5.2 The seasonal cycle of SSTs

The uncorrected COADS SST data set has been analysed to determine the mean seasonal amplitude of the anomalies at each available grid point for the periods 1950-79, 1905-40 and 1860-79. For 1950-79, as the data are anomalies from the mean over this period, there is virtually no residual seasonal cycle in the data (Figure 5.1). The little cycle that remains is confined to the boundaries of the data area and is a function of random effects such as relatively small samples and data gaps at some points, and the fact that a small amount of spatial smoothing of the data has been performed after calculation of the anomalies in order to ensure compatibility between adjacent grid points (Wright and Jones, 1986).

Figures 5.2 and 5.3 show results for 1905-40 and 1860-79. For these two periods, the seasonal cycles in the anomaly data are partly due to real changes in climate and partly due to instrumental effects. In Section 4.3.3 we concluded that real climatic change dominated for the nineteenth century data, while instrumental effects dominate for the 1905-40 data. If Figures 5.2 and 5.3 are compared, it can be seen that the seasonal cycle amplitudes for 1860-79 exceed those for 1905-40 at about 70% of the common grid points. For these various facts to be consistent, the nineteenth century seasonal cycle must have differed appreciably from the reference

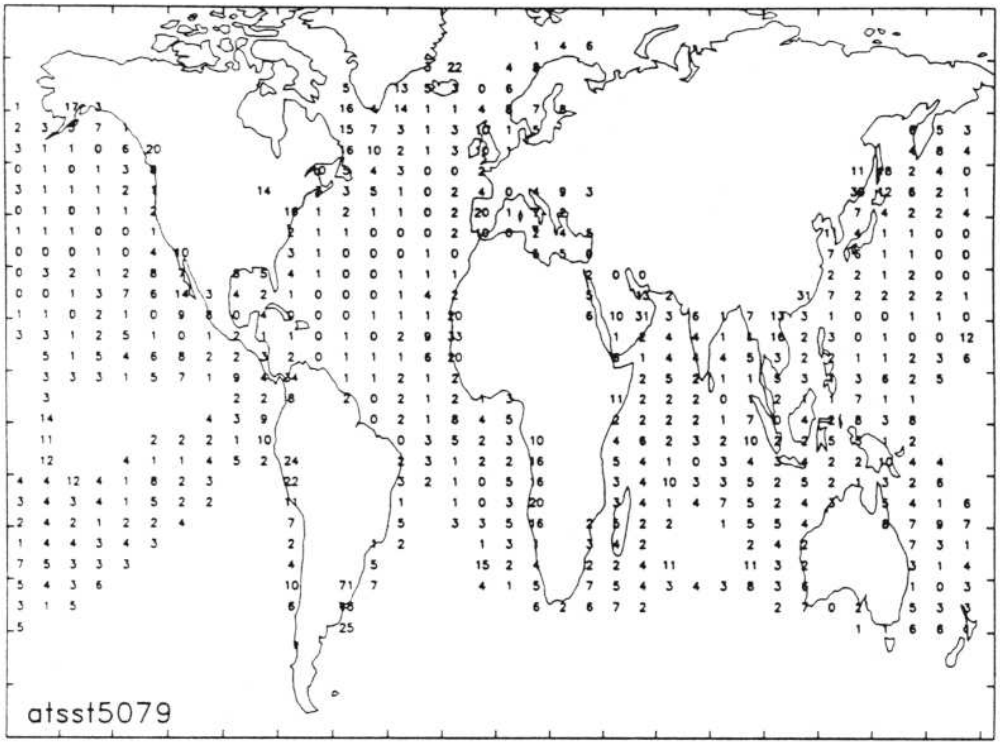

Fig. 5.1: Seasonal amplitude (°Cx0.01) in the 1950-79 COADS SST anomaly data. Anomalies are from the 1950-79 base period.

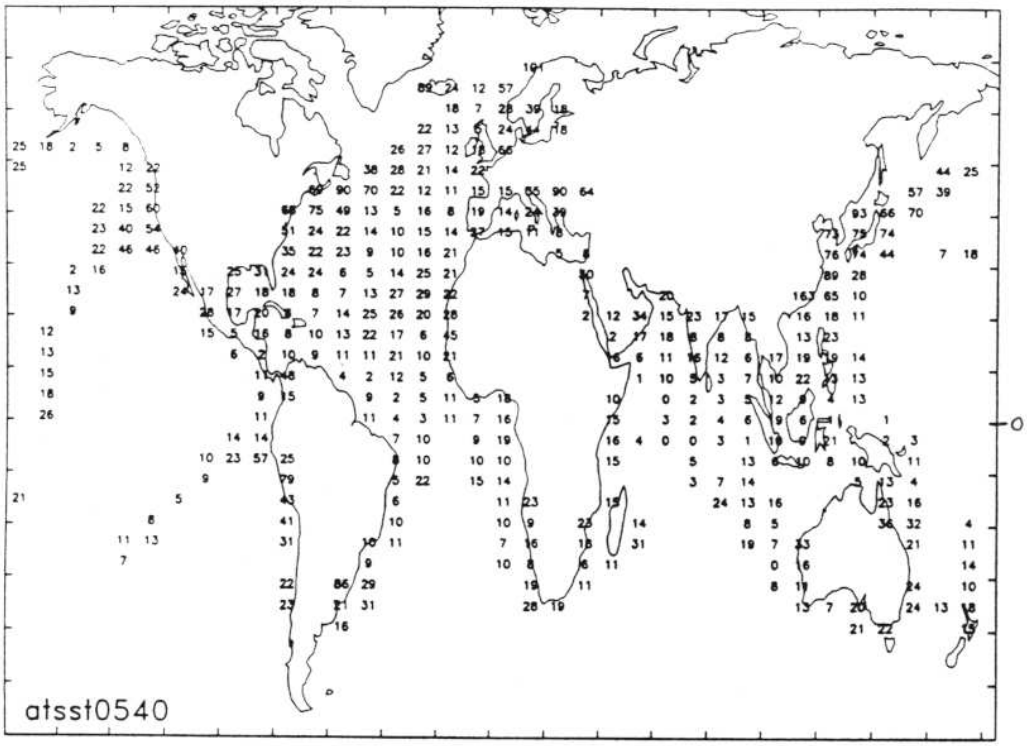

Fig. 5.2: Seasonal amplitude (°Cx0.01) in the 1905-40 COADS SST anomaly data. Anomalies are from the 1950-79 base period.

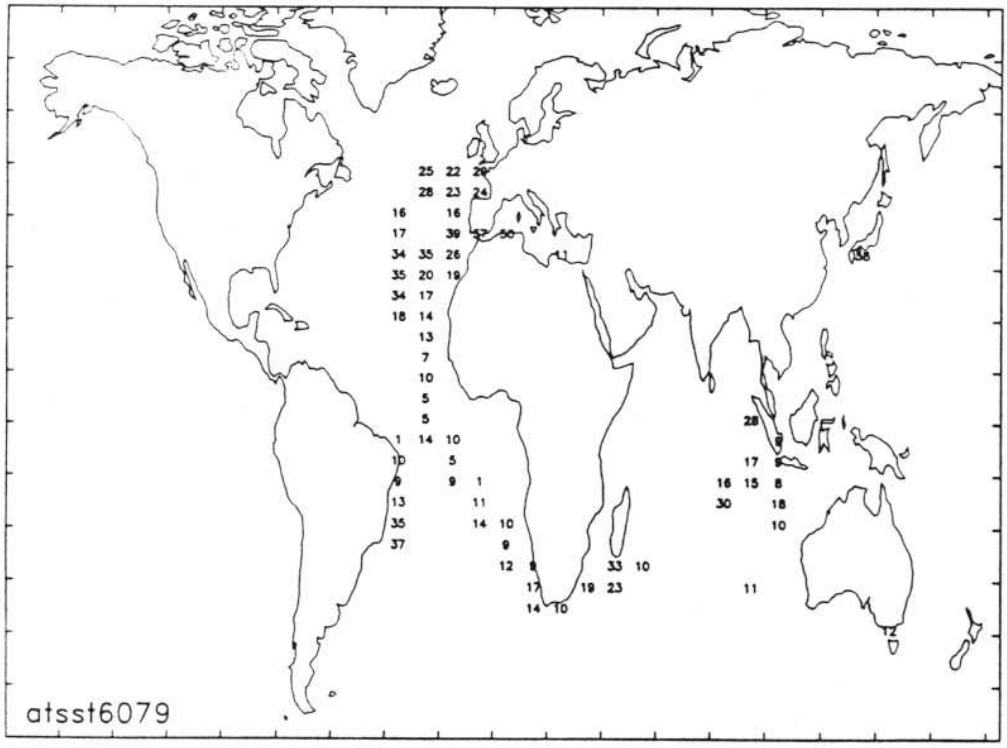

Fig. 5.3: Seasonal amplitude (°Cx0.01) in the 1860-79 COADS SST anomaly data. Anomalies are from the 1950-79 base period.

period value over wide areas, while the changes between 1905-40 and 1950-79 must have been relatively small. Precisely the same sort of behaviour was observed for the land data.

5.3 Seasonal cycles in the correction factor

To give some idea of the magnitude of the bucket-induced seasonal cycle amplitudes at individual grid points, we show typical results spanning the range of possibilities in Figures 5.4 and 5.5. In these calculations, ship speed has been taken as $7ms^{-1}$ and wind speed percentage taken to be 60%. The average amplitude of the seasonal cycle of the correction factor over 1905-40 was then calculated for exposure times of 3 minutes (Figure 5.4) and 6 minutes (Figure 5.5). The seasonal amplitude values in Figures 5.4 and 5.5 are comparable with those observed in the uncorrected data for 1905-40 (Figure 5.2) and show similar spatial variations, confirming that application of a bucket model with appropriately chosen parameters should be able to remove much of the spurious annual cycle in the 1905-40 data.

5.4 Time dependence of the hemispheric-mean correction factors

To show how the hemispheric-mean correction factors vary according to assumed ship speed and exposure time, area averages were calculated using the available SST coverage. These are shown in Figures 5.6 to 5.9. The year-to-year variations that can be seen in these Figures (rounded to $0.01^{o}C$) are due to coverage changes with time. These variations are most marked in the Southern Hemisphere where the coverage changes could introduce a change in hemispheric-mean correction factor by up to $0.06^{o}C$ (for an exposure time of 4.5 minutes).

The Figures confirm the analytical results derived earlier. The corrections can be seen to vary almost linearly with exposure time. Changing ship speed from $4ms^{-1}$ to $7ms^{-1}$ increases the correction factor by

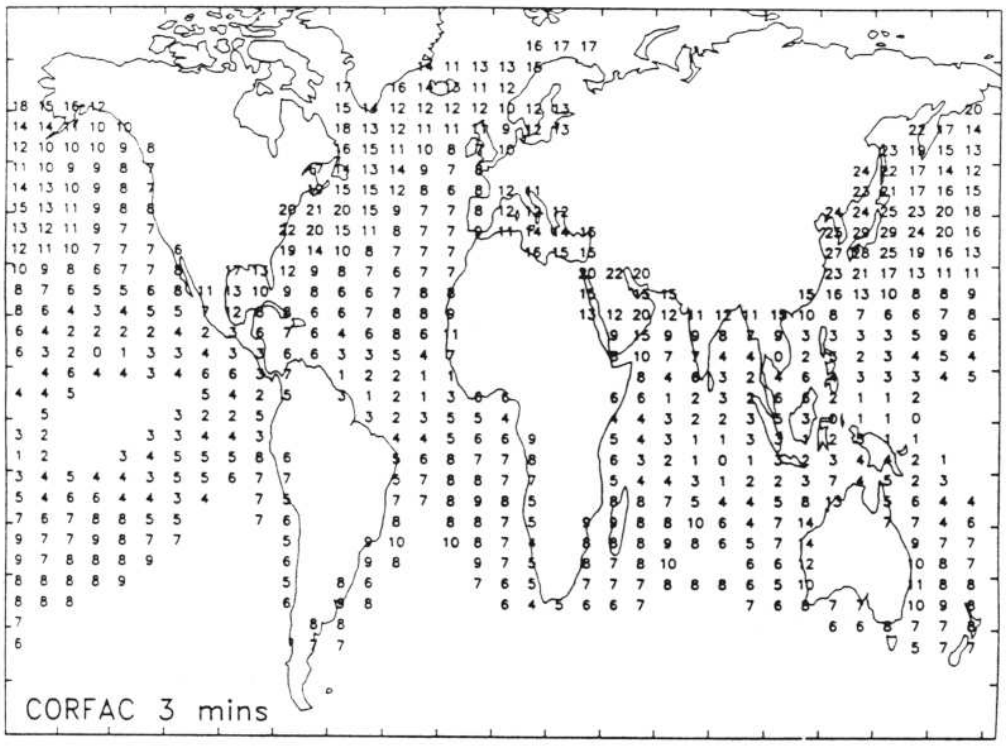

Fig. 5.4: Seasonal amplitude of the bucket model corrections for a ship speed of $7ms^{-1}$, 60% mean anemometer wind speed and a 3 minute exposure time.

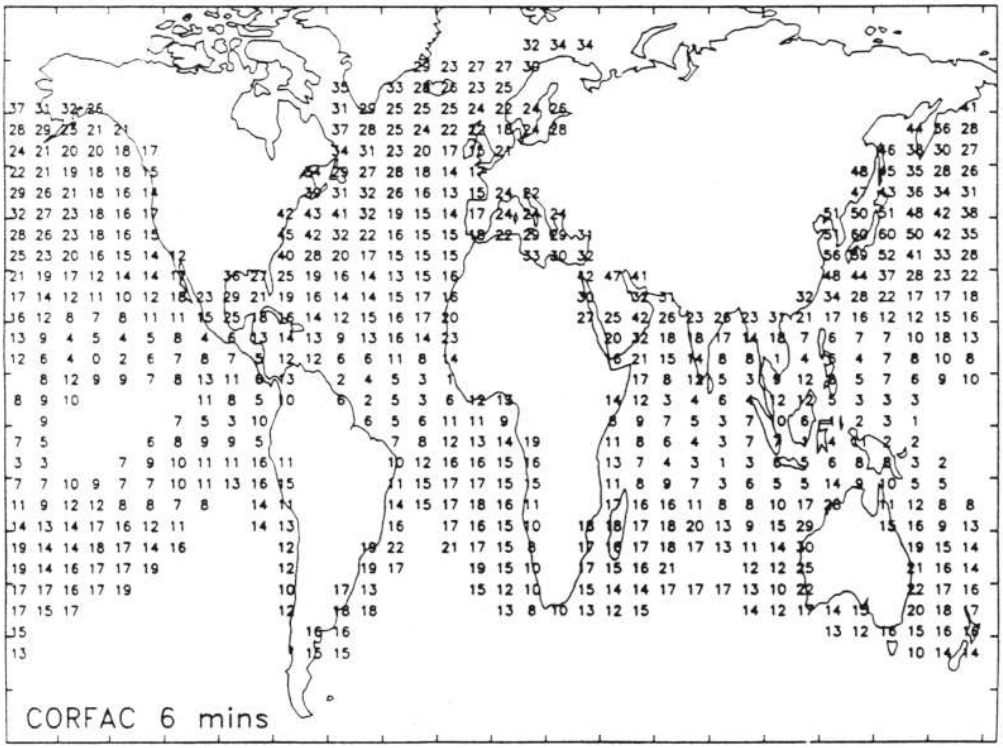

Fig. 5.5: Seasonal amplitude of the bucket model corrections for a ship speed of $7ms^{-1}$, 60% mean anemometer wind speed and a 6 minute exposure time.

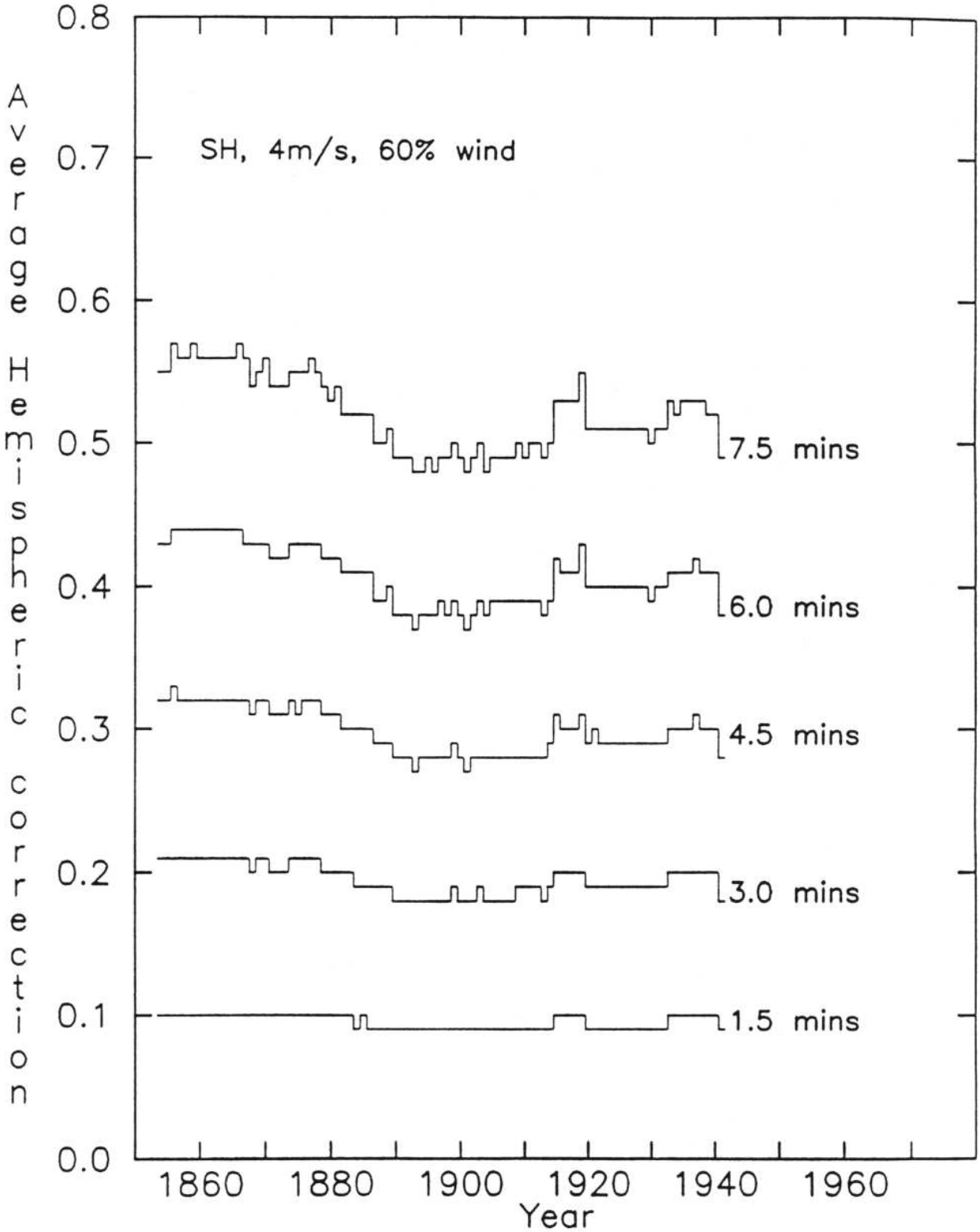

Fig. 5.6: Variations in hemispheric mean correction factor for different exposure times: Southern Hemisphere, ship speed $4ms^{-1}$ and a 60% mean anemometer wind speed.

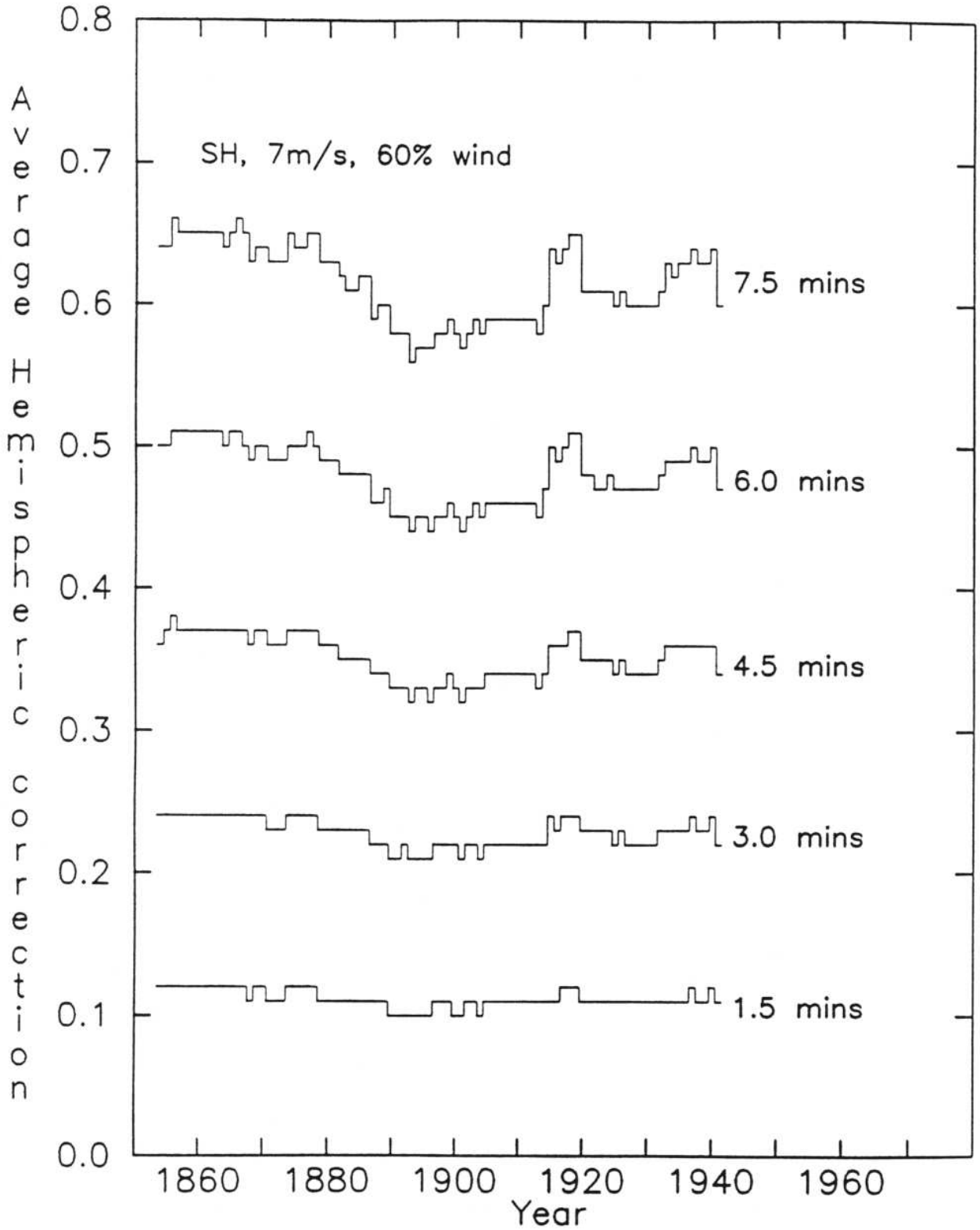

Fig. 5.7: Variations in hemispheric mean correction factor for different exposure times: Southern Hemisphere, ship speed $7ms^{-1}$ and a 60% mean anemometer wind speed.

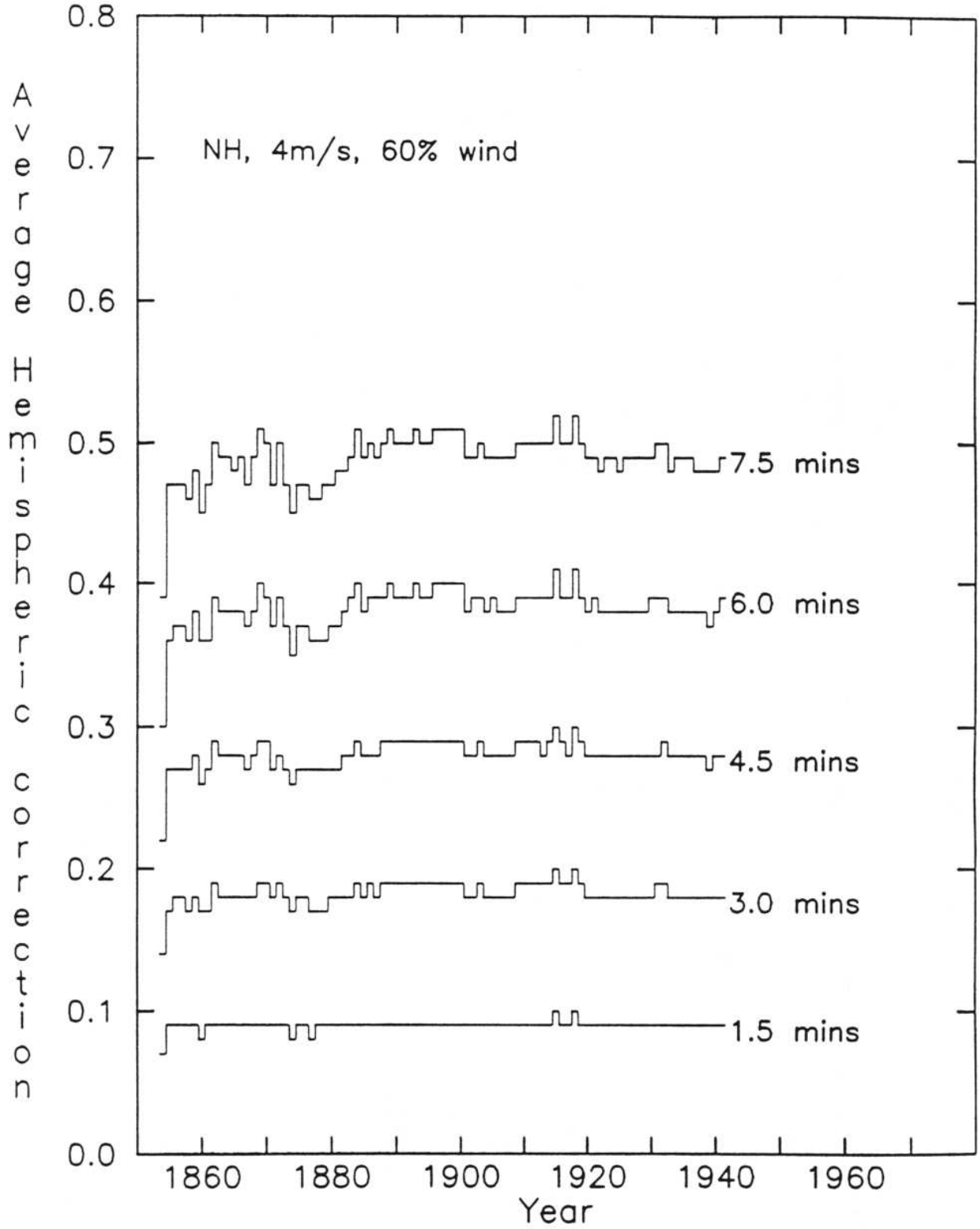

Fig. 5.8: Variations in hemispheric mean correction factor for different exposure times: Northern Hemisphere, ship speed $4ms^{-1}$ and a 60% mean anemometer wind speed.

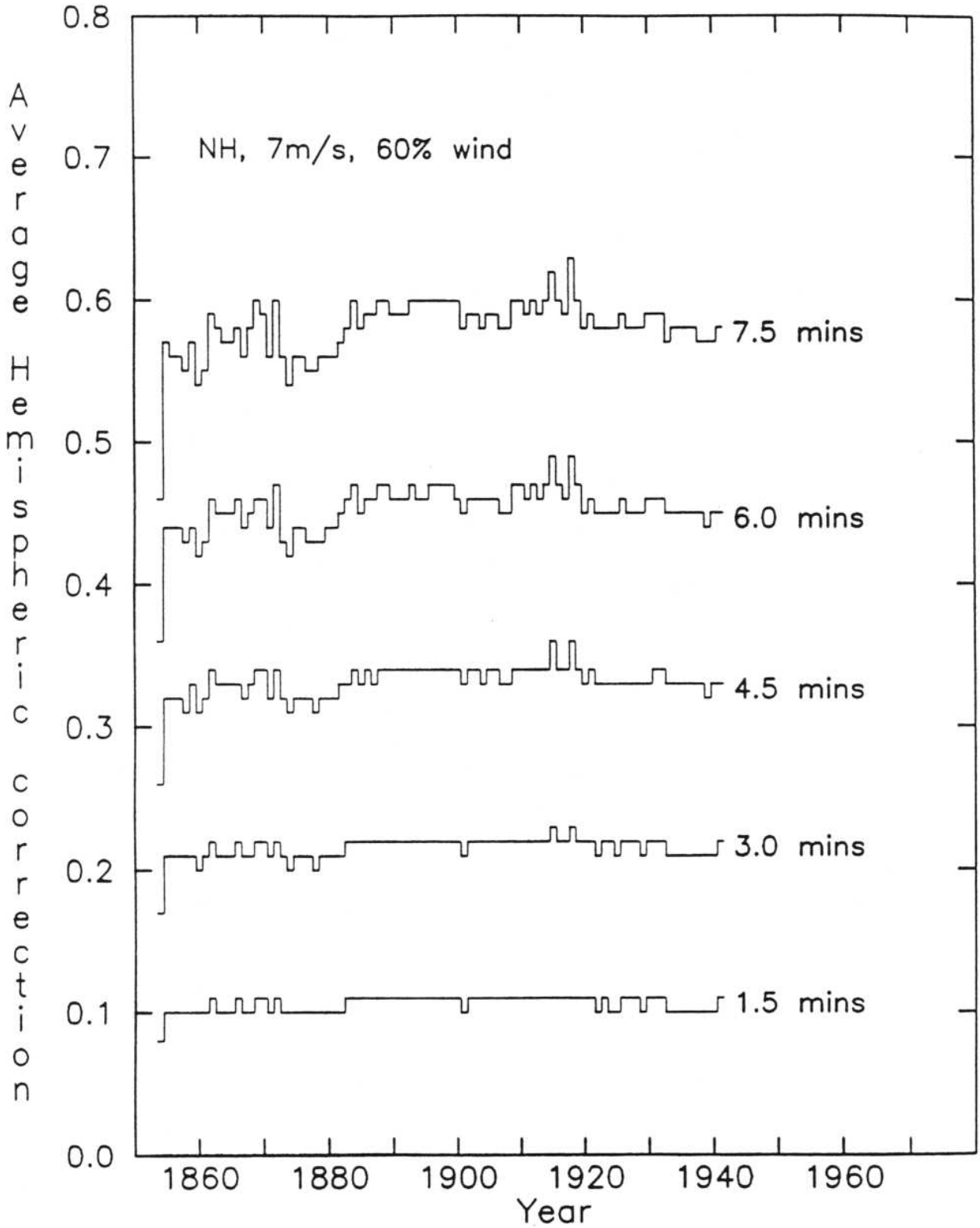

Fig. 5.9: Variations in hemispheric mean correction factor for different exposure times: Northern Hemisphere, ship speed $7ms^{-1}$ and a 60% mean anemometer wind speed.

about 20% (c.f. 17% estimated in Section 4.2.4). On average, for given exposure time and ship speed, Southern-Hemisphere-mean correction factors are slightly greater than for the Northern Hemisphere (except between 1885 and 1912). This is a coverage effect.

5.5 Zonal and seasonal variations in the correction factors

In general, hemispheric-mean correction factors are largest in the winter half year. Correction factors are invariably smallest in high northern latitudes. Since there are so few data south of 45°S, we have not calculated area-average correction factors in this region. Between 45°S and 45°N, the zonal-mean behaviour of the correction factors is linked to the dependence of the correction factor on season discussed above. The zonal differences here, however, are small. Further details are given in Section 6.2.

6. *CORRECTING SSTs USING THE A PRIORI APPROACH*

6.1 Optimum exposure time

Analyses in the previous chapters have led to the following conclusions, some based on the bucket model results and others on more general arguments:

(1) For 1905-40, SSTs may be corrected using the evaporating bucket model. Although average ship speed probably varied over this period, within the range of likely values ship speed does not noticeably affect the implied exposure time. We have used a ship speed of $7ms^{-1}$. Wind speeds of 60% of the anemometer speed produce slightly better results than the 40% reduction case, and lead to slightly lower optimum exposure times (by less than 1 minute on average) so we have used this value. The most likely exposure time lies in the range 3-6 minutes. We have used 4.5 minutes in making final corrections.

(2) For the nineteenth century data, the evaporating bucket model produces results which are noticeably less internally consistent compared with those for 1905-40. Based on somewhat sketchy evidence, wooden buckets were probably dominant up to 1870-1880, with a transition to uninsulated buckets occurring between then and the early twentieth century. We have assumed that canvas buckets, or their equivalent, accounted for 25% of all buckets prior to 1880, and that this fraction increased linearly to 100% in 1905. For ship speed we have used $4ms^{-1}$ prior to 1880, increasing linearly to $7ms^{-1}$ in 1905, and assumed wind speed on deck to be 60% of anemometer speed.

Although ship speed and wind speed are not critical in determining the optimum exposure time, they are important in determining the magnitudes of the corrections. This can be seen by an example which draws on results from the sensitivity analysis in Section 4.2.2. Suppose the anemometer wind speed is $10ms^{-1}$, so that the wind speed (U) near the bucket is either

$4ms^{-1}$ or $6ms^{-1}$. Suppose also that the ship speed (v) is either $4ms^{-1}$ or $7ms^{-1}$. The following results then obtain from equs. (3), (5c) and (14) if the Q_B term in (5c) is ignored

$$\text{(i)} \quad \Delta(U=6,v=4) = 1.11\ \Delta(U=4,v=4)$$

$$\Delta(U=6,v=7) = 1.04\ \Delta(U=6,v=4)$$

$$\text{(ii)} \quad \Delta(U=4,v=7) = 1.17\ \Delta(U=4,v=4)$$

$$\Delta(U=6,v=7) = 1.09\ \Delta(U=4,v=7)$$

$$\text{(iii)} \quad \Delta(U=6,v=7) = 1.22\ \Delta(U=4,v=4)$$

The effect of U variations is characterized by (i), (ii) characterizes the effect of v variations, while (iii) gives the combined effect. Confirmation of these results is provided by the complete analyses presented in Figs. 5.6-9. By comparing 5.6 and 5.7 or 5.8 and 5.9 it can be seen that $\Delta(U=6,v=7) \approx 1.18\ \Delta(U=6,v=4)$. This should be compared with (ii) above. The slightly higher value of the multiplying factor arises mainly through the neglect of Q_B in determining the analytical result. These effects are relatively small (a one minute error in exposure time would produce a noticeably larger error in Δ), but they are not insignificant.

The effect of an error in U or v could be offset by a small adjustment to the exposure time. This means that the optimum exposure times calculated earlier should differ slightly for different U or v, at least for 1905-40. Such a difference was noticeable when U was varied from $4ms^{-1}$ to $6ms^{-1}$, but only just. Theoretically, for this range of U values, the optimum exposure time (t) should vary by only 4-13% (i.e. 0.2-0.7 mins. for t = 5 mins.). This is in accord with the empirical observation that greater U requires only less than 1 minute less exposure time. For v varying between $4ms^{-1}$ and $7ms^{-1}$, the change in exposure time should be slightly larger, 9-17% (i.e. 0.5-0.9 mins. for t = 5 mins.). That this was not noticed is not surprising given the size of the effect and the lack of precision in estimating optimum exposure time. In fact, given these

factors, it is somewhat surprising that the U effect was noticeable at all.

6.2 The final correction factors

Final correction factors depend on the location, month and year. These variations are summarized in Figures 6.1 to 6.3. Figure 6.1 shows mean correction factors for the Northern Hemisphere. Southern Hemisphere mean corrections are shown in Figure 6.2. The seasons are offset by one month from conventional seasons so that their mean will correspond to a calendar year. The transition from small corrections in the early decades to larger corrections after 1905 is due to the change from wooden (i.e. insulated) to uninsulated buckets. Correction factors are largest in the winter half year. Northern Hemisphere corrections show slightly larger season-to-season variations. Figure 6.3 shows how the "winter" (JFM) and "summer" (JAS) - using Northern Hemisphere seasonal labels - corrections vary with latitude. Correction factors are lower in higher latitudes in general, particularly in the 45-75°N band where the "summer" corrections are near zero.

6.3 The corrected SST data set

Time series for the corrected, hemispheric-mean SST data are shown in Figures 6.4 and 6.5. As in Figures 6.1 to 6.3, offset seasons are used. The data shown have been smoothed using a 10-year Gaussian filter in order to facilitate comparisons. For the Southern Hemisphere (Figure 6.5), the seasons are remarkably consistent. The time series also show a steady warming trend over the whole period after the mid 1900s, with no long-term trend prior to that. For the Northern Hemisphere, there is some divergence between the seasons prior to 1890. As explained previously, we consider that there have been noticeable fluctuations in the seasonal cycle over the Northern Hemisphere land masses, and these seasonal variations over the oceans are in accord with this conclusion. Such seasonal differences could

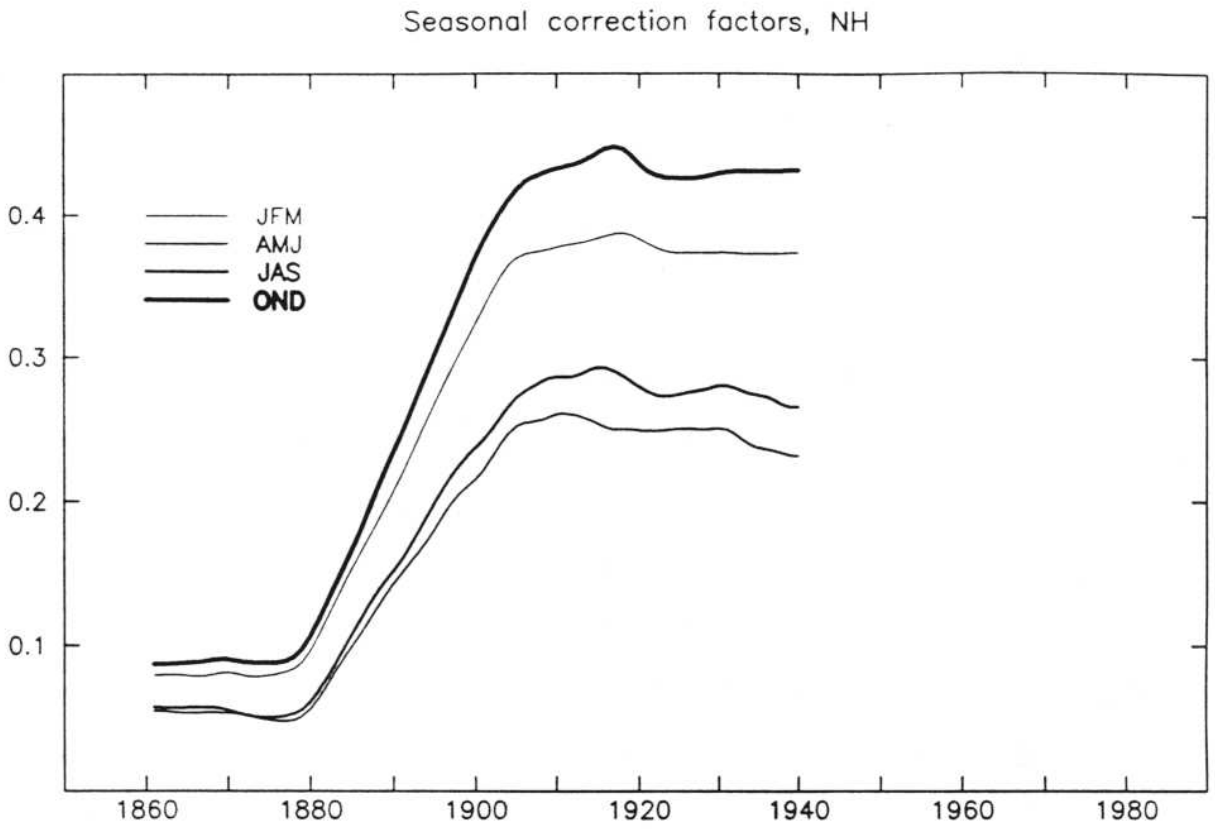

Fig. 6.1: Smoothed seasonal bucket model corrections: Northern Hemisphere. The four seasons are JFM (January, February and March), AMJ (April, May and June), JAS (July, August and September) and OND (October, November and December). Data are smoothed using a 10-year Gaussian filter.

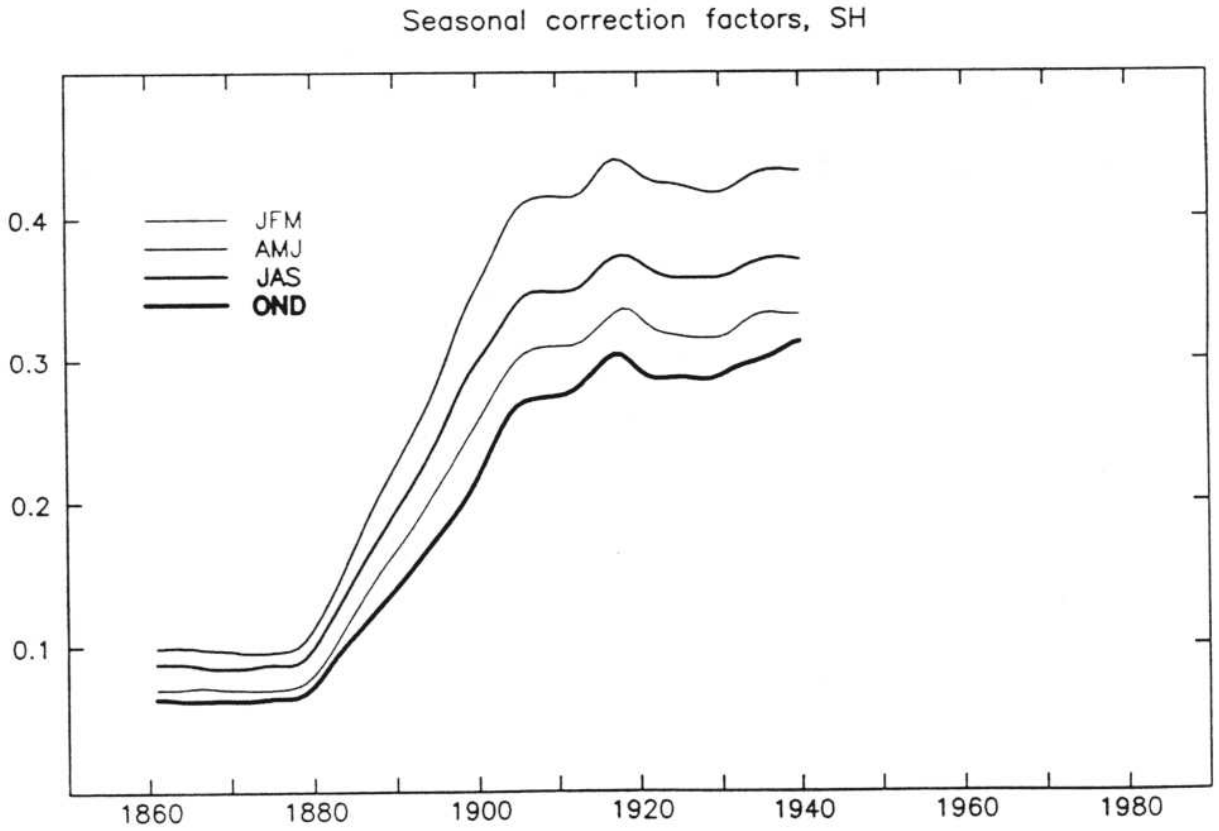

Fig. 6.2: Smoothed seasonal bucket model corrections: Southern Hemisphere.

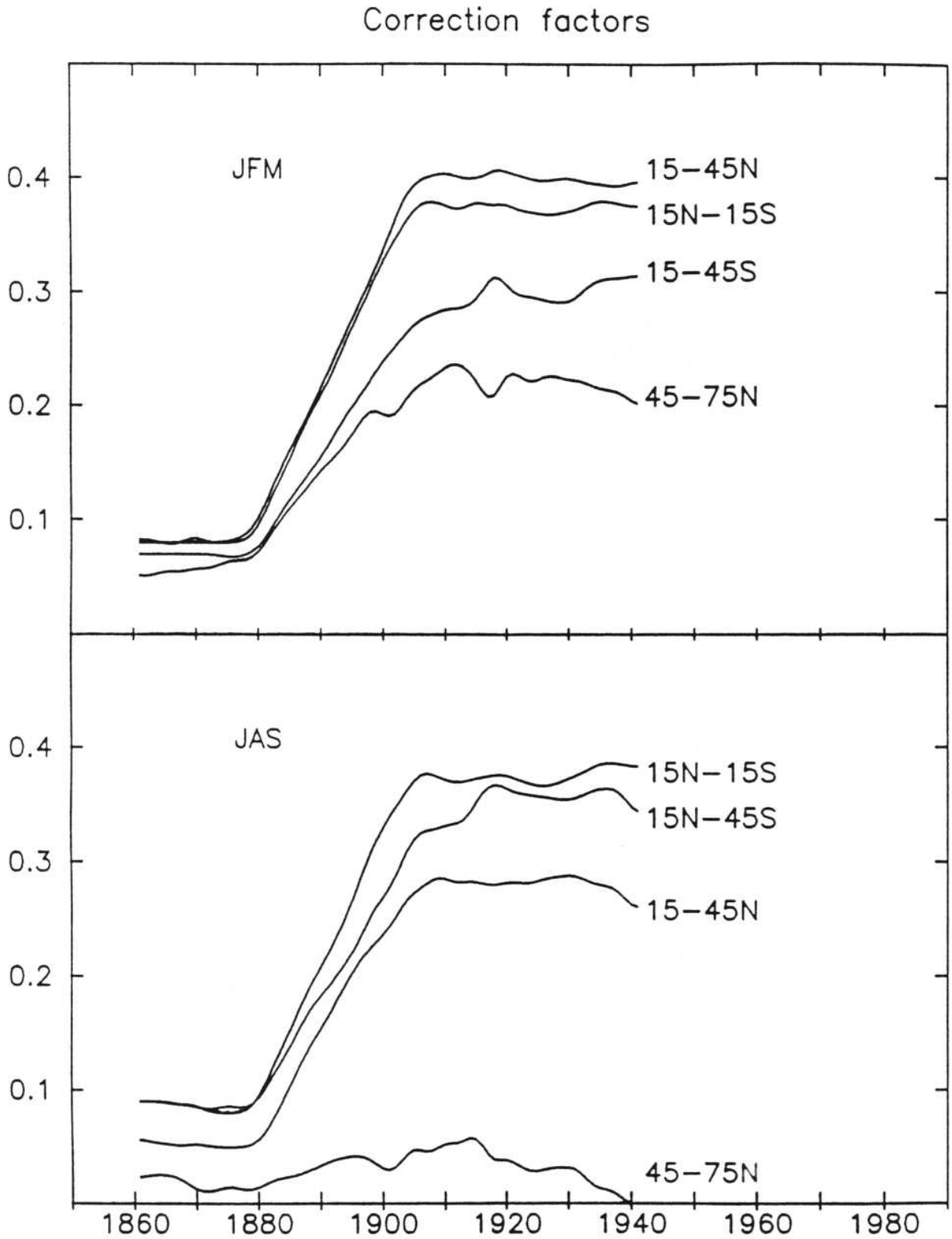

Fig. 6.3: Smoothed bucket model corrections for various latitude zones for the FJM (January, February and March) and JAS (July, August and September) seasons.

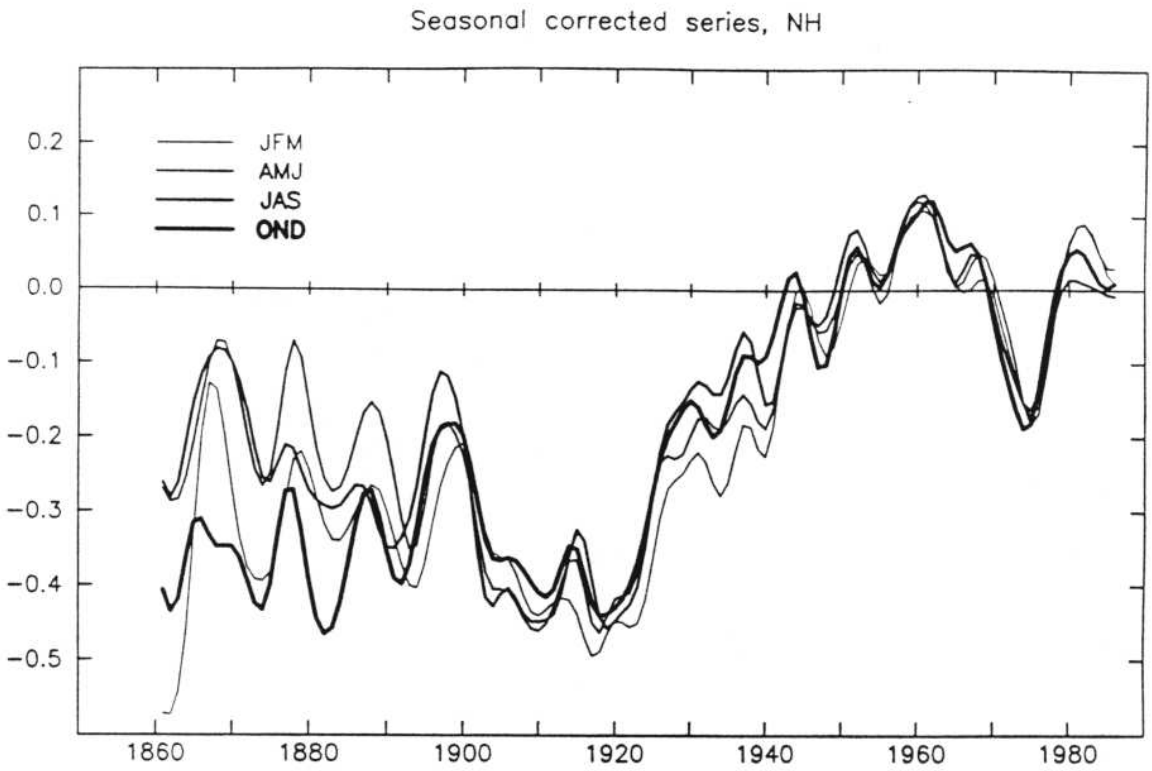

Fig. 6.4: Smoothed seasonal COADS SST time series after bucket model corrections: Northern Hemisphere.

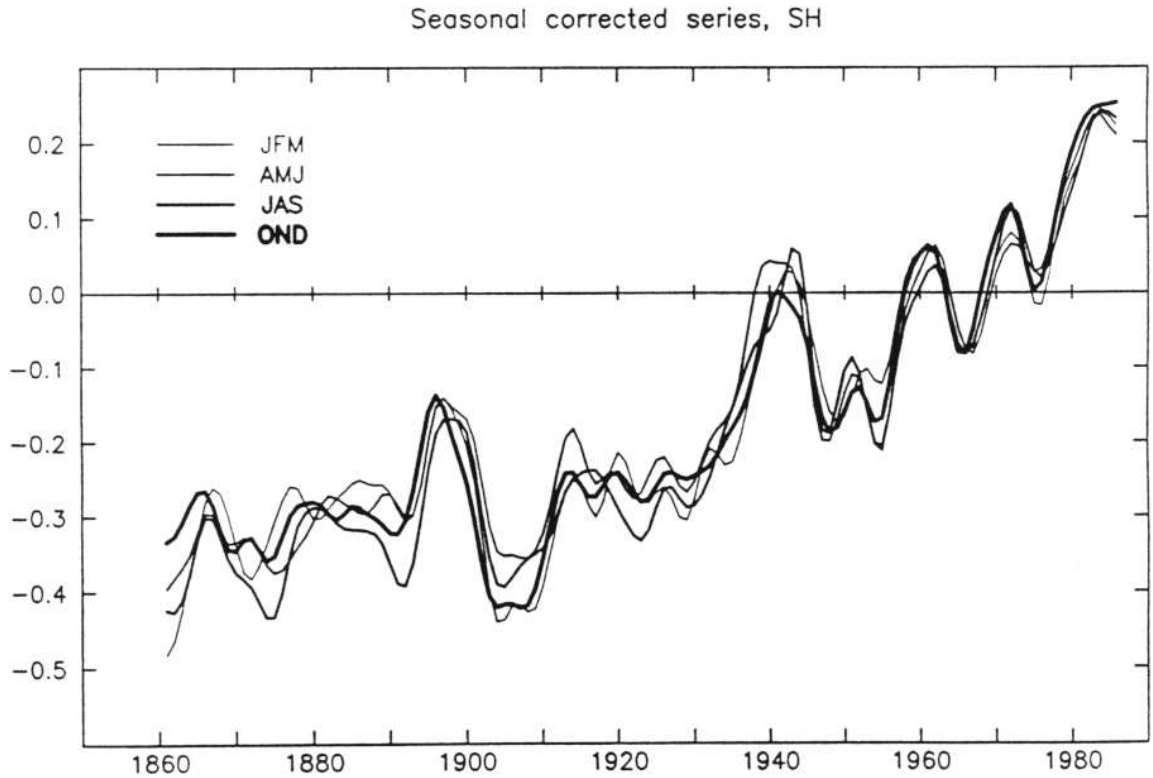

Fig. 6.5: Smoothed seasonal COADS SST time series after bucket model corrections: Southern Hemisphere.

be reduced by modifying the correction procedure, either by changing the exposure time, or by changing the assumed fraction of uninsulated buckets prior to 1905. However, this would increase the seasonal differences in the Southern Hemisphere and tend to make both hemispheric means less consistent with the land data.

Compatibility with the land data is examined further in Figures 6.6 to 6.9. Figure 6.6 shows the land data for the Northern Hemisphere (from Jones et al., 1986a, updated), while Figure 6.7 shows the land-sea difference (corrected SST minus land). Seasonal values are relatively consistent back to the early 1880s. The land-sea differences after 1905 are almost certainly real. They imply a cooling of the ocean relative to the land over 1890-1920, similar to the relative cooling that has occurred since the mid 1960s, and a relative warming of the oceans over 1940-1965. A possible explanation for these changes has been suggested by Wigley and Raper (1987), namely, changes in North Atlantic Deep Water formation rate. Such changes do not appear to be consistent with the possibility that a relative cooling over the oceans may have occurred in the twentieth century as a result of SO_2-derived cloud condensation nuclei changes (Wigley, 1989). Prior to 1880, the divergence of the seasonal difference curves in Figure 6.7 could either be a real effect arising from disparate variations in the seasonal cycle over land and oceans, or it could be an indication of errors in either the land data or the marine corrections.

For the Southern Hemisphere (Figures 6.8 and 6.9; land data from Jones et al., 1986b), the seasonal variations over land and ocean are more similar than in the Northern Hemisphere. This is as one might expect, given the smaller land area and the correspondingly greater influence of ocean changes on changes that might occur over the land masses.

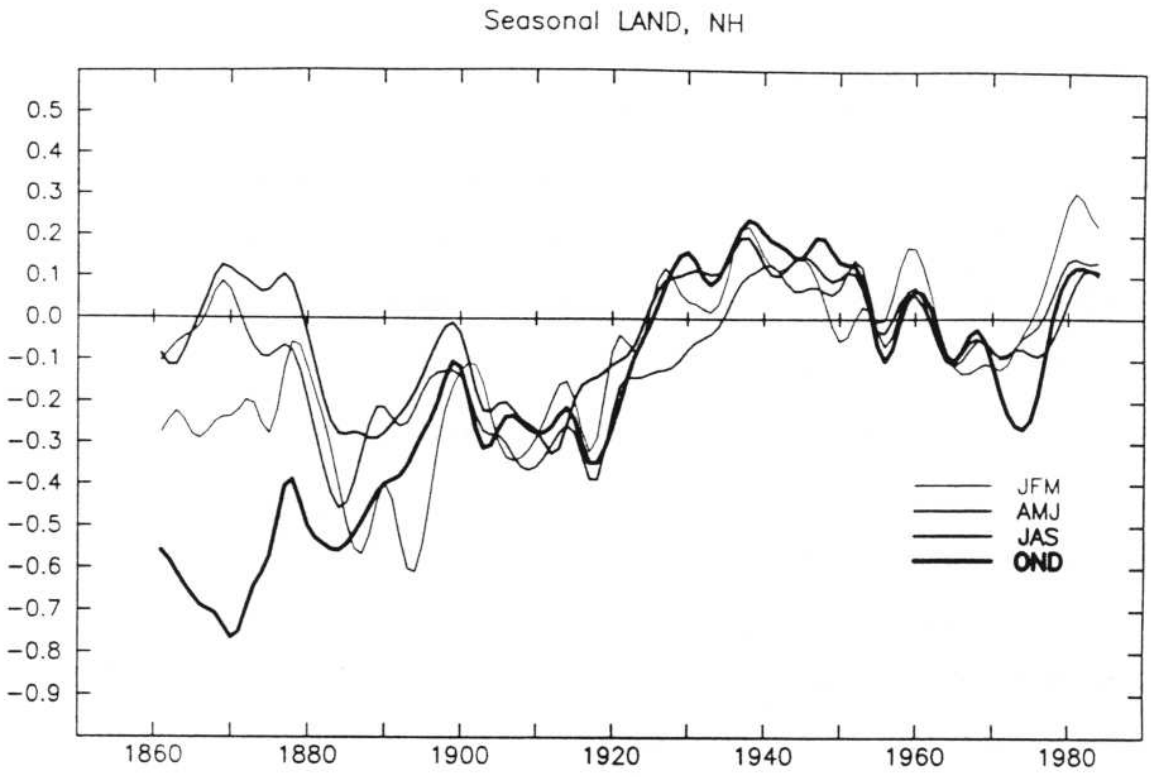

Fig. 6.6: Smoothed seasonal land time series: Northern Hemisphere.

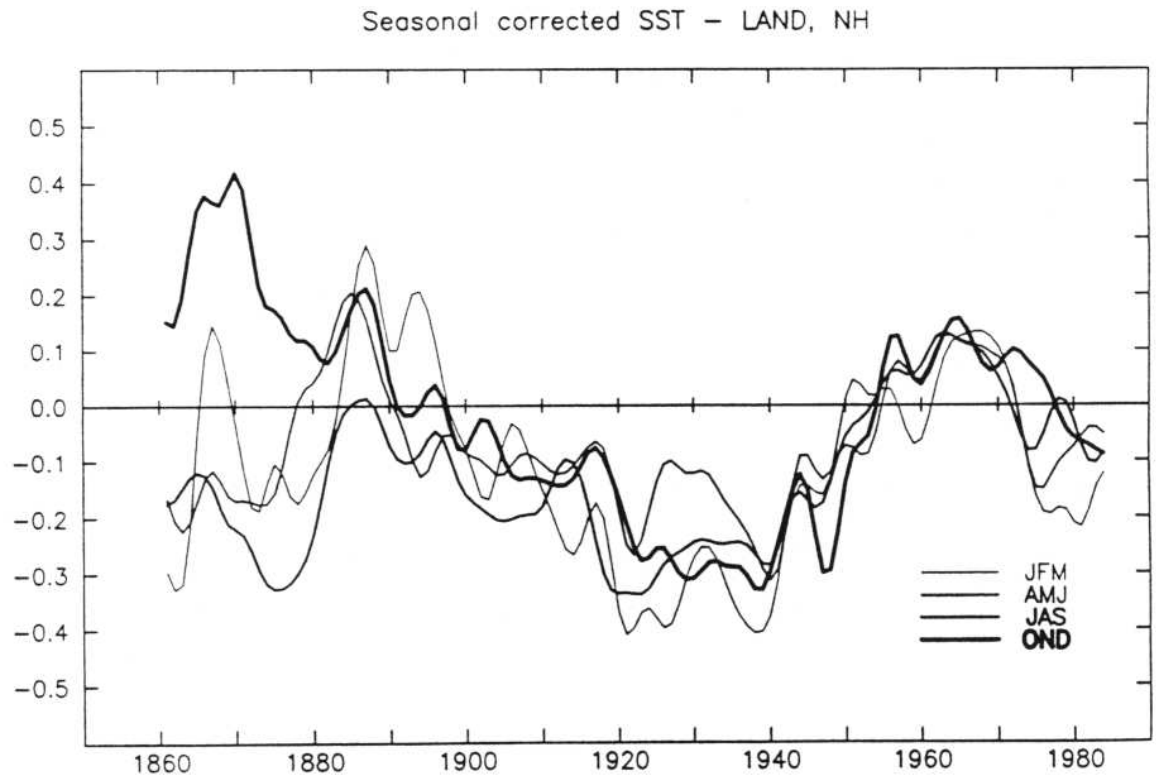

Fig. 6.7: Differences between the smoothed seasonal corrected COADS SST and land time series: Northern Hemisphere.

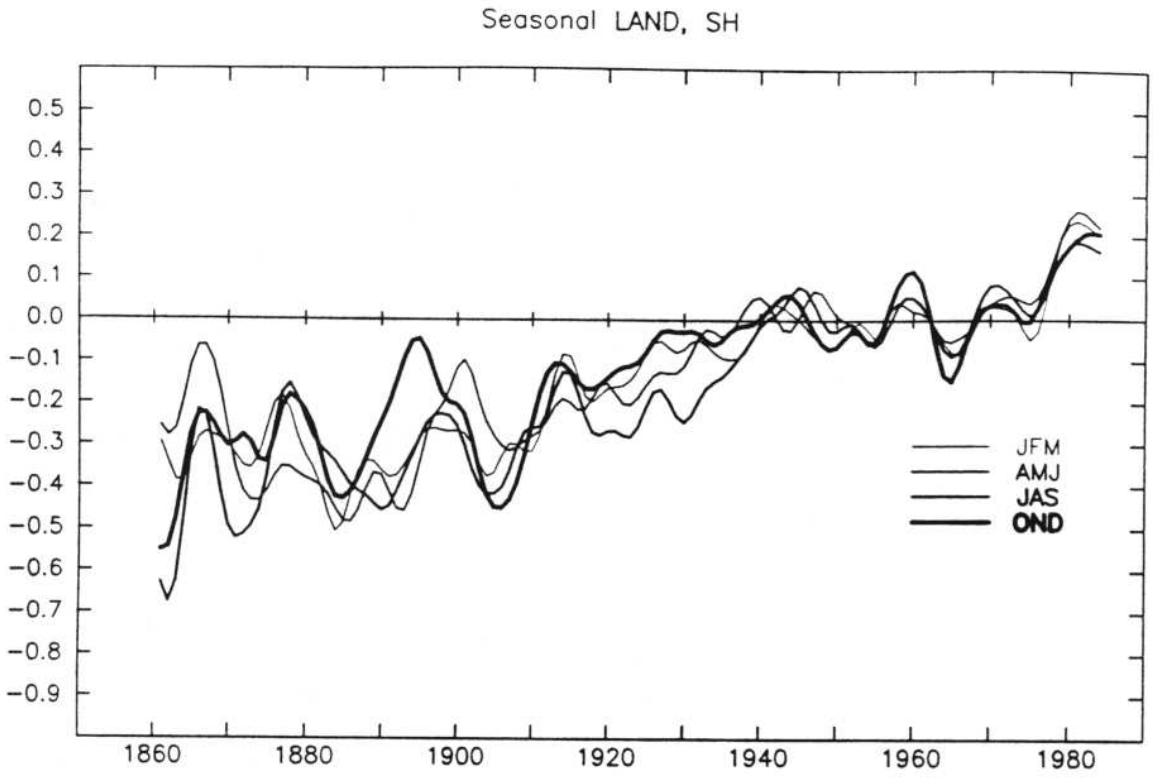

Fig. 6.8: Smoothed seasonal land time series: Southern Hemisphere.

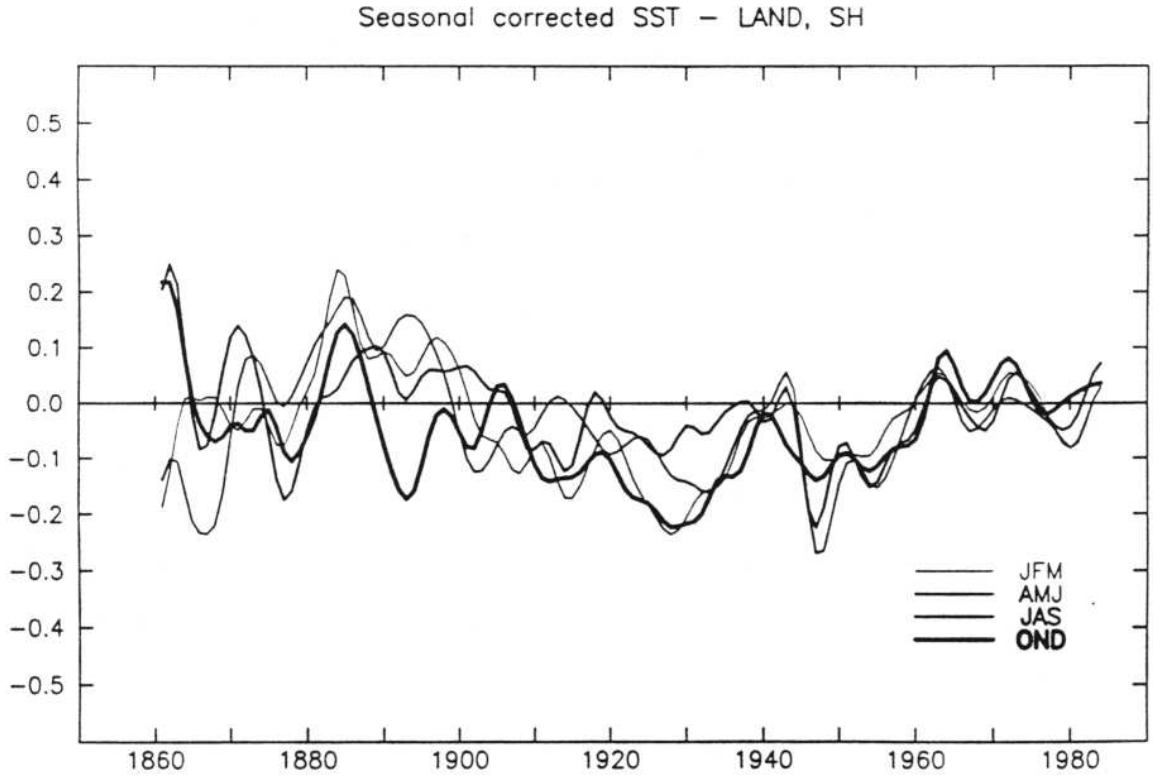

Fig. 6.9: Differences between the smoothed seasonal corrected COADS SST and land time series: Southern Hemisphere.

7. SUMMARY AND CONCLUSIONS

The main aims of this project were to compare different marine temperature data sets, to compare different methods of correcting these data, and to produce a corrected version of the COADS gridded SST data set. The UKMO and COADS compilations of marine data were considered. The two correction methods are referred to as the *a priori* method, which uses a physical model of the cooling of an evaporating bucket to derive corrections to SST data, and the *a posteriori* method in which SST corrections are derived by comparison with adjacent land-based temperature data. In our earlier work (Jones et al., 1986c), we used the latter method with the COADS data. This allowed only the production of hemispheric-mean, annual-mean temperatures - i.e. with no spatial or intra-annual detail. Our corrected results differed from those of Folland and co-workers (viz. Folland et al., 1984, and various revisions of this first version of the UKMO corrected data set). Folland and co-workers have, in general, used an *a priori* correction method with the uncorrected UKMO data set as a starting point.

In comparing the *uncorrected* UKMO and COADS data sets we found, surprisingly, that there are substantial differences. These are larger for MAT than for SST. For MAT, this is partly due to the fact that the UKMO data comprise only night-time marine air temperatures, so one is not strictly comparing like with like.

For the *corrected* data available prior to this report, the biggest discrepancies occur in the 19th century. It was thought that these might reflect errors in the land-based data, partly because these data show quite large inter-seasonal differences in their decadal and longer time scale changes. The analysis presented here, however, indicates that these inter-seasonal "trend" differences are real. They are consistent with circulation changes and with similar changes in the marine data. These results point to the existence of quite large decadal and longer time scale

changes in the amplitude of the seasonal cycle over land and marine areas on the hemispheric spatial scale.

In applying the *a priori* correction method in this report, we modified the procedure used by Folland and co-workers in three ways. First, we used an analytical solution of the bucket evaporative cooling equation, which gives a large savings on the computing time required to estimate correction factors. Second, we corrected the basic model of Folland and Hsiung (1986) by eliminating an approximation: the differences in the solutions between the old and revised models are, however, extremely small. Third, we assumed a varying fraction of evaporating buckets during the 19th century, with the variations based partly on historical information on the types of buckets used and partly on an analysis of the corrected data using different variations of the bucket fraction. Our results here suggest that most of the 19th century differences between the UKMO and Jones et al. corrected SST data can be explained through the change from dominantly non-evaporating buckets in the mid 19th century to dominantly evaporating buckets by the early 20th century.

The final, revised corrected SST time series (hemispheric and global annual-mean temperature changes) are shown in Figure 7.1 for 1854-1986, inclusive. These should be compared with our earlier time series (Jones et al., 1986c), which were based on the *a posteriori* correction method, in order to see the effect of the different correction methods. In making this comparison we first show the revised land-plus-marine time series (Figure 7.2). These have been produced using a slightly different method from that used by Jones et al. (1986c) to combine land and marine data.

To obtain Figure 7.2 we first produced a composite (land plus marine) gridded data set on a 5° latitude by 5° longitude grid. For coastal grid points representing both land and marine areas, we simply averaged the two values. Area averages were then calculated using all available grid points with cosine-latitude weighting. The method used by Jones et al. (1986c)

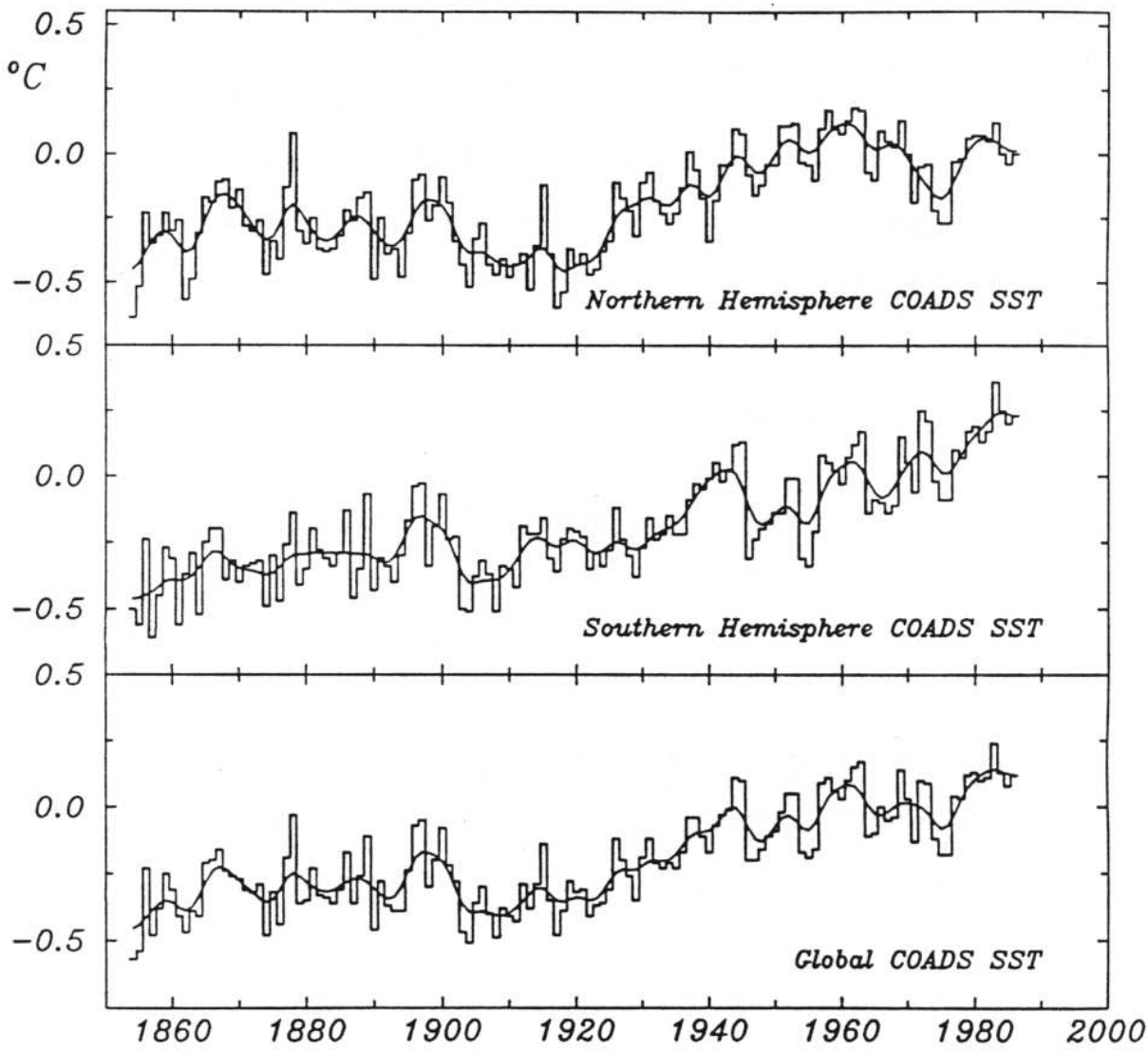

Fig. 7.1: Hemispheric and global SST time series based on COADS data after application of bucket model correction: 1854-1986.

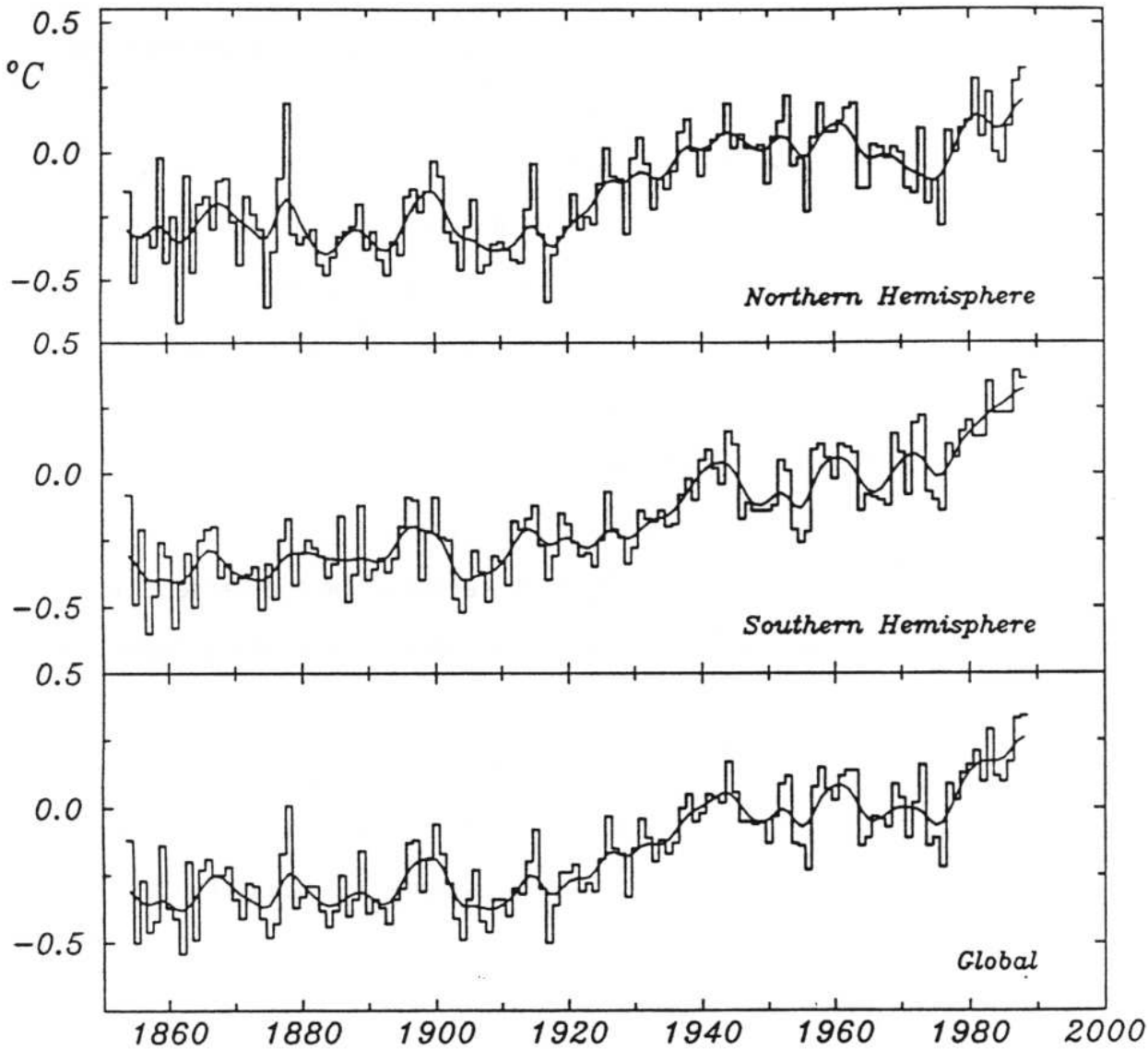

Fig. 7.2: Hemispheric and global time series combining bucket model corrected COADS SST and land data: 1854-1988. Marine data for 1987 and 1988 are from the UKMO data set.

was to begin with separate "hemispheric-mean" time series for the land and marine areas and to average these using appropriate weights. For the global-mean, the hemispheres were weighted equally. For the land and ocean weighting factors, Jones et al. showed the results were insensitive to the choice of land/ocean weights because of the high correlation between the land and marine series in each hemisphere.

In Figure 7.3 we show the original Jones et al. (1986c) results. Differencing Figures 7.2 and 7.3 (Figure 7.4) shows the effect of the different correction methods. There is, in this Figure, a small influence due to the different ways in which the hemispheric averages were produced, but this effect is negligible. The main difference between the correction factors occurs during the 1900-40 period, with the new (*a priori*) method giving smaller corrections by about 0.1°C. Visually, this has the effect of "delaying" the warming of the early 20th century, in the sense that, between 1900 and 1940, a particular level is reached 5-10 years later with the new data.

The relatively small difference between our old and new values for the 19th century implies that a discrepancy will still exist when our new data are compared with the UKMO SST data. To illustrate and quantify this we first show the latest UKMO results in Figure 7.5 (data obtained from C.K. Folland and D.E. Parker; see also Folland and Parker, 1989a,b). Figure 7.6 shows the difference between Figure 7.5 and our new SST results. The differences are up to 0.2°C, with the Folland/Parker method giving warmer temperatures in the mid 19th century (by around 0.2°C) through to the mid twentieth (by around 0.1°C). The differences are greater in the Northern Hemisphere; indeed, for the Southern Hemisphere there are essentially no differences after the mid 1880s.

Why are there these residual differences? Consider first the period 1900-40. Even after the extensive analysis presented in this report, it is difficult to identify the reasons for these small differences. *A priori*

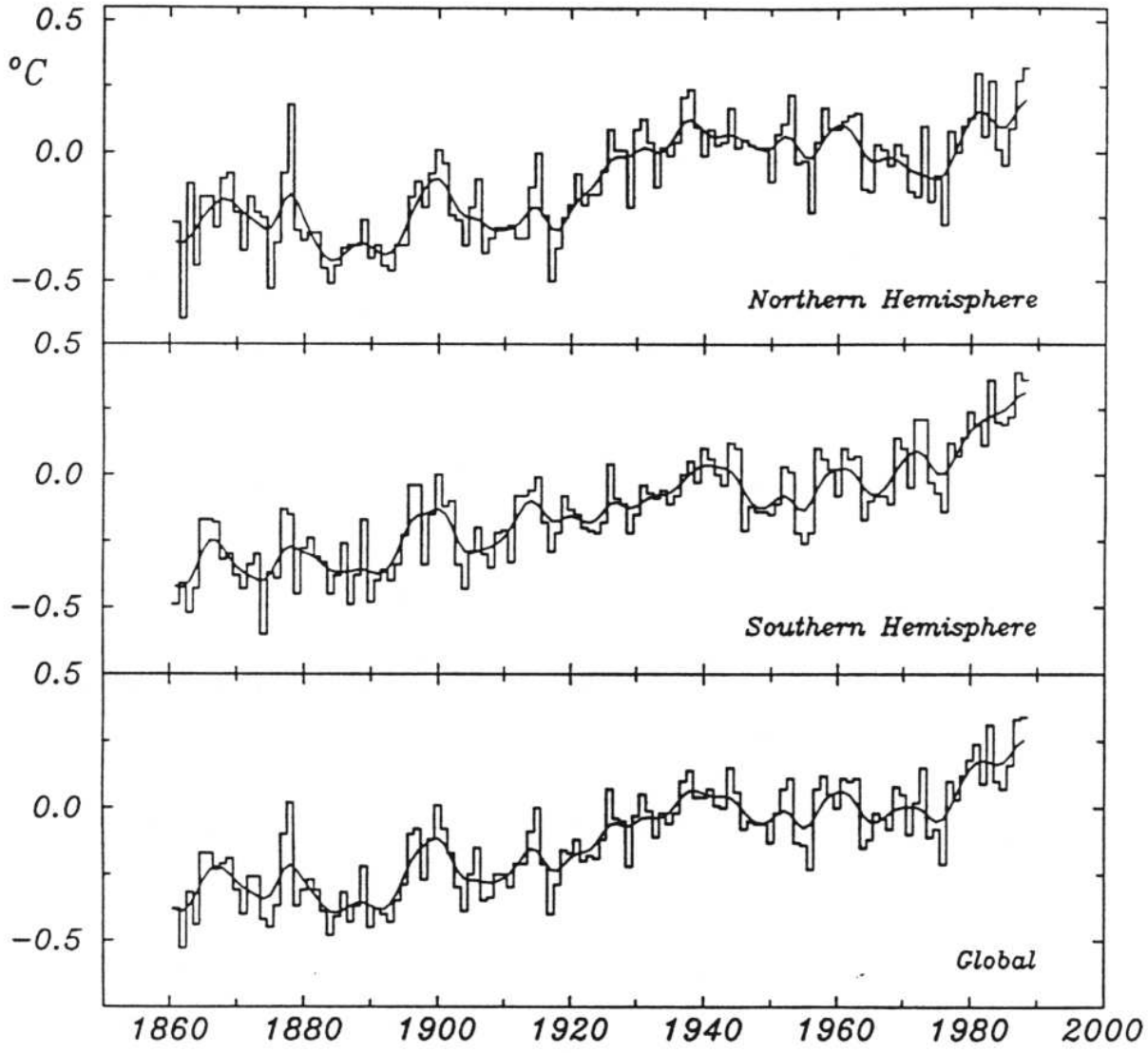

Fig. 7.3: Hemispheric and global time series combining COADS SST (corrected according to Jones et al., 1986c) and land data: 1861-1988. Marine data for 1987 and 1988 are from the UKMO data set. These curves are updated versions of those published in Jones et al. (1986c).

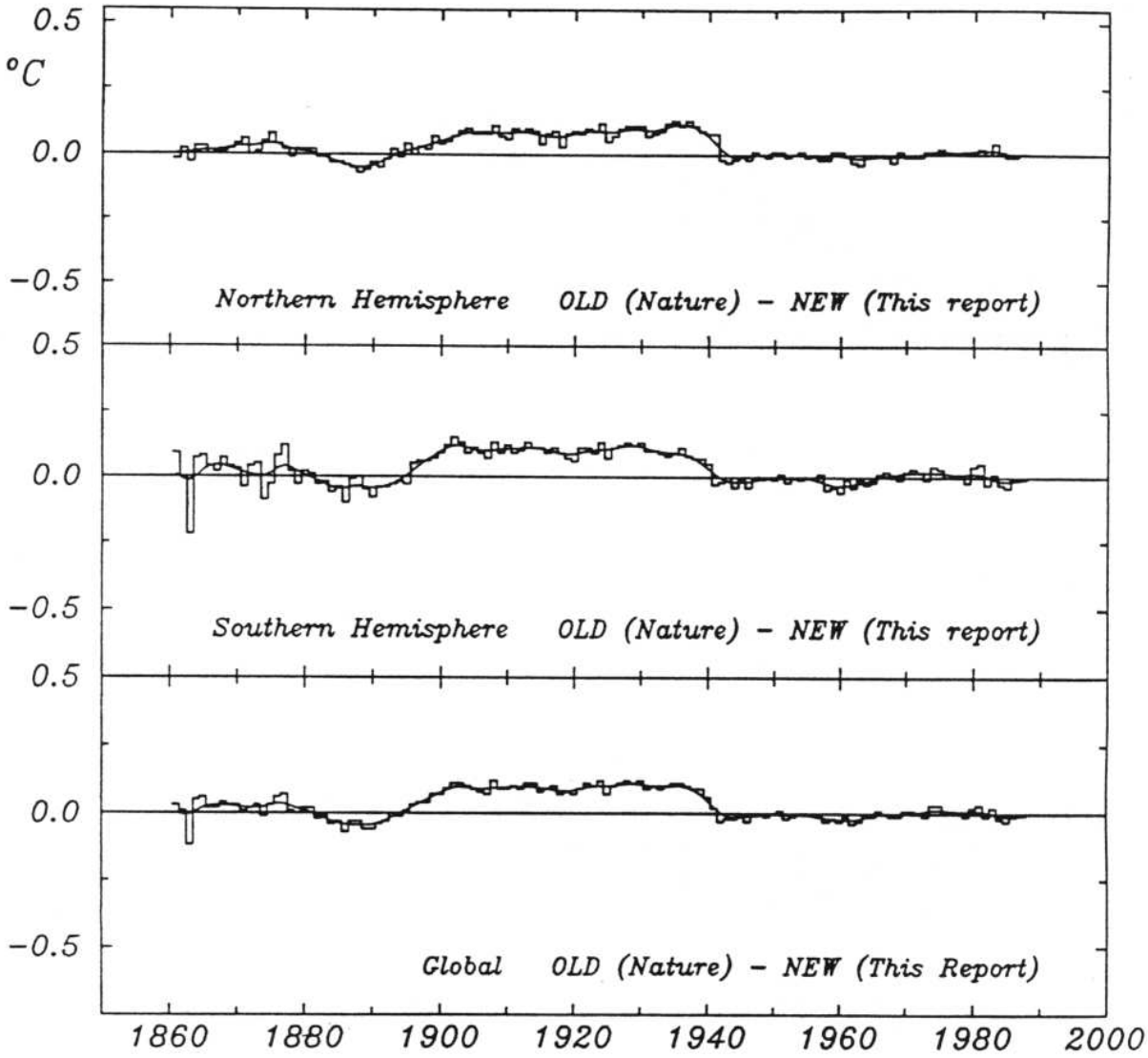

Fig. 7.4: Difference between the 'old' (Jones et al., 1986c) corrected COADS SST and land series and the 'new' (this report) bucket model corrected COADS SST and land series: 1861-1988 (Fig. 7.3 minus 7.2).

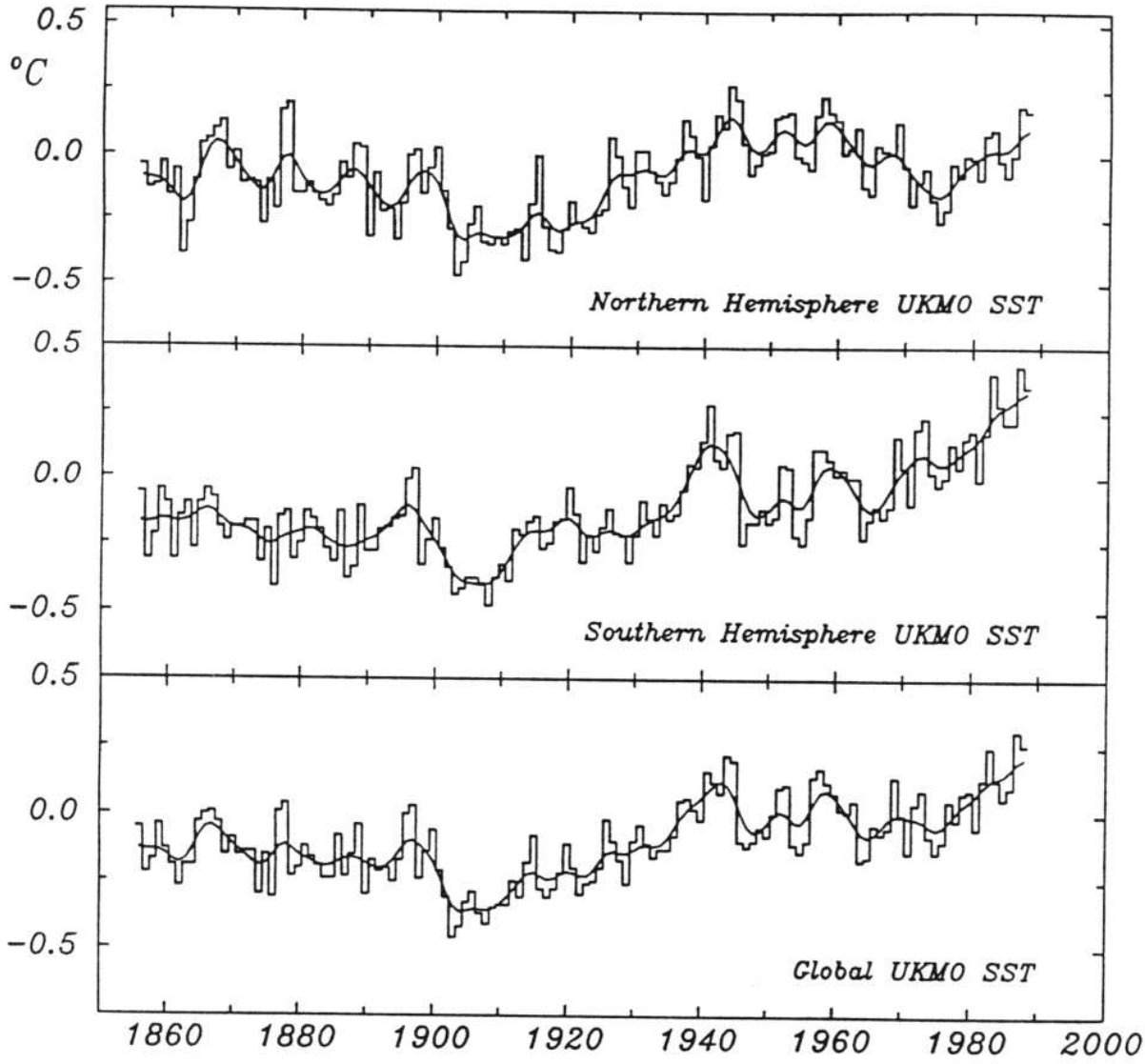

Fig. 7.5: Hemispheric and global time series based on corrected UKMO SST data: 1856-1988. Corrections to the UKMO data are detailed in Folland and Parker (1989a,b).

factors determined independently by ourselves and the UKMO are not immediately comparable at the hemispheric scale because of different conclusions drawn with regard to exposure time, and because coverage differences between the uncorrected UKMO and COADS data sets lead to correction factor differences. The issue is further complicated by the differences in the uncorrected data.

Comparison of Figures 7.4 and 7.6 shows that, if the latest UKMO results were compared with our *earlier* results, then they would show better agreement over the 1900-40 period in the Northern Hemisphere than do our present results. Similarly, our latest results agree better with the original Folland et al. (1984) results than with the most recent UKMO corrected data. This is because we have reduced the magnitude of our correction factor over 1900-1940, while the UKMO workers have increased the magnitude of their correction factor over this period (via a number of iterations).

For the period prior to 1900, the main reason for the differences between our results and those of the UKMO lies in the assumed evaporating bucket fraction. We have assumed that the percentage of evaporating buckets increased from 25% to 100% over the period from 1880-1905, while the UKMO workers have assumed that all measurements in the 19th century were made with evaporating buckets. This means that our (positive) corrections become progressively smaller as one goes back into the 19th century, so the resulting corrected temperatures become, in general, progressively cooler compared with the corrected UKMO data.

As a final point, we must judge whether or not our new corrected data are better than those derived earlier by the *a posteriori* method. It is clear that they are better in terms of spatial and temporal (i.e. intra-annual) coverage, since the earlier data were only hemispheric, annual means. In terms of overall quality, the new data are also almost certainly better. There is, however, an aspect that might lead one to suspect

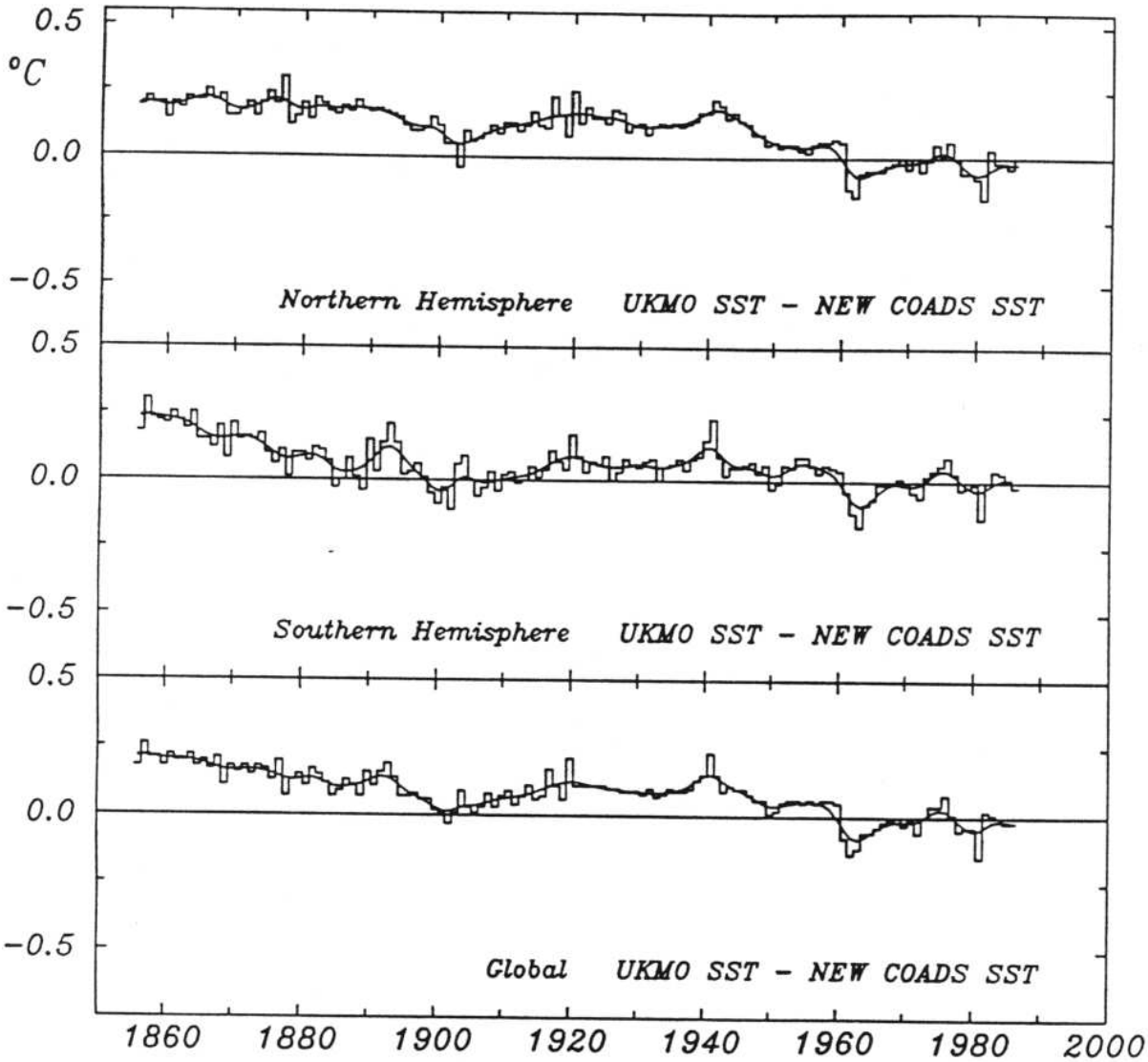

Fig. 7.6: Difference between the UKMO corrected SST data and the corrected COADS SST series derived in this report: 1856-1986 (Fig. 7.1 minus Fig. 7.5).

otherwise. The earlier corrected data were constrained to agree with the land data along coasts and near islands. This also had the effect of giving good agreement between the land and marine hemispheric means. With the new data, the hemispheric means over land and ocean areas do not agree so well (see Figures 6.7 and 6.9). Such differences, however, do *not* mean that the coastal/island land data are in conflict with the newly corrected marine data, because the new correction factors, in contrast to the old, differ spatially. As argued earlier, the land/marine differences we now observe must be largely real. The new SST data set produced by this project represents a substantial advance over earlier data.

REFERENCES

Abramowitz, M. and Stegun, I.A., 1965: Handbook of Mathematical Functions, Dover Publications, New York, 1046 pp.

Barnett, T.P., 1984: Long-term trends in surface temperature over the oceans. Monthly Weather Review 112, 303-312.

Barnett, T.P., 1985: Long-term climatic change in observed physical properties of the oceans. (In) Detecting the Climatic Effects of Increasing Carbon Dioxide. (M.C. MacCracken and F.M. Luther, Eds.). U.S. Dept. of Energy, Carbon Dioxide Research Division, 91-107.

Bottomley, M., Folland, C.K., Hsiung, J., Newell, R.E. and Parker, D.E., 1989: Global Ocean Surface Temperature Atlas, MIT press (in press).

Bradley, R.S. and Jones, P.D., 1985: Data bases for isolating the effects of increasing carbon dioxide concentration. (In) Detecting the Climatic Effects of Increasing Carbon Dioxide (M.C. MacCracken and F.M. Luther, Eds.) U.S. Dept. of Energy, Carbon Dioxide Research Division, 29-53.

Folland, C.K., Parker, D.E. and Kates, F.E., 1984: Worldwide marine temperature fluctuations 1856-1981. Nature 310, 670-673.

Folland, C.K. and Hsiung, J., 1986: Correction of seasonally-varying biases in uninsulated bucket sea surface temperature data using a physical model. Met. Office Synoptic Climatology Branch Memo No.154 (revised version of 1985 original).

Folland, C.K. and Parker, D.E., 1986: Worldwide and regional variations of surface marine temperature, 1856-1985. Proceedings of the Joint Royal Met. Soc./Hellenic Met. Soc. Meeting, Athens, April 1985.

Folland, C.K. and Parker, D.E., 1989a: Comparison of corrected sea surface and air temperature for the globe and the hemispheres, 1856-1988. Proceedings of the Thirteenth Annual Climate Diagnostics Workshop. U.S. Dept. of Commerce, 160-165.

Folland, C.K. and Parker, D.E., 1989b: Observed variations of sea surface temperature. (In) Climate-Ocean Interaction (M.E. Schlesinger, Ed.). NATO Workshop, Oxford, Kluwer Academic Publishers (in press).

Hansen, J.E. and Lebedeff, S., 1987: Global trends of measured surface air temperature. Journal of Geophysical Research 92, 13345-13372.

James, R.W. and Fox, P.T., 1972: Comparative sea-surface temperature measurements. Rep. No.5. Marine Science Affairs, WMO, No.336, 27 pp.

Jones, P.D., 1988: Hemispheric surface air temperature variations: recent trends and an update to 1987. Journal of Climate 1, 654-660.

Jones, P.D., Raper, S.C.B., Santer, B.D., Cherry, B.S.G., Goodess, C.M., Kelly, P.M., Wigley, T.M.L., Bradley, R.S. and Diaz, H.F., 1985: A Grid Point Surface Air Temperature Data Set for the Northern Hemisphere. U.S. Dept. of Energy, Carbon Dioxide Research Division, Technical Report TR022, 251 pp.

Jones, P.D., Raper, S.C.B., Bradley, R.S., Diaz, H.F., Kelly, P.M. and Wigley, T.M.L., 1986a: Northern Hemisphere surface air temperature variations, 1851-1984. Journal of Climate and Applied Meteorology 25, 161-179.

Jones, P.D., Raper, S.C.B. and Wigley, T.M.L., 1986b: Southern Hemisphere surface air temperature variations, 1851-1984. Journal of Climate and Applied Meteorology 25, 1213-1230.

Jones, P.D., Wigley, T.M.L. and Wright, P.B., 1986c: Global temperature variations, 1861-1984. Nature 322, 430-434.

Jones, P.D., Kelly, P.M., Goodess, C.M. and Karl, T., 1989: The effect of urban warming on the Northern Hemisphere temperature average. Journal of Climate 2, 285-290.

Karl, T.R. and Williams, C.N.Jr., 1987: An approach to adjusting climatological time series for discontinuous inhomogeneities. Journal of Climate and Applied Meteorology 26, 1744-1763.

Karl, T.R. and Jones, P.D., 1989: Urban bias in area-averaged surface air temperature trends. Bulletin of the American Meteorological Society 70, 265-270.

Kirkaldy, A.W., 1919: British Shipping, Its History, Organization and Importance, Kegal Paul, Trench, Trubner, London.

Krummel, O., 1907: Handbuch der Ozeanographie, Vol.1, Stuttgart, 373 pp.

Maury, M.F., 1855: Wind and Current Charts, 7th Edition, U.S. Navy, Philadelphia.

Murray, F.W., 1967: On the computation of saturation vapour pressure. Journal of Applied Meteorology 6, 203-204.

Oort, A.H., Pan, Y.H., Reynolds, R.W. and Ropelewski, C.F., 1987: Historical trends in the surface temperature over the oceans based on the COADS. Climate Dynamics 2, 29-38.

Paltridge, G. and Woodruff, S.D., 1981: Changes in global surface temperature from 1880 to 1977 derived from historical records of sea surface temperature. Monthly Weather Review 109, 2427-2434.

Parker, D.E., 1984: The statistical effects of incomplete sampling of coherent data series. Journal of Climatology 4, 445-449.

Parker, D.E., 1987: The sensitivity of estimates of trends of global and hemispheric marine temperature to limitations in geographical coverage. Long-Range Forecasting and Climate Research Series (LRFC) No. 12, Met. O. 13, Meteorological Office.

Quetelet, A., 1853: Report of the Maritime Conference held at Brussels in August/September 1853, for devising a uniform system of meteorological observations. 125 pp.

Ramage, C.S., 1984: Can shipboard measurements reveal secular changes in tropical air-sea heat flux? Journal of Climate and Applied Meteorology 23, 187-193.

Reynolds, R.W., 1988: A real-time global sea surface temperature analysis. Journal of Climate 1, 75-86.

Saur, J.F.T., 1963: A study of the quality of sea water temperatures reported in logs of ships' weather observations. Journal of Applied Meteorology 2, 417-425.

Shea, D.J., 1986: Climatological Atlas: 1950-79. Surface Air Temperature, Precipitation, Sea-Level Pressure, and Sea-Surface Temperature (45°S-90°N). NCAR Technical Note NCAR/TN-269+STR, National Center for Atmospheric Research, Boulder, Colorado, 35 pp. + Appendices.

Shearman, R.J., 1983: The Meteorological Office main marine data bank. Meteorological Magazine 112, 1-10.

Slutz, R.J., Lubker, S.J., Hiscox, J.D., Woodruff, S.D., Jenne, R.L., Joseph, D.H., Steurer, P.M. and Elms, J.D., 1985: Comprehensive Ocean-Atmosphere Data Set; Release 1, Environmental Research Laboratories, Climate Research Program, Boulder, Colorado, 268 pp. (NTIS PB86-105723).

Spalding, D.B., 1963: Convective Mass Transfer. McGraw-Hill, New York.

Tabata, S., 1978: Comparison of observations of sea surface temperatures at Ocean Station P and NOAA buoy stations and those made by merchant ships travelling in their vicinities, in the northeast Pacific Ocean. Journal of Applied Meteorology 17, 374-385.

Vinnikov, K.Ya., Groisman, P.Ya., Lugina, K.M. and Golubev, A.A., 1987: Variations in Northern Hemisphere mean surface air temperature over 1841-1985. Meteorology and Hydrology 1987(1), 45-53 (in Russian).

Wigley, T.M.L., 1989: Possible climate change due to SO_2-derived cloud condensation nuclei. Nature 339, 365-367.

Wigley, T.M.L., Angell, J.K. and Jones, P.D., 1985: Analysis of the temperature record. (In) Detecting the Climatic Effects of Increasing Carbon Dioxide (M.C. MacCracken and F.M. Luther, Eds.). U.S. Dept. of Energy, Carbon Dioxide Research Division, 55-90.

Wigley, T.M.L. and Jones, P.D., 1988: Do large-area-average temperature series have an urban warming bias? Climatic Change 12, 313-319.

Wigley, T.M.L. and Raper, S.C.B., 1987: Thermal expansion of sea water associated with global warming. Nature 330, 127-131.

Woodruff, S.D., 1985: The Comprehensive Ocean-Atmosphere Data Set. Third Conference on Climate Variations and Symposium on Contemporary Climate: 1850-2100, American Meteorological Society, Boston, Mass., 14-15.

Woodruff, S.D., Slutz, R.J., Jenne, R.J. and Steurer, P.M., 1987: A Comprehensive Ocean-Atmosphere Data Set. Bulletin of the American Meteorological Society 68, 1239-1250.

Wright, P.B. and Jones, P.D., 1986: A gridded data set for the global oceans, 1854-1979. (In) Proceedings of a COADS workshop, Boulder, Colorado, January 22-24, 1986 (S.D. Woodruff, Ed.). NOAA, Technical Memorandum ERL ESG-23.